To the Graduate Council:

I am submitting herewith a thesis written by Amy Elizabeth Schoner entitled "The Sedimentology and Sedimentary Petrology of the Lower Silurian Clinch Sandstone at Beans Gap, Grainger County, Tennessee." I have examined the final copy of this thesis for form and content and recommend that it be accepted in partial fulfillment of the requirements for the degree of Master of Science, with a major in Geology.

Steven G. Driese

Steven G. Driese, Major Professor

We have read this thesis and recommend its acceptance:

Kenneth R. Walker

Richard W. Arnseth

Accepted for the Council:

C W Minkel

The Graduate School

STATEMENT OF PERMISSION TO USE

In presenting this thesis in partial fulfillment of the requirements for a Master's degree at The University of Tennessee, Knoxville, I agree that the Library shall make it available to borrowers under rules of the Library. Brief quotations from this thesis are allowable without special permission, provided that accurate acknowledgment of source is made.

Permission for extensive quotation from or reproduction of this thesis may be granted by my major professor, or in his absence, by the Head of Interlibrary Services when, in the opinion of either, the proposed use of the material is for scholarly purposes. Any copying or use of the material in this thesis for financial gain shall not be allowed without my written permission.

Signature Amy Elizabeth Schoner

Date March 5, 1985

THE SEDIMENTOLOGY AND SEDIMENTARY PETROLOGY OF THE LOWER SILURIAN CLINCH SANDSTONE AT BEANS GAP, GRAINGER COUNTY, TENNESSEE

A Thesis

Presented for the

Master of Science

Degree

The University of Tennessee, Knoxville

Amy Elizabeth Schoner

June 1985

ACKNOWLEDGMENTS

I would like to express my gratitude to my advisor, Dr. Steven Driese, for being a constant source of help and encouragement. I would also like to thank my committee members, Dr. Richard Arnseth and Dr. Kenneth Walker, for their suggestions and comments. My colleagues, Mary Cudzil and Craig Clement, were invaluable as sources of ideas and input as I tried to find the best answers to all the questions posed in this study. Profuse thanks are extended to Bill Copeland, whose rappelling equipment and proficiency tremendously simplified the sampling process. I would also like to express my appreciation to Newman Smith for his support and encouragement throughout this study. My final thanks go to my parents, without whose financial and moral support I never could have begun this project, much less completed it.

Financial aid was provided by the Professors Honor Fund of the Department of Geological Sciences at the University of Tennessee, Knoxville, Sigma Xi, and the Appalachian Basin Industrial Associates. My thanks are extended to George H. Davis of Sun Exploration and Production Company for his interest in this project and for financing preparation of almost half of the thin sections.

ABSTRACT

The Clinch Sandstone is exposed along a 2 kilometer transect through Beans Gap on Clinch Mountain in northeastern Tennessee. The two members of the Clinch Sandstone, the lower Hagan Shale Member (14.9 m) and the upper Poor Valley Ridge Member (55.7 m), are both present and can be divided into distinct facies. The three facies of the Hagan Shale Member compose a coarsening-upward sequence that includes shelf-mud deposition at the base and transition-zone deposition at the contact with the Poor Valley Ridge Member. These deposits are characterized by a rather diverse assemblage of trace fossils including Arthrophycus, Skolithos, Rusophycus, Monocraterion, Planolites, and possible Chondrites. The Hagan Shale Member is composed of subarkosic clayshale, siltstone, interbedded clayshale and siltstone and thin- to medium-bedded quartzitic sandstone. Paleocurrent indicators are rare in the Hagan Shale Member.

The Poor Valley Ridge Member can be subdivided into four facies at Beans Gap. Each represents different environments of deposition. Facies 1, characterized by medium- to large-scale trough cross-stratification, represents depositional conditions with flow velocities of 70 to 90 cm per second but interrupted by suspension deposition of clays and bioturbation. Facies 2 exhibits medium- to very large-scale planar-tabular cross-stratification and represents flow velocities of 60 to 80 cm per second during episodes of deposition more continuous than those of facies 1. Facies 3 is

characterized by very densely bioturbated sandstone, which represents periods of low-energy and reduced sediment influx. Facies 4 represents deposition characterized by alternating high-energy events (which deposited horizontally laminated and rippled sandstone) and low-energy events (suspension deposition of clays followed by bioturbation). The Poor Valley Ridge Member contains Arthrophycus, Skolithos, Rusophycus, Cruziana, Monocraterion, Diplocraterion, Planolites, and possible Thalassinoides. Each of the facies and trace fossils present represent deposition in a subtidal, marine environment with probable water depths between approximately 3 and 20 m. Vertical sequences within the Poor Valley Ridge Member were analyzed with a statistical comparison to random occurrence. The analysis yielded two preferred paths which can be described as "low-energy" and "high-energy." Paleocurrent directions for the Member, when examined in conjunction with facies and facies sequences suggest deposition in three laterally shifting shallow-marine environments: the shoreface, rip channel/tidal inlets, and a back-bay or lagoon. A prograding sequence from the top of the Hagan Shale Member to a thinly laminated siltstone in the middle of the Poor Valley Ridge Member reverses to a brief transgressive sequence consisting of rip current/tidal inlet and shoreface deposits. These are in turn overlain near the top of the Formation by more rip current/tidal inlet and uppermost shoreface deposits. An unconformity occurs at the top of the Clinch Sandstone at Beans Gap.

Detailed sampling and point-counting yielded extensive mineralogic data which was compiled and statistically treated with

correlation coefficients to determine occurrence relationships between the minerals. Few noticeable trends and relationships were found in the Formation, but the compilation allowed comparisons to be drawn between the Clinch Sandstone in northeastern Tennessee and the Tuscarora Formation in Virginia and Pennsylvania. The Clinch Sandstone in Tennessee is apparently derived from a more mature source (throughout almost its entire deposition, unlike the Tuscarora Formation in Virginia), perhaps the Cambrian Chilhowee Group, and represents deposition in a shallow-marine setting; it does not show any fluvial facies, such as are found in the Tuscarora Formation to the north.

Post-burial features have been noted and porosity has been measured from the thin sections. These suggest several stages of authigenic mineral precipitation and dissolution which occluded much of the original porosity but also formed secondary and hybrid pores that are present today in amounts averaging 3% and ranging up to 11%.

TABLE OF CONTENTS

SECTION		PAGE
I.	INTRODUCTION	1
II.	HISTORICAL BACKGROUND AND SITE DESCRIPTION	3
	Background	3
	Site Description	6
III.	FIELD AND ANALYTICAL METHODS	12
	General	12
	Photomosaic Construction	12
	Field Measurements	19
	Sampling	19
	Petrography	20
	Trace Fossils	21
	Paleocurrents	22
IV.	LITHOLOGIC DESCRIPTION	24
	Facies Descriptions	24
	Facies Relationships	40
	Petrographic Description	60
	Mineral Associations	80
	Textural Maturity	97
	Rounding	97
	Sorting	102
	Overall Textural Maturity	105
	Post Burial Features	105
	Cementation	105
	Replacement and Alteration	110
	Total Porosity	112
V.	TRACE FOSSILS	120
VI.	PALEOCURRENT ANALYSIS	139
	Results	139
	Interpretation of Data	142
VII.	LITHOLOGIC INTERPRETATION	154
	Sedimentology	154
	Facies	154
	Depositional Setting	163

SECTION PAGE

Petrography 181
Diagenetic History 189

VIII. SUMMARY AND CONCLUSIONS 196

REFERENCES 200

APPENDICES 210

A. TOTAL POINT-COUNT DATA 211

B. DETRITAL PERCENTAGES RECONSTRUCTED FROM POINT-COUNTED DATA 213

C. PALEOCURRENT MEASUREMENTS 215

D. LITHOLOGIC DESCRIPTION 219

VITA 227

LIST OF TABLES

TABLE		PAGE
1.	History of Clinch Sandstone Nomenclature	4
2.	Observed Frequency Matrix	51
3.	Expected Frequency Matrix	53
4.	Difference Matrix	54
5.	Means, Standard Deviations, Ranges and Occurrences for All Minerals in the Clinch Sandstone	61
6.	Visually Estimated Correlations Between Constituents and Properties	84
7.	Calculated Correlation Coefficients (r) Using $\alpha = 0.05$ to Determine Significance	85
8.	Ranges of Constituents and Properties for Each Facies	86
9.	Paleocurrent Studies on Clinch Sandstone Lithostratigraphic Equivalents	149
10.	Similarities Between the Clinch Sandstone and Modern Bar and Associated Environments	169
A-1.	Total Point-Count Data	212
B-1.	Detrital Percentages Reconstructed from Point-Counted Data	214
C-1.	Paleocurrent Measurements	216
D-1.	Lithologic Description	220

LIST OF FIGURES

FIGURE		PAGE
1.	Outcrop Locality Map	7
2.	Vertical Outcrop Relationships at Beans Gap	10
3.	Outcrop 1 Sedimentology	13
4.	Outcrop 2 Sedimentology	15
5.	Outcrop 4 Sedimentology	17
6.	Facies Relationships in Hagan Shale Member	25
7.	Hagan Shale Member facies C (Slightly Clayey Siltstone to Very Fine-Grained Sandstone)	27
8.	Skolithos in Hagan Shale Member	27
9.	Diagrammatic Sketch of All Trace Fossils Found in the Clinch Sandstone at Beans Gap	29
10.	Hagan Shale Member facies A (Clayshale)	32
11.	Hagan Shale Member facies B (Interbedded Siltstone and Sandstone)	32
12.	Poor Valley Ridge Member Facies 1, Between Arrows (Trough Cross-Beds)	36
13.	Poor Valley Ridge Member Facies 2, Between Arrows (Planar-Tabular Cross-Beds)	36
14.	Poor Valley Ridge Member Facies 3 (Bioturbated Beds)	38
15.	Poor Valley Ridge Member Facies 4 (Horizontally Laminated Beds)	38
16.	Facies Relationships in Outcrop 1	42
17.	Facies Relationships in Outcrop 2	44
18.	Facies Relationships in Outcrop 4	46
19.	Generalized Stratigraphic Column for Clinch Sandstone at Beans Gap	48

FIGURE PAGE

20. Facies Transitions which Occur More Often Than Expected Under Random Depositional Conditions (Constructed from Tables 2, 3 and 4) 55

21. Photograph and Tracing Showing Lateral Facies Shift in Immediately Overlying Beds 58

22. Stratigraphic Distribution of Monocrystalline Quartz . . 64

23. Stratigraphic Distribution of Quartz Overgrowths (Using 0.5 for All Values Between 0 and 1) 66

24. Stratigraphic Distribution of Illite/Sericite 68

25. Stratigraphic Distribution of Amorphous Iron Oxide/ Clay Aggregates 70

26. Stratigraphic Distribution of Polycrystalline Quartz . . 73

27. Stratigraphic Distribution of Kaolinite/Dickite 75

28. Stratigraphic Distribution of Smectite 77

29. Classification for Visual Comparison of Point-Counted Constituents and Properties 81

30. Stratigraphic Variation in Textural Maturity 87

31. Stratigraphic Distribution of Grain Size 89

32. Photomicrograph of Quartz Overgrowth (Visible Grain Boundary on Large, Rounded Monocrystalline Quartz) . . . 98

33. Stratigraphic Variation in Rounding 100

34. Stratigraphic Variation in Sorting 103

35. Photomicrograph of Pressure Solution Features: Sutured Grain Boundary and Stylolite 108

36. Photomicrograph of Lateral Elongation 108

37. Photomicrograph of Squashed Mica 108

38. Photomicrograph of Grain Fracturing Present in Large, Oblong, Monocrystalline Quartz Grain 113

39. Photomicrograph of Whole-Rock Fracture Which Has Been Occluded with Authigenic Kaolinite 113

FIGURE PAGE

40. Stratigraphic Distribution of Porosity 115

41. *Arthrophycus* in Clinch Sandstone Float 121

42. *Skolithos* Type A and Type B 124

43. *Planolites* (*) and *Pelecypodichnus* (+) in Clinch Sandstone Float 127

44. *Diplocraterion* with Spreite in Poor Valley Ridge Member 127

45. *Rusophycus* in Hagan Shale Member 129

46. *Cruziana* Among *Rusophycus* in Hagan Shale Member 129

47. *Monocraterion* in Clinch Sandstone Float 129

48. Photograph Tracing of *Arenicolites* in Clinch Sandstone Sandstone 132

49. Photograph Tracing of *Thalassinoides*(?) on Underside of Bed Viewed from Below 135

50. Possible *Chondrites* in Clinch Sandstone Float 137

51. *Paleophycus* in Clinch Sandstone Float 137

52. *Corophioides* (*) in Clinch Sandstone Float 137

53. Bidirectional Paleocurrent Indicators in Clinch Sandstone (Length of Wedges is Proportional to Number of Observations) 140

54. Comparison of Planar-Tabular vs. Trough Cross-Bed Paleocurrent Indicators (Length of Wedges is Proportional to Number of Observations) 143

55. Stratigraphic Breakdown of Paleocurrent Means in Clinch Sandstone 145

56. Unidirectional Paleocurrent Indicators in Clinch Sandstone (Length of Wedges is Proportional to Number of Observations) 147

57. Map of Paleocurrent Vector Means for Clinch Sandstone Equivalents 151

FIGURE PAGE

58. Portion of Thinly Laminated Siltstone Interval (2.46 m Thick) in Poor Valley Ridge Member 165

59. Generalized Profile of a Nearshore Marine Environment (After Reinson, 1979) 170

60. Ideal Prograding Beach-to-Offshore Sequence (Modified from Howard and Reineck, 1979; and McCubbin, 1982) 174

61. Proposed Paleoenvironments for Clinch Sandstone at Beans Gap (Adapted from Reinson, 1979) 177

62. Approximate Composite Paragenetic Sequence for Clinch Sandstone at Beans Gap 191

I. INTRODUCTION

The Lower Silurian Clinch Sandstone is the most prominent ridge-forming unit in east Tennessee, cropping out along Clinch Mountain, Powell Mountain, and Newman Ridge. Regional studies of the Clinch Sandstone have included outcrops in east Tennessee (Nicholson, 1978) but, prior to this study, there has been no detailed paleoenvironmental analysis of these rocks.

New outcrops were created during the Spring of 1978 along US Route 25E over Clinch Mountain at Beans Gap. These outcrops constitute the best-exposed Clinch Sandstone outcrop locality in Tennessee.

Laterally correlative stratigraphic units equivalent to the Clinch Sandstone in the northern and central Appalachians include the Tuscarora Sandstone, the Medina Group, and the lower part of the Shawangunk Conglomerate (Berry and Boucot, 1970; Colton, 1970). Westerly and southerly lateral equivalents in the southern Appalachians include the Rockwood Formation and the Red Mountain Formation (Miller, 1976; Chowns, 1972).

The Clinch Sandstone is composed of two members (Miller and Fuller, 1954): the lower Hagan Shale Member and the upper Poor Valley Ridge Member (Chapter 2 for description by Miller and Fuller, 1954). These two members have not been differentiated elsewhere along this strike belt or in adjacent strike belts to the northeast containing equivalent stratigraphic units.

The purpose of this study is to document the sedimentology of the Clinch Sandstone at the four extensive outcrops at Beans Gap and

to propose a paleoenvironmental model for its deposition. Three facies were defined for the Hagan Shale Member and four facies for the Poor Valley Ridge Member. Detailed petrographic data are used to supplement field study of physical and biogenic sedimentary structures.

An attempt was also made to compare Clinch depositional environments with stratigraphic equivalents to the north (Smith, 1970, 1972; Cotter, 1982, 1983; Folk, 1960) as well as to propose modern analogs for the depositional environments that are inferred for the study.

The Beans Gap locality is scientifically significant because it provides more information about the Lower Silurian in east Tennessee, detailed studies of which are lacking. This study provides the basis for a comparison between the southern Clinch Sandstone and northern Tuscarora Formation, important for gaining knowledge of regional paleoenvironmental relationships.

II. HISTORICAL BACKGROUND AND SITE DESCRIPTION

Background

Safford first defined the "Clinch Mountain Sandstone," in 1869, as all strata above the red-colored strata of the "Clinch Shale" (now called the Juniata Formation) and below the Chattanooga Shale. Rogers (1953) referred to these strata as the Clinch Sandstone. Miller and Fuller (1954) divided the Clinch Sandstone into two lithologic units: the basal unit (composed predominantly of shale) was termed the Hagan Shale Member; the upper ridge-forming sandstone was named the Poor Valley Ridge Member. Dennison and Boucot (1974) limited Safford's original description to those rocks lying between the Upper Ordovician Juniata and the Lower Devonian Wildcat Valley Sandstone along Clinch Mountain. Further to the northeast the Lower Silurian Clinch Sandstone is overlain by the Middle Silurian Clinton Group (Colton, 1970; Miller and Fuller, 1954). Recent nomenclature changes, though limited, are significant (Table 1). The Clinch Sandstone is considered Lower Silurian (Llandovery), not on the basis of megafossils (because these are absent on Clinch Mountain in Tennessee) but by regional stratigraphic relationships (Dennison and Boucot, 1974).

The Clinch Mountain Sandstone was first described as a white to gray-white, hard sandstone containing Skolithos tubes and some shaley layers (Safford, 1869). Rodgers (1953) amended this

Table 1. History of Clinch Sandstone Nomenclature.

	Safford 1869	Rodgers 1953	Miller & Fuller 1954	Colton et al. (SW Virginia) 1970	Dennison & Boucot (NE Tennessee) 1974
	Chattanooga Shale (Devonian			Clinton Grp. (Middle Silurian)	Wildcat Valley Sandstone (Lower Dev.)
LOWER SILURIAN	Clinch Mountain Sandstone	Clinch Sandstone	Clinch Sandstone: Poor Valley Ridge Member; Hagan Shale Member	Clinch Sandstone	Clinch Sandstone
UPPER ORDOVICIAN	Clinch Shale	Juniata Formation	Sequatchie Formation	Juniata Formation	Juniata Formation

description by stating that the Clinch Sandstone is a thick-bedded to massive, medium- to coarse-grained, well-sorted and well-rounded, pure quartz sandstone that locally includes fine pebbles. Miller and Fuller (1954) described the two Clinch Sandstone Members separately: the Hagan Shale Member as a green-gray shale with sparse body fossils, and the Poor Valley Ridge Member as consisting of interbedded sandstone and shales present as massive beds, with some laminations, cross-beds and ripple-marked upper surfaces.

The Clinch Sandstone, though named in 1869 for Clinch Mountain, did not have a type section until Dennison and Boucot (1974) suggested a type section on TN Route 70 at Little War Gap. Miller (1976) subsequently proposed Little Moccasin Gap (northwest of Abingdon, Virginia) as the reference section. Miller mentioned several outcrops along Clinch Mountain including those which were examined in this study. He described the Beans Gap outcrops along TN Route 25E as "base excellently exposed . . . few outcrops near top." During a road improvement project begun in 1976, blasting exposed new outcrops of the Clinch Sandstone in the Beans Gap area. These new outcrops are, therefore, the freshest Clinch Sandstone exposures in east Tennessee. Other outcrops of the Clinch Sandstone may be more vertically extensive but, due to weathering, do not show the degree and quality of preservation and hence may not display the most accurate depositional and early-stage diagenetic features as have been found at the Beans Gap outcrops. Only 70.6 m of Clinch Sandstone is exposed in the study area due to erosion at the top of the Formation prior to Chattanooga Shale deposition. The Clinch Sandstone

has been measured at the type section (Little War Gap) as 95.7 m, and at the reference section (Little Moccasin Gap) as 89.6 m. The unit is conformably underlain by the Upper Ordovician Juniata Formation and, as previously mentioned, has an erosive upper boundary. The next unit present above the Clinch Sandstone along US Route 25E on Clinch Mountain is the Wildcat Valley Sandstone (Lower Devonian), followed by the Mississippian/Devonian Chattanooga Shale (Hardeman, 1966; Miller, 1976).

These outcrops were chosen for this study for their freshness (outstanding preservation) and excellent exposure of physical and biogenic sedimentary structures, as well as broad lateral and vertical extent. Additionally the variety of outcrop styles present at Beans Gap (cliff face, terraced face, slope face and quarry amphitheater) offered multiple avenues of investigation.

Site Description

Four extensive Clinch Sandstone outcrops occur at the top of Clinch Mountain along a 2 km transect through Beans Gap adjacent to US Route 25E in Grainger County (Figure 1). The outcrops lie at 36°21'6"N, 83°22'51"E in the Avondale and Bean Station 7.5 minute U.S. Geological Survey topographic quadrangles. Clinch Mountain lies on the Copper Creek thrust sheet in the Valley and Ridge physiographic province of the Southern Appalachians, where the Clinch Sandstone is a principal ridge-forming unit. At Beans Gap, the Clinch Sandstone is exposed at the top of the ridge and along the southern dip slope.

Figure 1. Outcrop locality map.

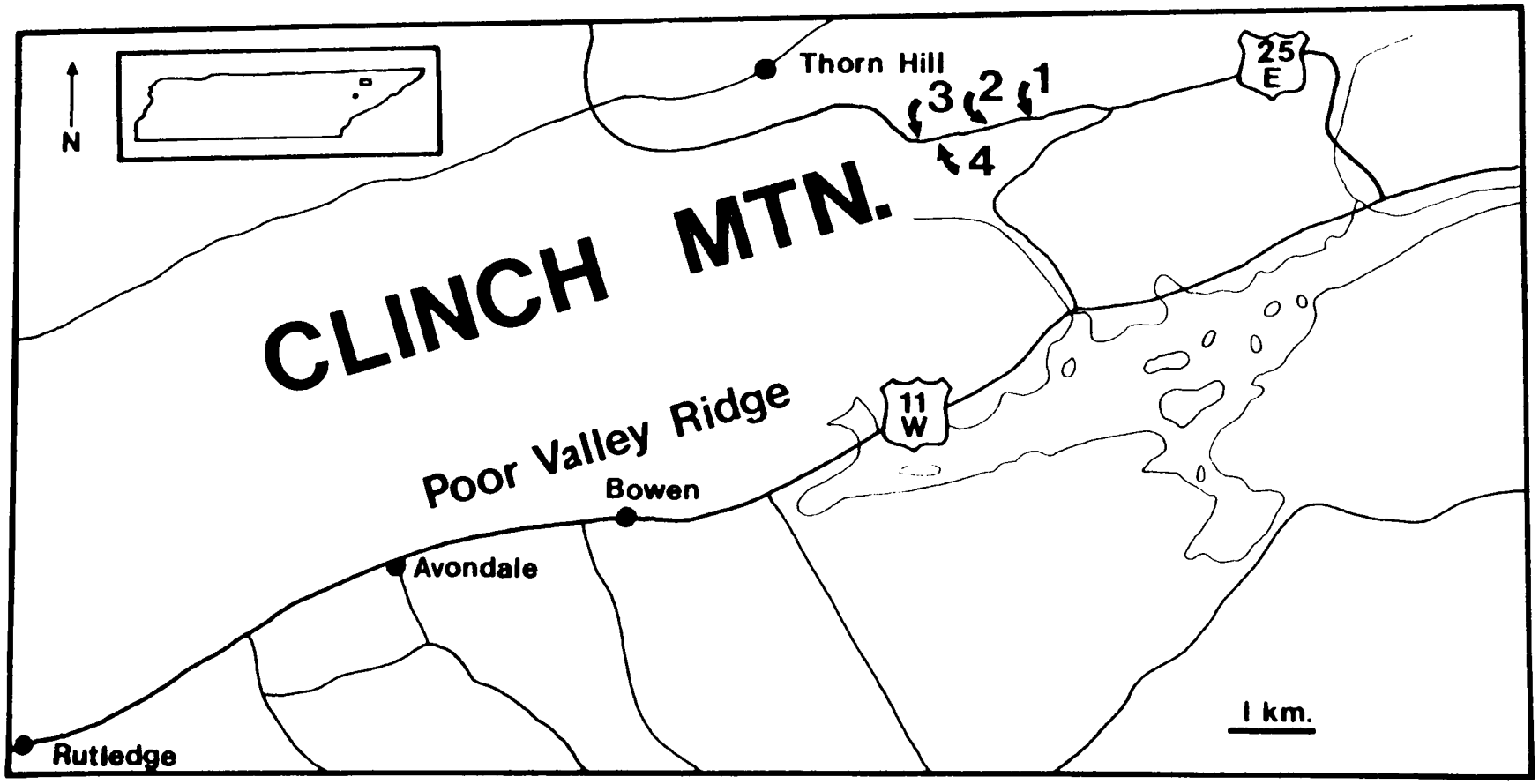
N
Thorn Hill
3
2
1
4
25
E
CLINCH MTN.
Poor Valley Ridge
11
W
Bowen
Avondale
Rutledge
1 km.

Figure 1

Outcrop 1 is a two-dimensional roadcut, 75 m wide and 11 m high; it is almost continuous with outcrop 2, a two-dimensional roadcut which is 205 m wide and 16 m high. Outcrop 3 is a roadcut-to-quarry transition including all but the top 5 m of the Clinch Sandstone on Clinch Mountain (approximately 65.5 m out of 70.6 m total). The very top of the Clinch Sandstone exposure at Beans Gap is present in outcrop 4, the lower portion of which is equivalent to the upper beds of outcrop 3. Outcrop 4, 76 m wide and 6 m high, is two-dimensional and is within line of sight of outcrop 3, which allows stratigraphic correlation. Outcrops 1 and 2 are stratigraphically lower than outcrop 4, yet are equivalent to a portion of the very extensive outcrop 3. These relationships are shown schematically in Figure 2.

Figure 2. Vertical outcrop relationships at Beans Gap. Vertical scale is 1:500. Horizontal relationships are not to scale.

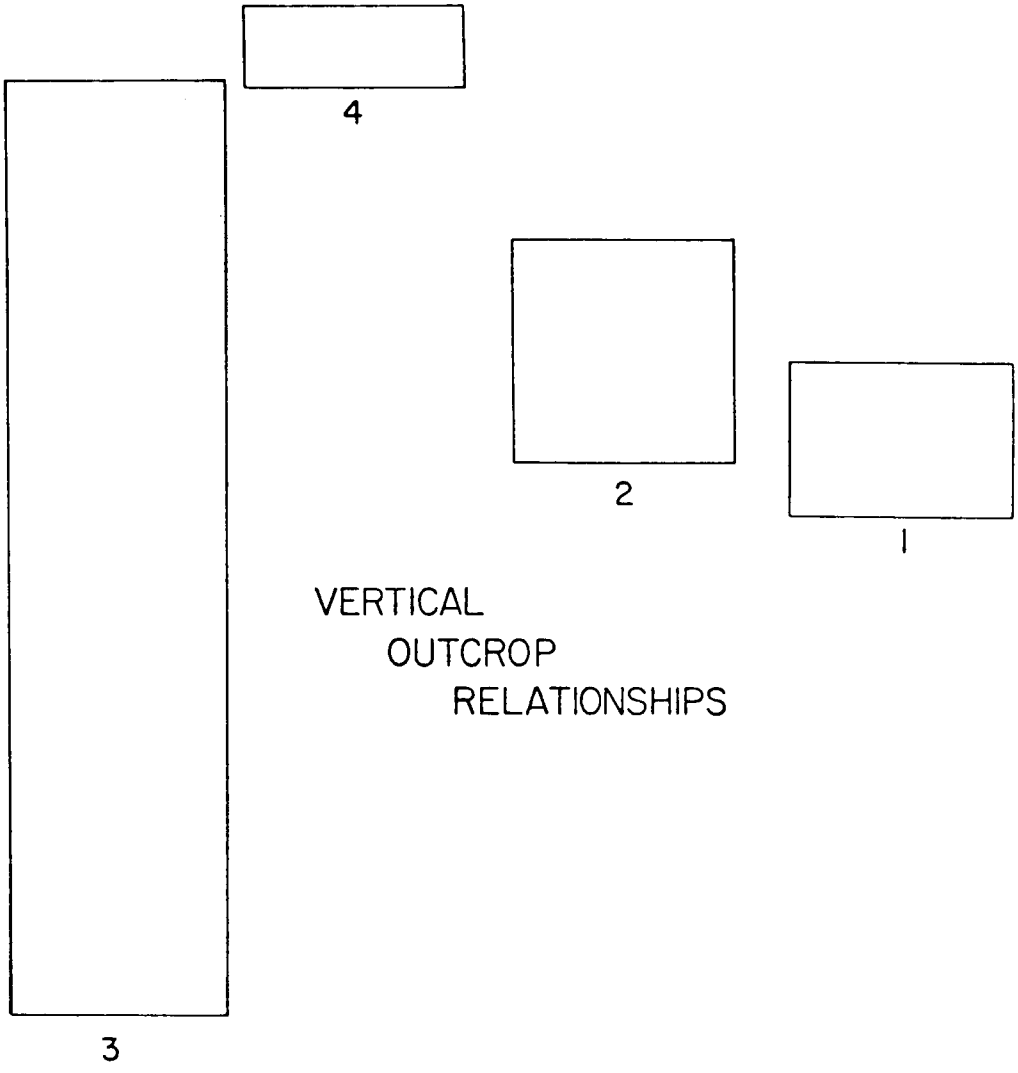

Figure 2

III. FIELD AND ANALYTICAL METHODS

General

While searching for suitable outcrops, several traverses were made across Clinch Mountain at accessible windgaps and roadcuts to examine the Clinch Sandstone. Due to the degree of preservation present, the Beans Gap location was chosen (as mentioned in Section II). A single locality investigation allowed far more detail than could have been accomplished had more outcrops been involved.

Photomosaic Construction

To create a base on which lateral relationships could be evaluated, extensive photomosaics were made of the three outcrops with broad lateral exposure (outcrops 1, 2 and 4) (Figures 3, 4, and 5). Photographs were taken at intervals of approximately 3 to 5 m from distances of about 20 to 25 m. Photographic tracings, enhanced by on-site addition of structural details, were drafted for outcrops 1 and 4. Outcrop 2 is a much higher and longer outcrop and required redrafting to eliminate distortion. This was accomplished using a Bonne projection (division of the distorted image into equal area grids which were transferred to orthogonal coordinates). In this manner vertical and lateral geometric relationships were preserved.

Figure 3. Outcrop 1 sedimentology.

Outcrop 1

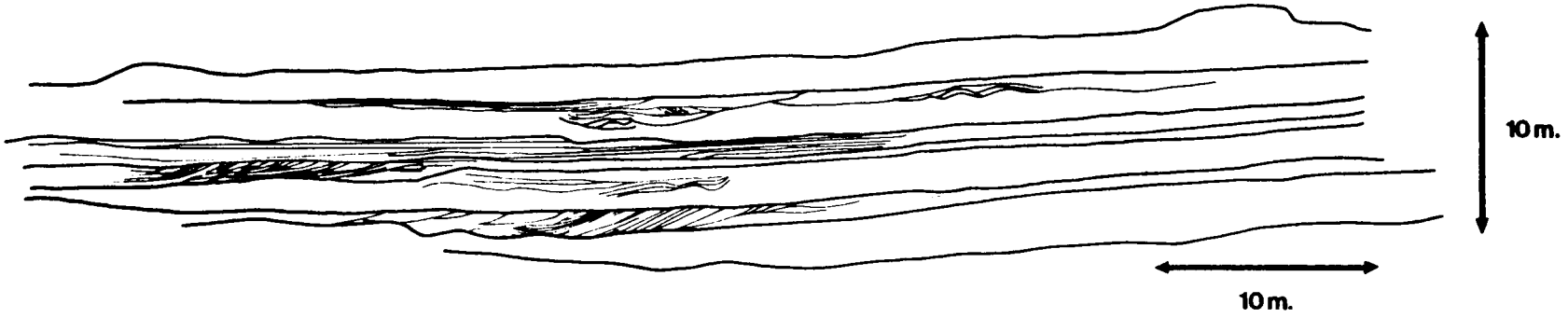

Figure 3

Figure 4. Outcrop 2 sedimentology.

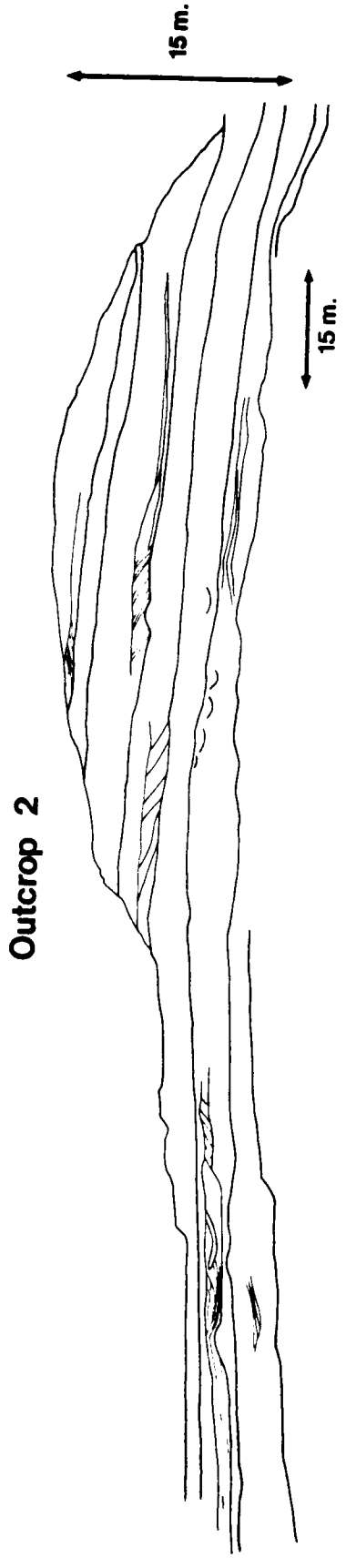

Figure 4

Figure 5. Outcrop 4 sedimentology.

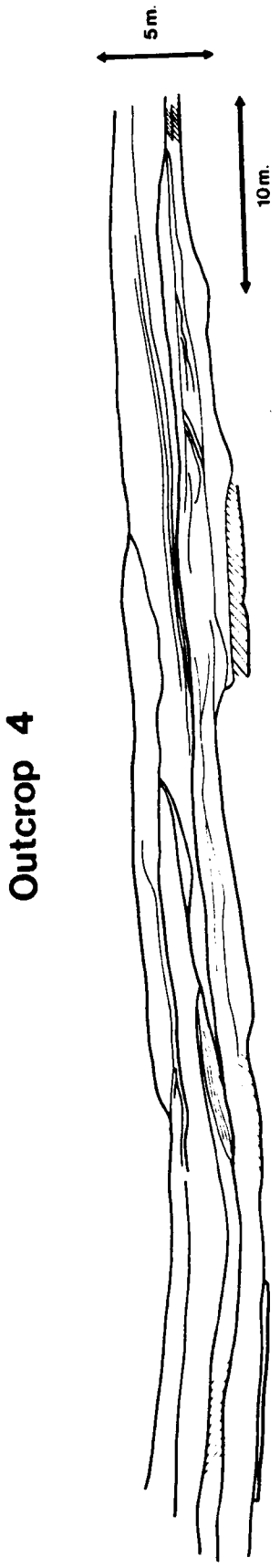

Figure 5

Field Measurements

Each outcrop was measured using a steel tape and/or a Jacob's staff, whichever was appropriate. Measurements were also made at each bedding interval to recheck relationships gathered from the photomosaics.

A plane table and alidade traverse was made between outcrops 1, 2 and outcrop 4 (separated by approximately 770 vertical meters) to determine the amount of section covered by colluvium and vegetation. This also placed outcrops 1 and 2 in a vertical relationship with outcrops 3 and 4. Outcrops 3 and 4 together constitute the entire vertical section. The stratigraphic relationships between each of the four outcrops are diagrammatically shown in Figure 2, p. 10.

Sampling

One hundred eleven hand samples were taken from the four outcrops. Outcrops 1 and 2 were sampled by rappelling to a change in facies or a noticeable change within facies. At this point the orientation was marked on the sample while still part of the rock wall, the sample was broken loose, the sample was then dropped to an individual on the ground and numbered and catalogued with exact sample location. Outcrops 3 and 4 were sampled, where possible, at a facies change or change in lithology. It proved difficult to gather cohesive, workable shale, siltstone and conglomerate samples. Therefore, these lithologies are relatively underrepresented in the petrographic descriptions.

Each hand sample was assigned to a facies based on grain size, lithology and sedimentary structures.

Petrography

Preliminary thin sections were made of seven of the samples to determine whether or not there was sufficient variability between facies and samples over the entire section to warrant extensive thin section work. It was then decided that, although the Clinch Sandstone had been described in the literature as a rather lithologically monotonous formation, there was in fact a great deal of variability over the section. Fifty-nine 27 by 46 mm chips were then cut, vacuum-impregnated with dyed epoxy to retain clays and aid in identification of porosity, mounted and cut to 30 μm-thickness.

Several of the resultant 59 thin sections were scanned to ascertain general characteristics of the rocks. Each was then point counted using a Swift automatic point counter to a total of 300 points. The counting interval was determined for each slide by measuring the diameter of the largest grain occurring on the slide and then using an interval slightly greater than that distance. The slides were counted in a random order without regard to facies, height in section or relationship with other thin sections. This served to keep operator bias from affecting the point-counting procedure. In addition to mineralogic composition, other characteristics were noted for each thin section. Average and range of grain size and average size of pores were estimated using a microscope grain size comparator

(Swanson, 1981). Sedimentary features such as fining-upward sequences were noted as well and sorting and rounding were visually estimated. Variability of rounding with size was also noted when appropriate. Rounding and sorting was estimated using the charts developed by Powers (1953). Textural maturity was determined using Folk's (1974) criteria. Extinction was measured for three representative thin sections and found to be undulatory in >98% of the quartz grains. At this point measurement ceased and undulatory vs. nonundulatory nature was only qualitatively noted. Replacement minerals and those which were replaced were noted, if possible. However, the replaced grain was typically completely obliterated by the secondary mineral and was, therefore, unidentifiable.

Plagioclase composition was determined using the Michel-Levy method (Kerr, 1977). All observed grains cut parallel to (010) were measured on each sample; however, a maximum of six grains was reached on only one slide. This low number leaves questions as to the exact composition of the plagioclase but these measurements aid in narrowing down the possible compositional range and, to some extent, the source region.

Point-count data were then normalized to produce a percentage of total counts for each sample as well as percentage of detrital material. These data are included in Appendix A and Appendix B.

Trace Fossils

Trace fossils were noted, measured and described when found. Photographs were taken when particularly significant or unfamiliar

specimens were discovered. Identification (on the generic level) was made in the laboratory from field sketches, descriptions and photographs.

Paleocurrents

Paleocurrent measurements were taken for 82 unidirectional and 11 bidirectional current indicators. These were cross-beds, channel axes, ripples and oriented Rusophycus. In many cases obliteration due to extensive induration prohibited placement of the Brunton compass directly on foreset planes because only two-dimensional outcrop faces were exposed. In such cases a board was placed co-planar with the trace of the cross-laminations to give a good estimate of cross-bedding strike and dip (Yeakel, 1962). When foreset planes were present but no ledge was available, the board was wedged between foresets to provide an extension of the plane and yield a good estimate for the strike and dip. Other features were measured directly.

Measurements for strike and dip of foresets and bedding were taken and used to restore bedding to horizontal, thus providing original current direction in the form of dip azimuths (Ragan, 1973). Circular histograms were constructed to illustrate the distribution of current directions for different parts of the Formation. Because most of the data were unimodal, a program for vector analysis was employed. The program, ORIENT, developed by Maher and Dott (1979, Univ. of Wisconsin), calculates the mean vector azimuth, variance,

standard deviation, and the magnitude of the resultant vector for a set of data. The paleocurrent data for the Clinch Sandstone are included in Appendix C.

IV. LITHOLOGIC DESCRIPTION

Facies Descriptions

The Clinch Sandstone facies are described separately for the two members due to the historical subdivision that results from their lithologic dissimilarity.

The Hagan Shale Member is composed of three facies: facies A, B, and C. Facies assignments were based primarily on grain size, in addition to bedding characteristics and other sedimentologic features. Overall grain size coarsens upward and bed thickness increases upward as well (Figure 6; Appendix D). The rocks range from olive clay-shales through gray-green siltstones to multi-colored, iron-stained sandstones. When beds display more than one color, the colors are typically mottled.

The most common lithology of the Hagan Shale Member is a very slightly clayey siltstone to very fine-grained sandstone (Facies C). Beds in this facies are <1 to 20 cm thick, typically parallel laminated but also rarely cross-bedded in sets up to 50 cm thick (Figure 7). Cross-bedded sandstones commonly contain Skolithos (Figure 8), whereas horizontal beds show abundant Arthrophycus, Planolites, and Rusophycus on exposed bases. Planolites is also present within beds. Diagrammatic sketches of all trace fossils in the Clinch Sandstone are included in Figure 9; detailed descriptions are covered in Section V.

Figure 6. Facies relationships in Hagan Shale Member.

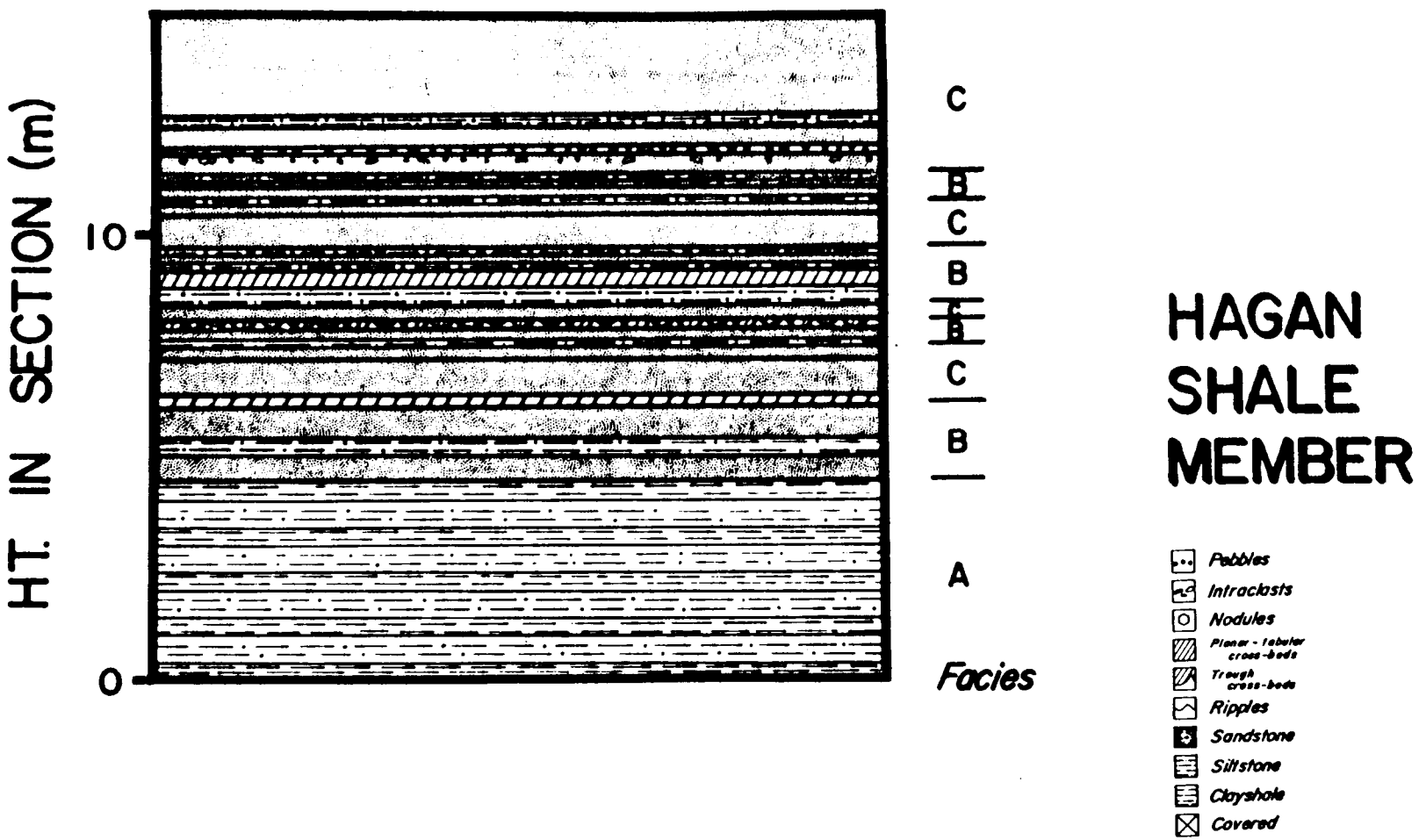
HT. IN SECTION (m)
10
0
C
B
C
B
C
B
A
Facies
HAGAN SHALE MEMBER
Pebbles
Intraclasts
Nodules
Planar - tabular cross-beds
Trough cross-beds
Ripples
Sandstone
Siltstone
Clayshale
Covered

Figure 6

Figure 7. Hagan Shale Member facies C (slightly clayey siltstone to very fine-grained sandstone). White marks on scale indicate 5 cm intervals.

Figure 8. Skolithos in Hagan Shale Member. Centimeter scale is on right. Arrows point to examples.



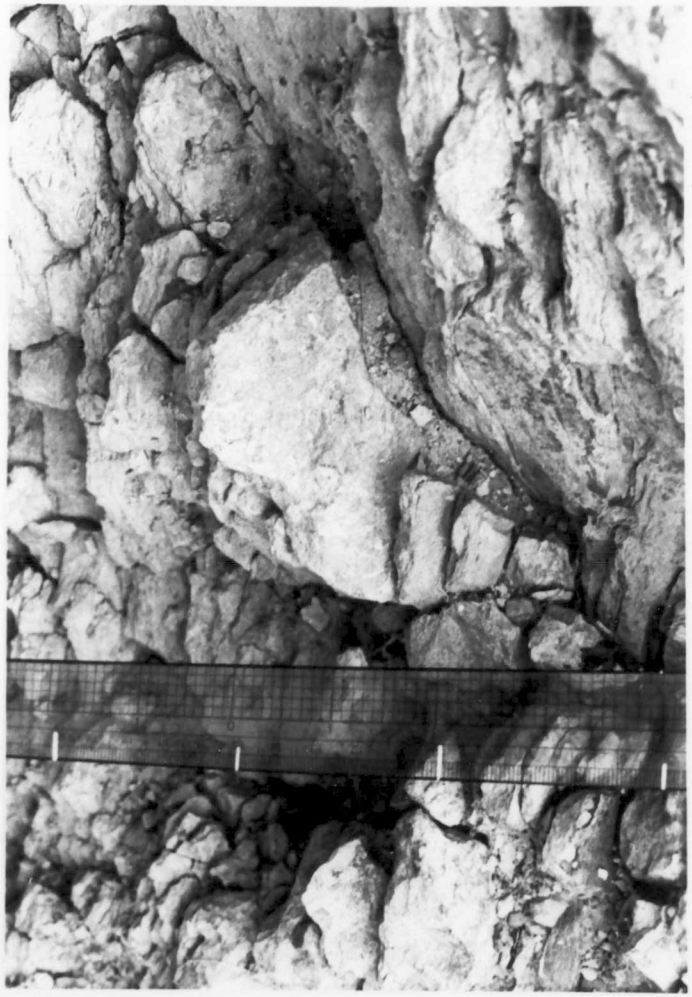

Figure 9. Diagrammatic sketch of all trace fossils found in the Clinch Sandstone at Beans Gap. A = Arenicolites, B = Arthrophycus, C = Chondrites, D = Corophioides, E = Cruziana, F = Diplocraterion, G = Monocraterion, H = Rusophycus, I = Paleophycus, J = Pelecypodichnus, K = Planolites, L = Skolithos type A, M = Skolithos type B, N = Thalassinoides.

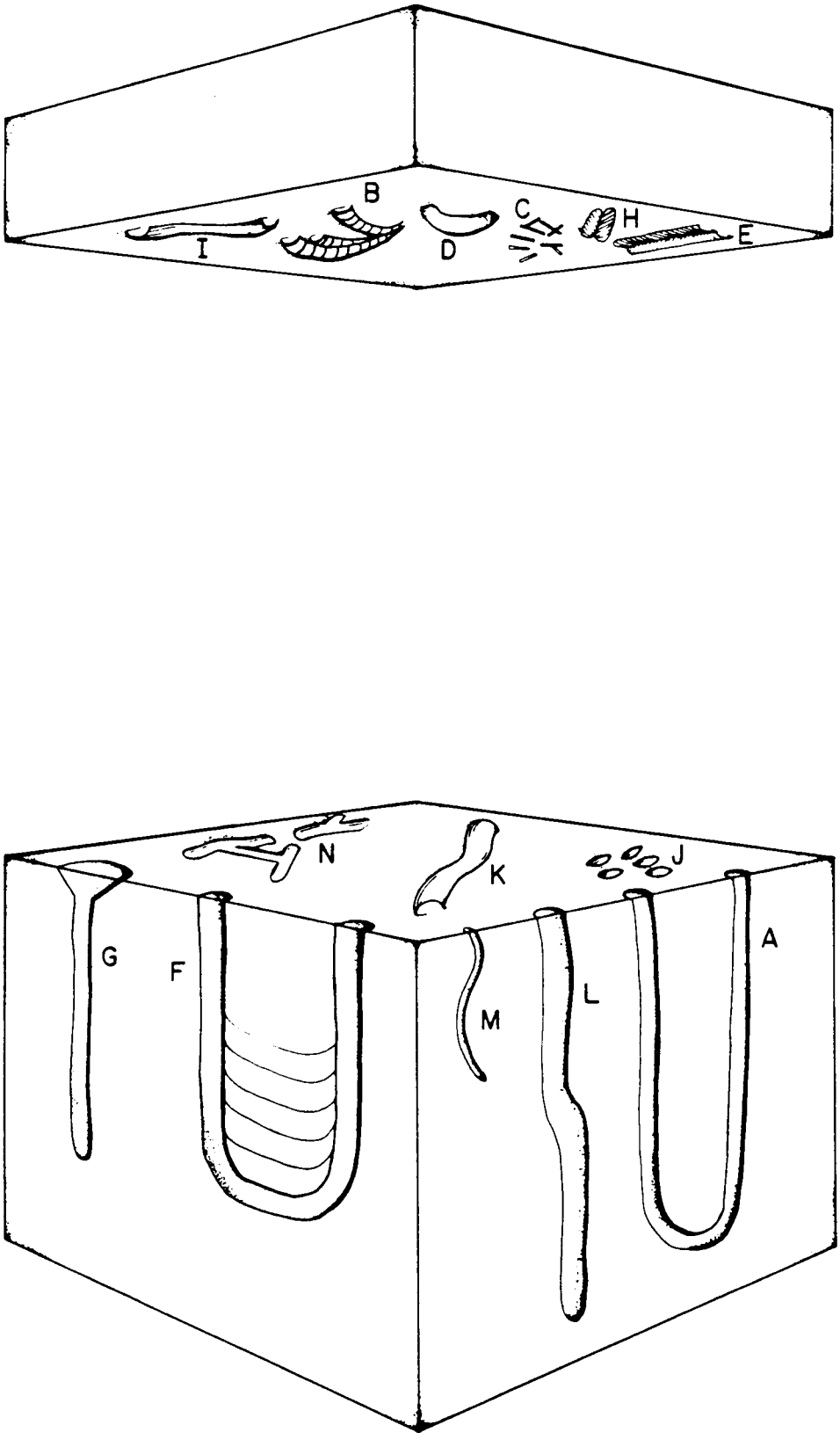

Figure 9

Facies C first occurs in the middle of the Member but is most prevalent towards the top of the unit where it forms medium to thick beds of siltstone and sandstone. Facies C is associated with facies B, typically occurring as moderately thick beds interstratified with facies B.

Facies A is a very slightly silty clayshale, typically interbedded with clayey siltstone (Figure 10). The clayshales are commonly very thinly laminated (2-3 mm). These laminae are devoid of both physical and biogenic sedimentary structures.

Facies A constitutes the lowermost 4.4 m of the yellow-gray to green-gray Hagan Shale Member. The lower contact with the maroon to pale-yellow Juniata Formation is gradational.

Facies B is composed of siltstone and fine sandstone irregularly interbedded with a very slightly silty clayshale (in beds) <1 to 20 cm thick) (Figure 11). This lithology grades upward into dominantly sandy interbeds (2 to 3 cm thick), wavy bedded with clayey siltstone. The sandstones of Facies B rarely exhibit trough cross-stratification and oscillation ripple marks. Facies B commonly contains Skolithos, abundant Monocraterion, an unidentifiable deposit-feeding trace as well as possible Chondrites traces. Planolites may be present on the upper surfaces of beds and Rusophycus on the bases. Intraclasts of deep maroon, Juniata Formation shale-like lithology are present in some of the facies B sandstone beds.

Facies B occurs in the middle portion of the Hagan Shale Member, from approximately 4.4 m to about 9.65 m above the contact

Figure 10. Hagan Shale Member facies A (clayshale). Centimeter scale is on right. Dark lines mark a 10 cm interval.

Figure 11. Hagan Shale Member facies B (interbedded siltstone and sandstone). Ruler is 30.5 cm long.



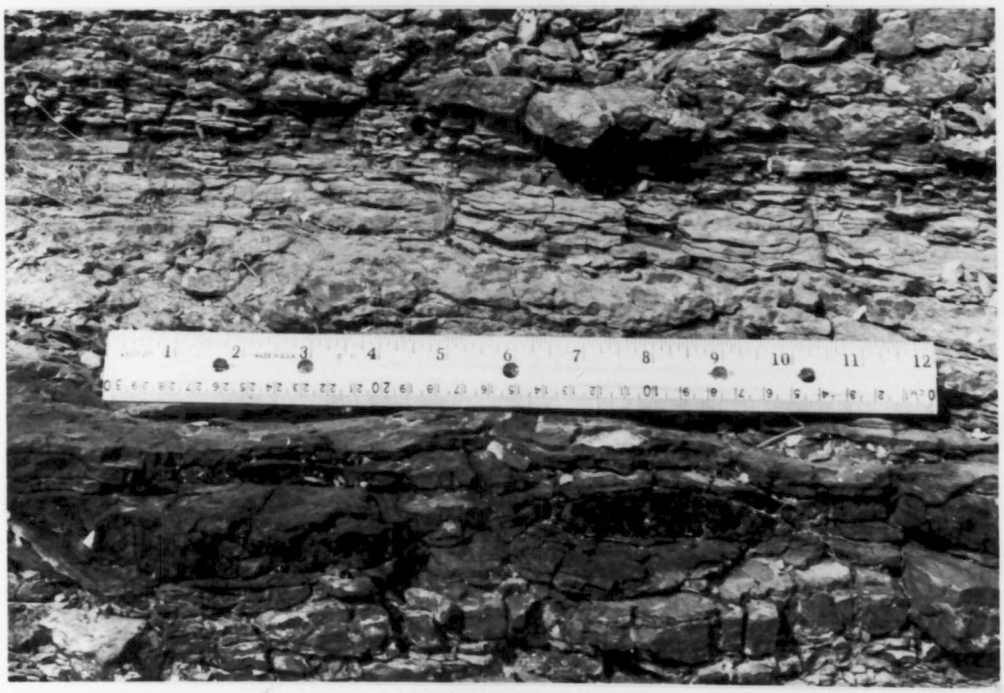

with the Juniata Formation (Figure 6, p. 25). This facies grades upward from the clayshales of Facies A at its lower extent to a conglomeratic unit of Facies C at its upper extent.

The contact between the Poor Valley Ridge Member and the Hagan Shale Member is gradational. At Beans Gap the contact has been placed 14.9 m above the contact between the Clinch Sandstone and the Juniata Formation.

Although five facies have been recognized in the Poor Valley Ridge Member (Driese et al., 1984), only four are present along Route 25E: facies 1, 2, 3, and 4. Overall grain size ranges from silt to pebbles and intraclasts up to 2 cm in diameter. Siltstones are commonly dark gray or gray-green in color. Most sandstone beds are white but can be gray, light gray, very pale brown or olive. Late-stage groundwater percolation (?) has led to irregular iron staining. This staining, if present, masks the original color of the sandstone beds.

Bedding thickness ranges from 3 cm in siltstone to approximately 1 m or more in bioturbated sandstone. Cross-beds are 1 mm to 10 cm thick; sets range from 7 cm up to 2 m.

Facies in the Poor Valley Ridge Member were assigned primarily on the basis of physical sedimentary structures, but also included grain size and trace fossil assemblages.

Facies 1 consists of medium- to large-scale trough cross-beds up to 1 m thick developed in fine- to coarse-grained sandstone. Trough sets consist of centimeter-thick, tangential foreset bundles

separated by mm-thick clay drape laminae that contain Arthrophycus (Figure 12). Small-scale current ripple marks are superimposed on some foreset bed surfaces, and shale intraclasts line the bases of scour surfaces. Individual sets persist laterally over distances up to 20 m.

Facies 2 consists of medium- to very large-scale planar-tabular cross-beds up to 2 m thick developed in medium- to very coarse-grained sandstone (Figure 13). Planar sets are composed of centimeter-thick planar-abrupt foresets, which are commonly separated by reactivation surfaces. Clay drape laminae and trace fossils are rare. A typical vertical sequence consists of a basal large-scale set overlain by smaller sets, which decrease in thickness upward. Winnowed quartz pebble lags are common at the tops of planar sets as are gray shale intraclasts. Individual sets persist laterally over distances of up to 10-20 m.

Facies 3 and 4 most typically do not contain cross-stratification (Figures 14 and 15). Facies 3 consists of massive, densely bioturbated, medium- to coarse-grained sandstone beds up to 3 m thick. Although some bedding planes are preserved, internal stratification is rarely visible (Figure 14). Diplocraterion, with well-developed spreite, Arenicolites and Skolithos tubes are the most abundant trace fossils. Basal surfaces of burrowed beds are horizontal and contain abundant Arthrophycus and Paleophycus. Individual beds persist laterally over distances in excess of 150 m.

Facies 4 consists of thin to medium, horizontally laminated beds of very fine- to medium-grained sandstone, which are

Figure 12. Poor Valley Ridge Member facies 1, between arrows (trough cross-beds). Ruler is 30.5 cm long.

Figure 13. Poor Valley Ridge Member facies 2, between arrows (planar-tabular cross-beds). Black bar represents 20 cm.

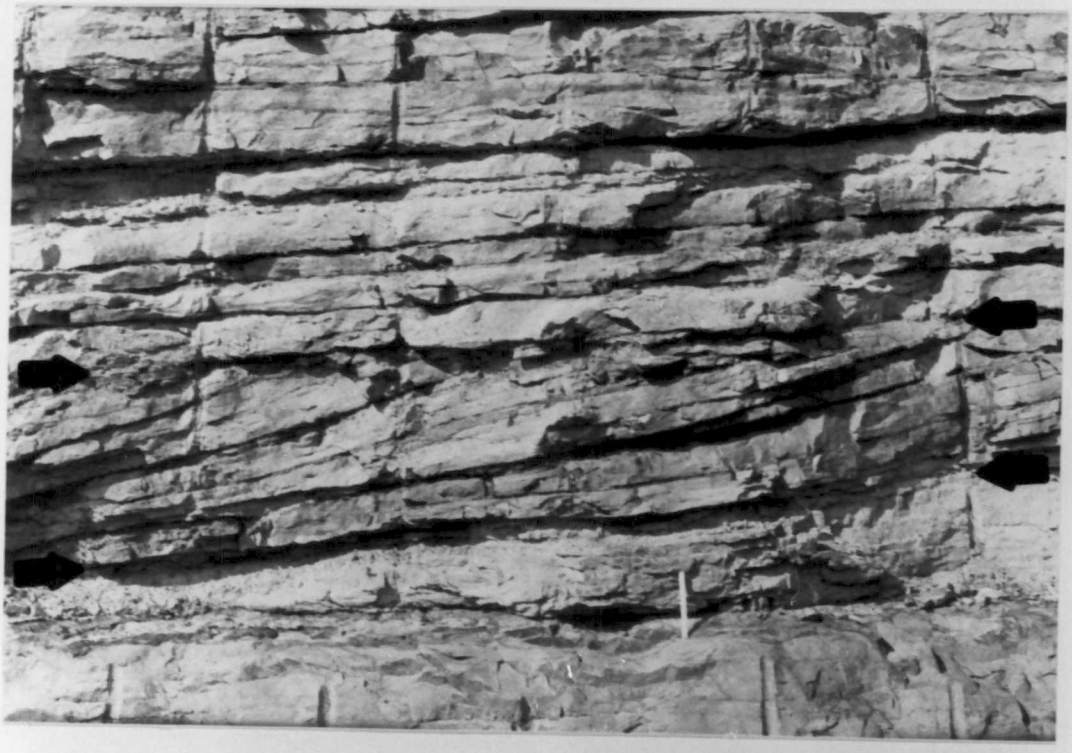



Figure 14. Poor Valley Ridge Member facies 3 (bioturbated beds). Distance between large vertical drillholes is approximately 90-100 cm.

Figure 15. Poor Valley Ridge Member facies 4 (horizontally laminated beds). Shown above dashed line. Ruler on cross-bedded unit is 30.5 cm long.

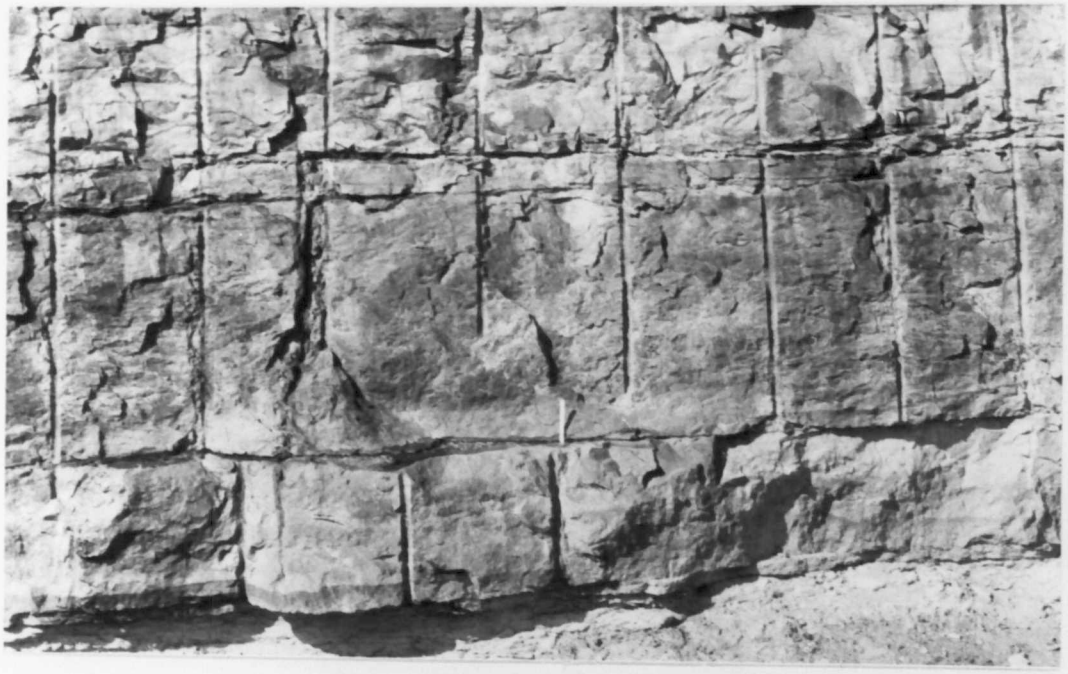

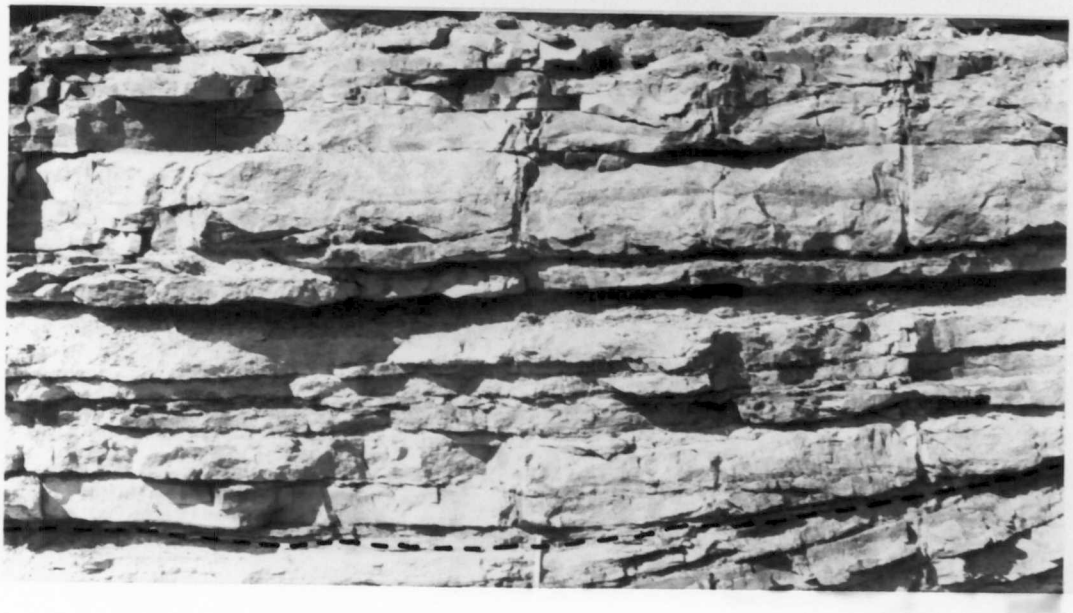

interstratified with centimeter-thick, gray-green shales and ripple cross-laminated sandstones (Figure 15). The bases of most sandstone beds contain abundant Arthrophycus and Paleophycus and rare Rusophycus and Cruziana trace fossils. Individual beds persist laterally up to 20 m. Rare conglomeratic layers can be found within Facies 4 laminated sandstone beds.

Facies 3 and facies 4 are associated with very rare dish structures. These features are only visible in outcrop 2 (Figure 4, p. 15) and range in size from 1 to 2 m wide and average approximately 0.5 m high. Dish structures form during the gradual consolidation of rapidly deposited sediment but provide no significant depositional environmental interpretations (Lowe and LoPiccolo, 1974).

Facies Relationships

The Hagan Shale Member exhibits an overall upward-coarsening trend, and the three facies recognized follow this vertical trend. The three Hagan Shale Member facies are diagrammatically shown in Figure 6, p. 25. The finest-grained facies (A) occurs at the base of the Member. It is overlain by facies B, interbedded siltstone, sandstone and clayshale, which is in turn overlain by the coarser siltstone to sandstone beds of facies C.

Lateral continuity of each Hagan Shale Member facies is much greater than that of the Poor Valley Ridge Member facies. Beds commonly persist for more than 20 m. Nonetheless, the character of the lower Member does not remain completely constant, exhibiting lateral changes in grain size, lithology and ichnology.

Figures 16, 17 and 18 illustrate the major relationships between the four Poor Valley Ridge Member facies at three of the outcrops along Route 25E. Burrowed units (Facies 3) may extend laterally for more than 150 m (e.g., bed B-1 in Figures 16 and 17) whereas most cross-bedded units are limited in lateral extent to only 25-50 m and many are quite limited (as little as 1.5 m horizontally). Laminated beds (Facies 4) are variable, averaging about 20 m in lateral extent.

As a result of this lateral variability only a generalized stratigraphic column can be created for the Clinch Sandstone (Figure 19). Several important aspects, however, can be noted in the stratigraphic column. In outcrops 3 and 4 (the two which combine to compose the entire column), burrowed facies 3 shows up as the dominant facies in the lower 15 m of the Formation. Towards the middle of the unit facies 4 horizontal beds become dominant and include a 2.46 m thick sandy siltstone unlike any other unit in the Poor Valley Ridge Member. This finer-grained, thinly bedded, otherwise structureless unit resembles facies C of the Hagan Shale Member. It is characterized by bedding that thins upward, is light gray colored and weathers to yellowish brown. Comparatively, the coarsest units in the Poor Valley Ridge Member are medium- to coarse-grained sandstones, which commonly show pebble stringers. These stringers are uneven and are not associated with scour or channel surfaces. Commonly the pebbly areas also include pebble-sized clayshale intraclasts. These intraclasts are typically gray or light pink-maroon. Light pink-maroon beds, similar to these intraclasts, are present in

Figure 16. Facies relationships in outcrop 1. Outcrop averages 10 m high.

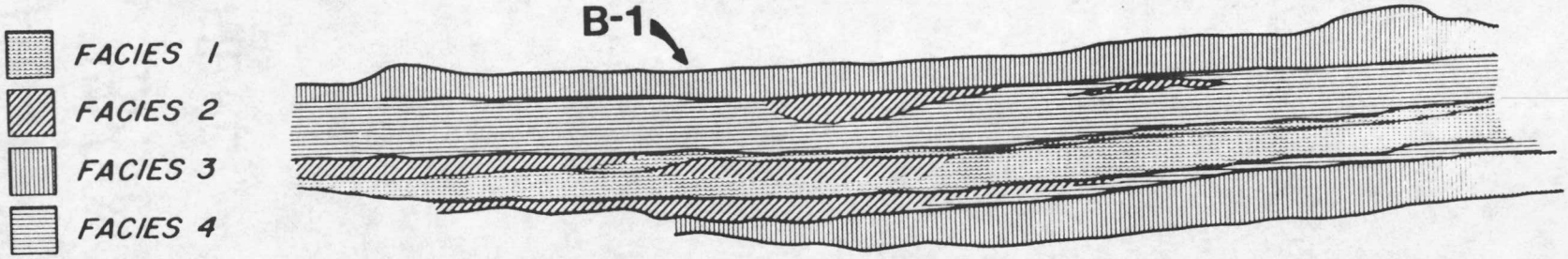

Figure 16

Figure 17. Facies relationships in outcrop 2. Outcrop averages 15 m high. Same legend as Figure 16.

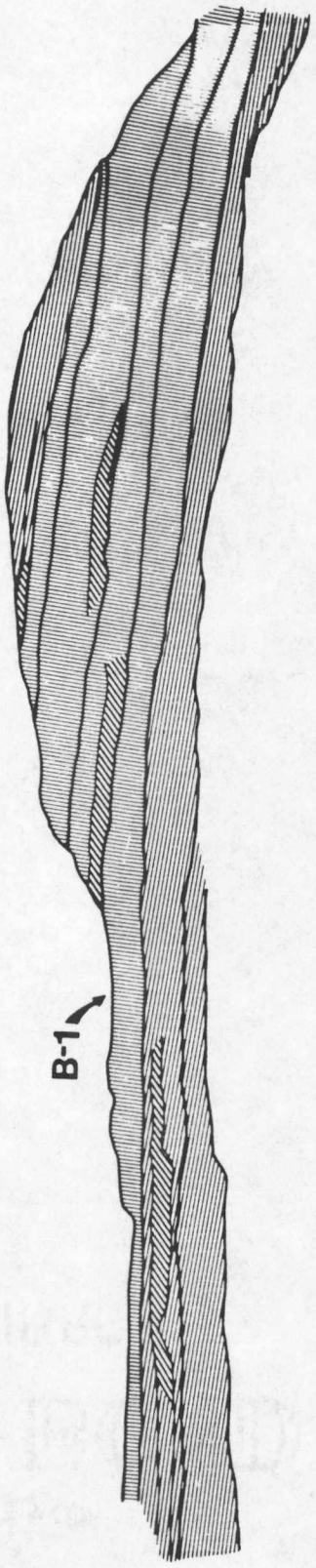

Figure 17

Figure 18. Facies relationships in outcrop 4. Outcrop averages 5 m high. Same legend as Figure 16.

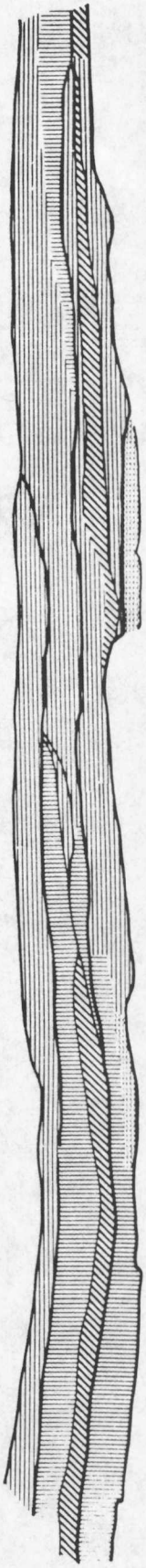

Figure 18

Figure 19. Generalized stratigraphic column for Clinch Sandstone at Beans Gap.

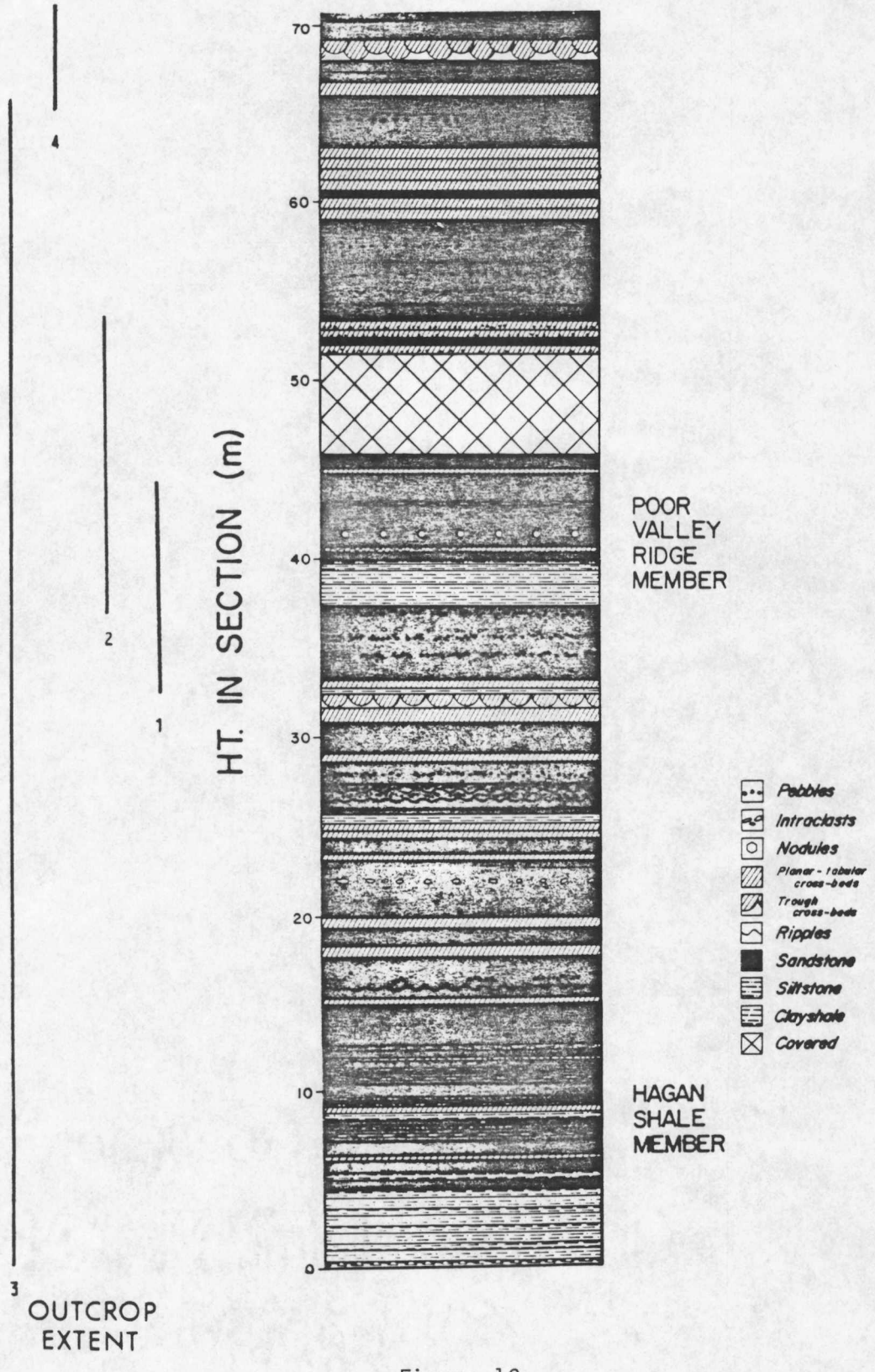
4
2
1
3
OUTCROP EXTENT
HT. IN SECTION (m)
70
60
50
40
30
20
10
0
POOR VALLEY RIDGE MEMBER
HAGAN SHALE MEMBER
Pebbles
Intraclasts
Nodules
Planar - tabular cross-beds
Trough cross-beds
Ripples
Sandstone
Siltstone
Clayshale
Covered

Figure 19

the very lowest 8.2 m of the Poor Valley Ridge Member. Both the light pink-maroon intraclasts and beds resemble the maroon beds of the Juniata Formation, though they are lighter in color. The paler nature of the Poor Valley Ridge Member intraclasts and beds may represent a Juniata-like lithology diluted with a higher quartz sand content. Coarse sand and pebbles apparently occur randomly, but are most common in facies 3 bioturbated beds and facies 4 horizontally laminated beds. In one bed near the top of the Member coarse sand and pebbles are present in a localized fining-upward sequence. Also more prevalent in the upper part of the member are planar-tabular cross-beds. The planar-tabular cross-beds rarely contain pebbles, whereas trough cross-beds, which are less abundant and more evenly distributed, are more homogeneous in grain size and almost never contain coarse sand or pebbles. Oscillation ripples, however, are commonly associated with pebble stringers. Oscillation ripples, though rare, are distributed throughout the Member.

In order to study the vertical pattern of facies (facies sequences) in the Poor Valley Ridge Member, the number of transitions between each of the four facies were noted and tabulated for the most vertically continuous section, outcrops 3 and 4. Thirty-five transitions were noted, and recorded in an observed frequency matrix (Table 2). An expected frequency matrix was then constructed by using:

$$Ei_j = \frac{n_j}{N - ni} \times ni$$

Table 2. Observed Frequency Matrix.

Overlying Facies / Underlying Facies	Trough Cross-Beds	Planar-Tabular Cross-Beds	Bioturbated Beds	Horizontally Laminated Beds	Total
Trough cross-beds	-	0	1	2	3
Planar-tabular cross-beds	1	-	6	7	14
Bioturbated beds	0	5	-	3	8
Horiz. laminated beds	2	7	1	-	10
Total	3	12	8	12	35

where n_j = the number of transitions involving the underlying facies, ni = the number of transitions involving the overlying facies and N = the total number of transitions (Table 3). The two matrices were compared and a difference matrix was generated (Table 4). Positive values indicated transition frequencies more common than would be expected if the facies were randomly stacked and negative values, the opposite (Walker, 1979). However, this technique is not statistically valid because it ignores the fact that facies transitions in which a facies succeeds itself are undefined and/or not recognized (Selley, 1970; Carr, 1982). Nonetheless, it does allow a rough ordering of facies. Although a statistically valid procedure has been proposed by Carr (1982), it was not used in this study because the total number of noted facies transitions was so low.

The difference matrix shows a complex possible ordering (Figure 20) in which facies 1 trough cross-stratified beds are most commonly overlain by facies 3 burrowed beds and facies 4 horizontally laminated beds. Facies 2 planar-tabular cross-beds are most commonly overlain by facies 3 burrowed beds, which are, in turn, also overlain by facies 2 beds. Facies 4 is overlain by facies 2 and facies 1 most commonly. One set of transitions may denote a high-energy path including upper flow-regime flat beds whereas the other may indicate lower energy, which allowed more bioturbation.

Horizontal relationships are more difficult to ascertain in the Poor Valley Ridge Member. Lateral facies changes seem random in most instances, though predictable patterns of environment shifts

Table 3. Expected Frequency Matrix.

Overlying Facies / Underlying Facies	Trough Cross-Beds	Planar-Tabular Cross-Beds	Bioturbated Beds	Horizontally Laminated Beds
Trough cross-beds	-	1.12	.75	1.12
Planar-tabular cross-beds	2	-	5.33	8
Bioturbated beds	.88	3.55	-	3.55
Horiz. laminated beds	1.2	4.8	3.2	-

Table 4. Difference Matrix.

Overlying Facies / Underlying Facies	Trough Cross-Beds	Planar-Tabular Cross-Beds	Bioturbated Beds	Horizontally Laminated Beds
Trough cross-beds	-	-1.88	.08	1.29
Planar-tabular cross-beds	-.07	-	.38	-.07
Bioturbated beds	-.11	.18	-	-.07
Horiz. laminated beds	.08	.22	-.22	-

Figure 20. Facies transitions which occur more often than expected under random depositional conditions (constructed from Tables 2, 3 and 4).

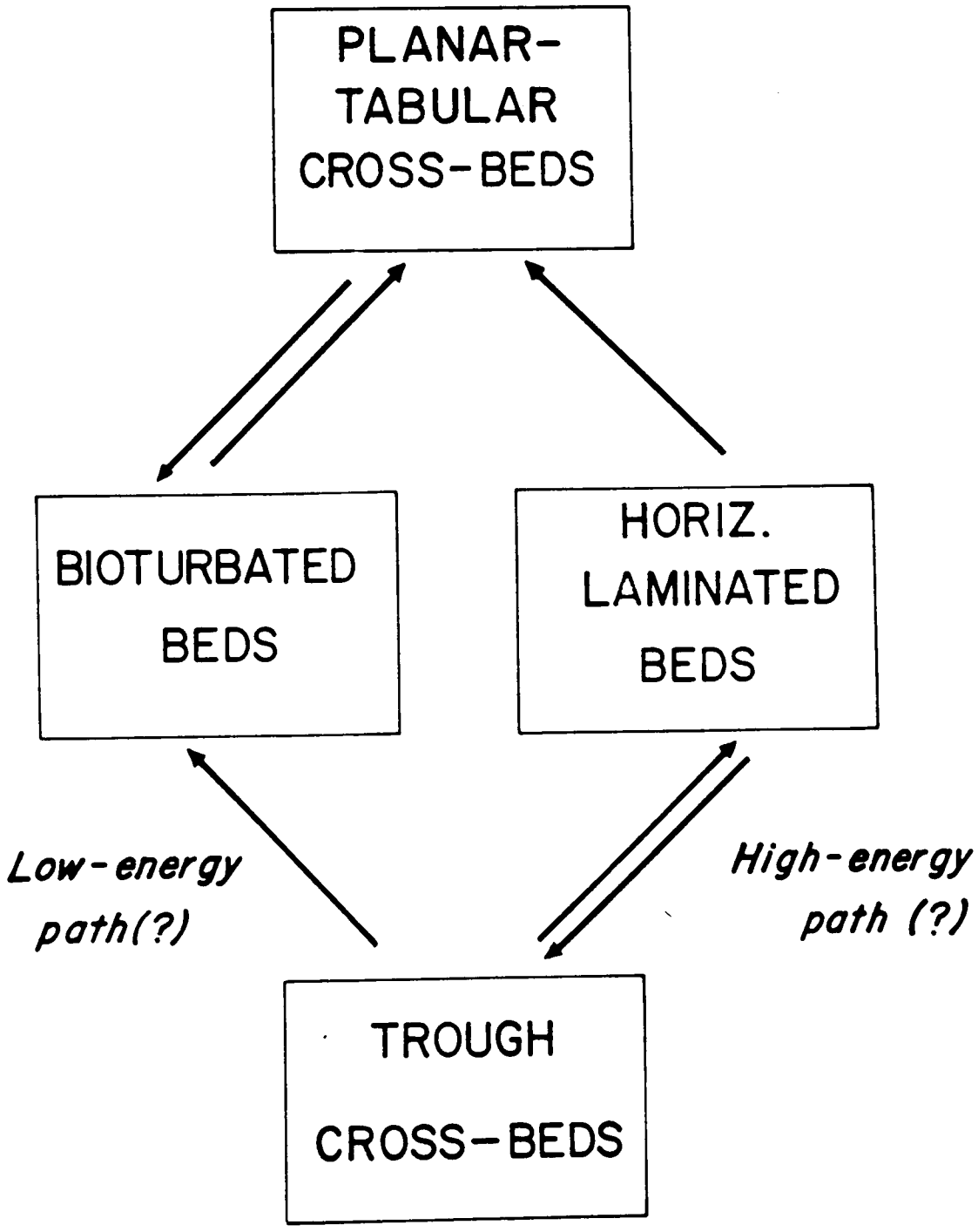
PLANAR-
TABULAR
CROSS-BEDS
BIOTURBATED
BEDS
HORIZ.
LAMINATED
BEDS
Low-energy
path(?)
High-energy
path (?)
TROUGH
CROSS-BEDS

Figure 20

over time are rarely recognized. In such instances, a limited area of one particular sedimentary structure is overlain by a different structure but a nearby area of the original structure is now present in the overlying bed. Both outcrops 1 and 2 show excellent examples of this oblique relationship in the displacement over time of cross-bedded units (Figure 21).

Outcrop 4, as well as outcrops 1 and 2, is sufficiently laterally extensive that several horizontal relationships can be examined. In outcrop 1, facies 2 planar-tabular cross-beds grade laterally into facies 4 horizontally laminated beds or into facies 1 trough cross-beds (Figure 16, p. 42). Because facies 3 is the most laterally extensive, it cannot be easily related to any other facies horizontally. In outcrop 2 the most common lateral transition is from facies 2 to facies 4 (Figure 16), as in outcrop 1. Conversely, though, in outcrop 2, facies 2 planar-tabular cross-beds commonly grade horizontally into burrowed facies 3 beds. Outcrop 4 is even more complex, exhibiting its most common lateral transition between facies 3 and facies 4 (Figure 18, p. 46). Facies 4 also grades into facies 1 and 2. Facies 2 is also horizontally related to facies 3. Outcrop 4 exhibits all possible lateral transitions except those which include facies 1 (which is uncommon in outcrop 4).

The complexity and randomness of the lateral facies relationships is without modern analog. In few instances do they relate logically as would two expected adjacent depositional environments.

Figure 21. Photograph and tracing showing lateral facies shift in immediately overlying beds. From the base of the photograph to the top of the outcrop (center) is approximately 10 m.

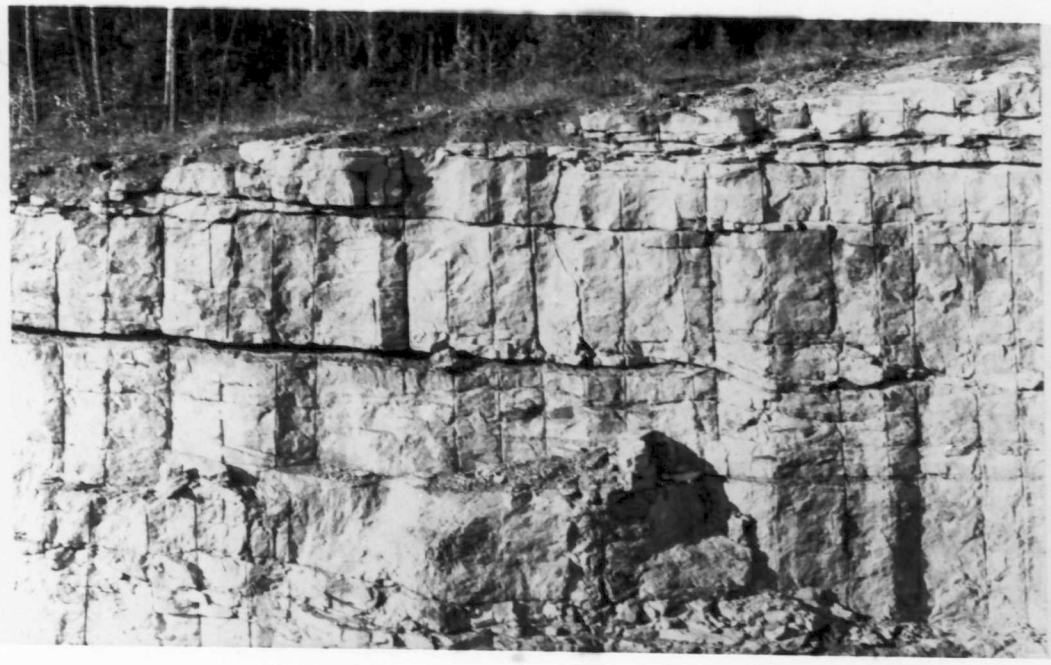

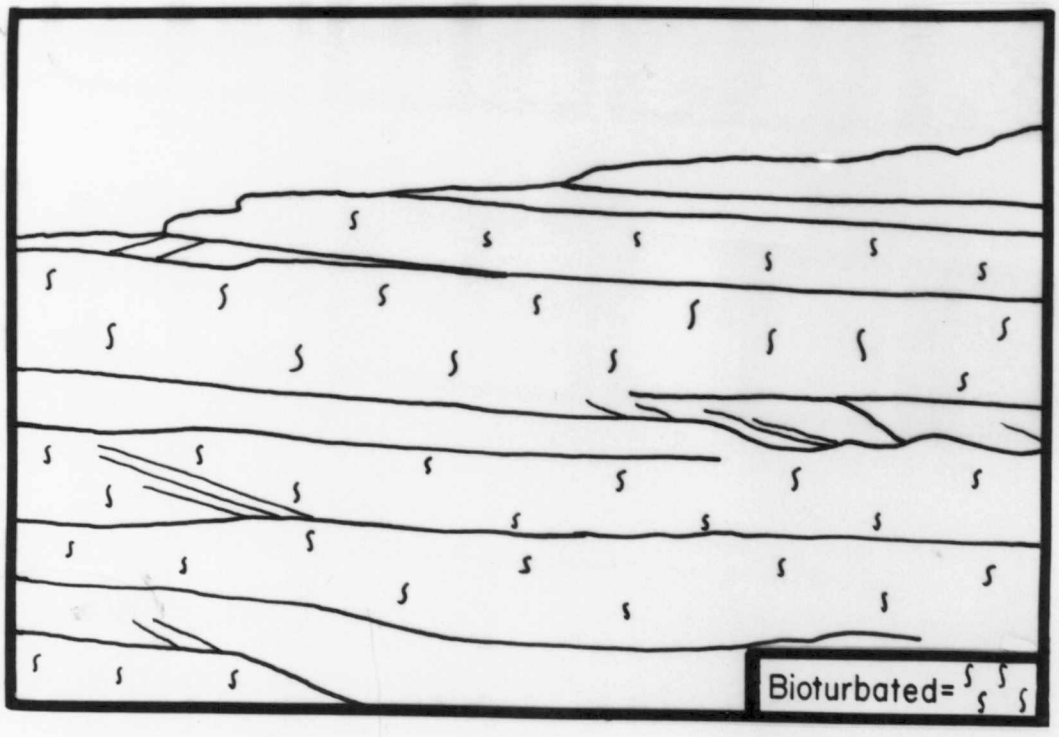
Bioturbated=

Petrographic Description

The 7 samples of the Hagan Shale Member and 50 samples of the Poor Valley Ridge Member were point-counted to a total of 300 points per slide. Each point count was then tabulated to determine percentages of total slide constituents (Appendix A). Detrital components were normalized to obtain original depositional percentages (Appendix B). Table 5 shows the average quantity for each mineral, its standard deviation, range and the samples which exhibit the maxima and minima.

Monocrystalline quartz was, by a significant margin, the dominant mineral (Figure 22). Second in dominance were the ubiquitous quartz overgrowths (Figure 23).

Illite-sericite was present in 31 of the 50 Poor Valley Ridge Member samples and 6 of the 7 Hagan Shale Member samples (Figure 24). Illite and sericite have been grouped together because distinguishing between the two minerals under a normal light microscope is only possible by measuring the length of each crystal. Individual crystal resolution was not possible so no attempt at distinguishing between the two minerals was made. Illite-sericite is concentrated toward the base of the Poor Valley Ridge Member and in the Hagan Shale Member. Other irresolvable fine-grained phyllosilicates present in the Clinch Sandstone are the amorphous iron oxide-clay aggregates (Figure 25). These minerals are so fine-grained that they do not produce peaks on x-ray analysis. In this study, when an amorphous, rust-colored mass was encountered it was counted as amorphous iron oxide-clay aggregates.

Table 5. Means, Standard Deviations, Ranges and Occurrences for All Minerals in the Clinch Sandstone.

Part 1

Mineral	$\bar{X}$	s	Range	Occurrence
Monocrystalline quartz	82.9%	8.54%	47% to 93	(sample 3-3 from Hagan facies C, 38.2 m above contact with Juniata) (sample 1/7-4, Poor Valley Ridge [PVR] facies 3, 44.5 m above the contact)
Quartz overgrowths	5.9	3.8	<1 to 21	(sample C-3 from Hagan facies B, 9.4 m above contact) (sample 2/5-2, PVR facies 1, 42.6 m above contact)
Illite/ sericite	2.35	3.25	<1 to 40	(12 samples) (sample 3-13, PVR facies 4, 38.2 m above the contact)
Amorphous iron oxide/clay aggregates	2.2	3.14	0 to 13	(10 samples) (samples 3-4, Hagan facies C, 11.4 m above the contact, and 1/6-2b, PVR facies 1, 43.9 m above the contact)
Polycrystalline quartz	1.3	1.68	0 to 8	(16 samples) (sample 4-2, PVR facies 2, 66.4 m above the contact)
Kaolinite/ dickite	0.75	0.72	0 to 4	(4 samples) (sample A-5, PVR facies 2, 62.4 m above the contact)
Smectite	0.67	1.06	0 to 6	(31 samples) (sample C-1, Hagan facies A, 3.7 m above the base)
Muscovite	∿0.23	∿0.32	0 to <1 to 1	(36 samples) (21 samples)

Table 5 (continued)

Part 1 (continued)

Mineral	$\bar{X}$	s	Range	Occurrence
Chlorite	∿0.17	∿0.46	0 to 3	(43 samples) (sample 2/7-2, PVR facies 3, 44.1 m above the contact)
Plagioclase	∿0.12	∿0.43	0 to 3	(48 samples) (sample C-1, Hagan facies A, 3.7 m above the contact)
Biotite	∿0.09	-	0 to 1	(37 samples) (sample 3-2, Hagan facies B, 7.7 m above the contact)
Chert	∿0.08	-	0 to <1	(50 samples) (5 samples)
Microcline	∿0.07	-	0 to 1	(52 samples) (sample 3-1, Hagan facies B, 7.4 m above the contact)
Rock Fragments	-	-	0 to 5	(56 samples) (sample 3-3 Hagan facies C, 11.4 m above the contact)
SRF's				
MRF's	-	-	0 to <1	(55 samples) (samples 3-10, PVR facies 3, 30.4 m above the contact and 3-11, PVR facies 4, 35.9 m above the contact)
Fossil Fragments		-	0 to <1	(56 samples) (sample 3-3 Hagan facies C, 11.4 m above the contact)

Table 5 (continued)

Part 2

Heavy Minerals and Opaques Present	No. of Samples (All Quantities = <1%)
Tourmaline	39
Zircon	37
Hornblende	22
Garnet	4
Rutile	1
Sphene	1
?Apatite	1
?Epidote	1
?Hematite	4
?Pyrite	3
?Magnetite	2

Figure 22. Stratigraphic distribution of monocrystalline quartz. Legend for all facies symbols: open star = facies A; closed square = facies B; open square = facies C; open triangle = facies 1; closed triangle = facies 2; closed circle = facies 3; open circle = facies 4.

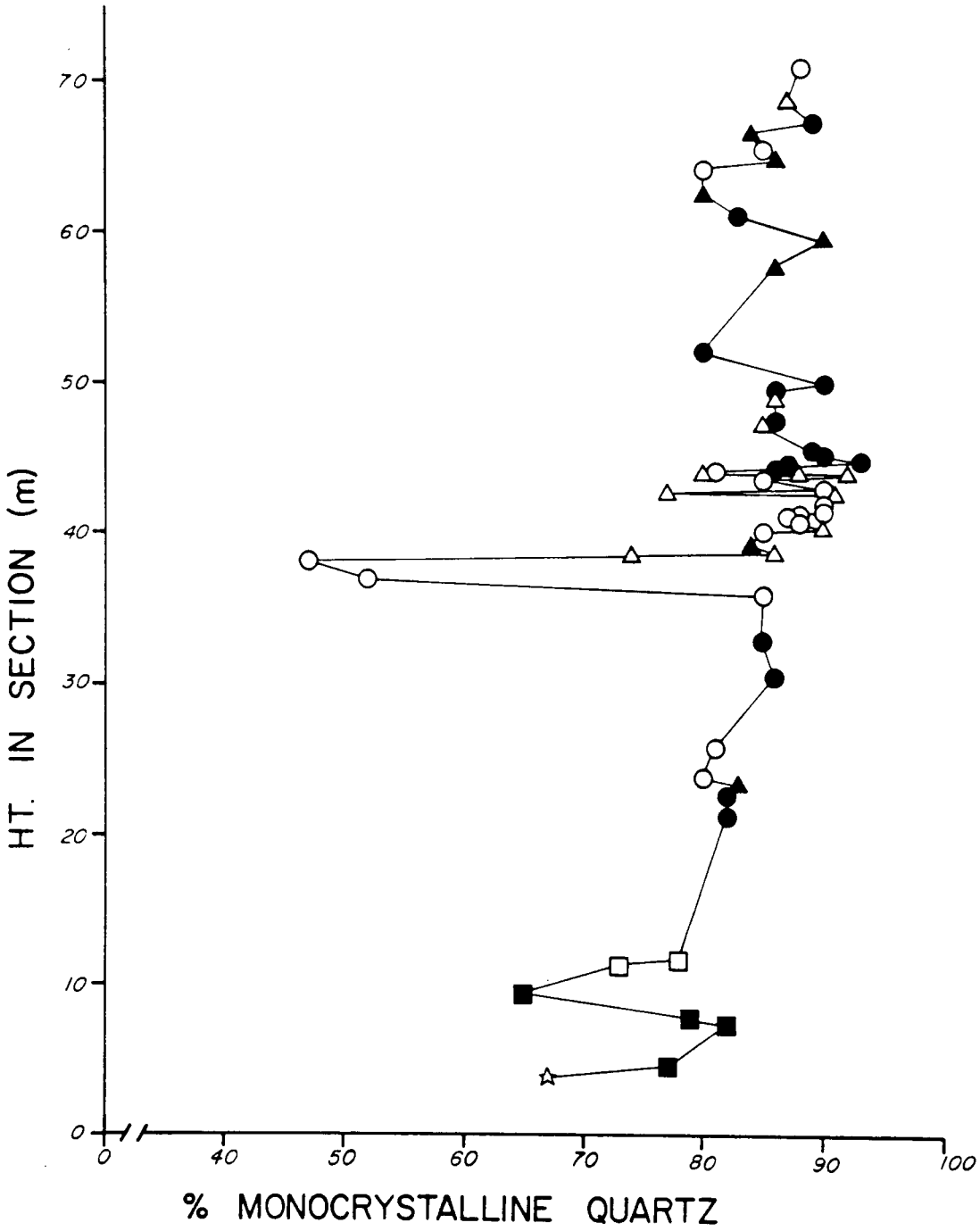
HT. IN SECTION (m)
0
10
20
30
40
50
60
70
0
40
50
60
70
80
90
100
% MONOCRYSTALLINE QUARTZ

Figure 22

Figure 23. Stratigraphic distribution of quartz overgrowths (using 0.5 for all values between 0 and 1).

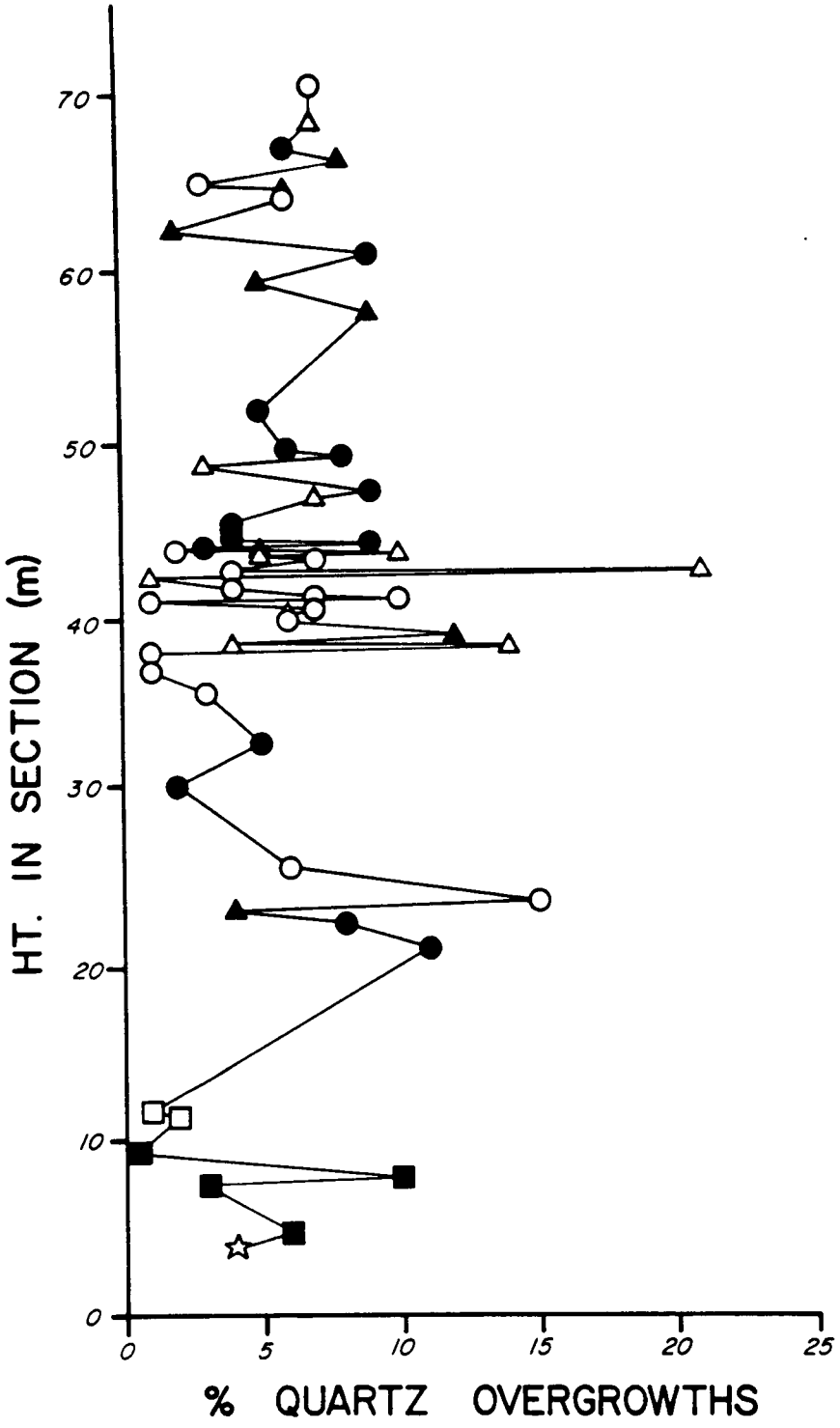
70
60
50
40
30
20
10
0
HT. IN SECTION (m)
0
5
10
15
20
25
% QUARTZ OVERGROWTHS

Figure 23

Figure 24. Stratigraphic distribution of illite/sericite.

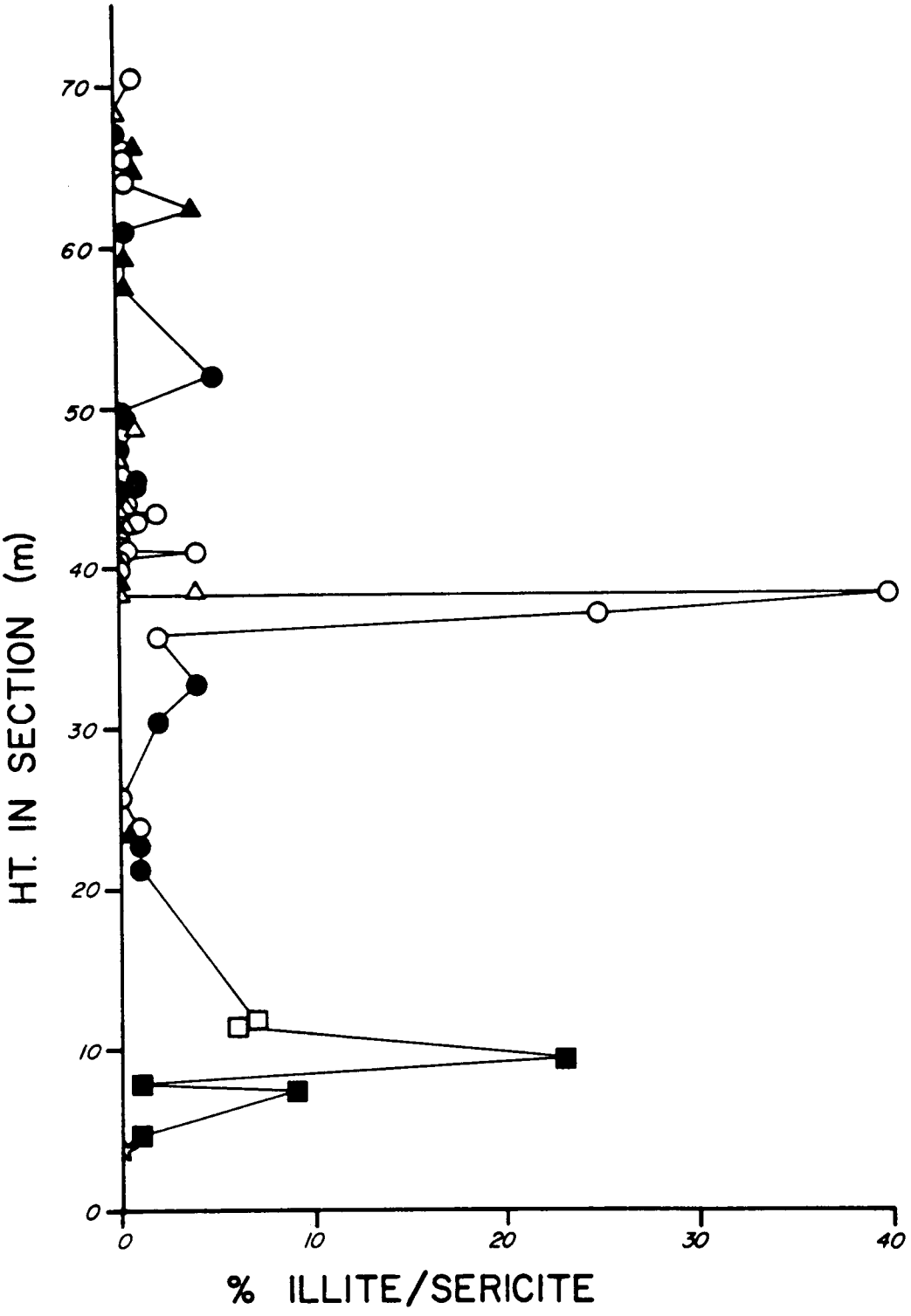
HT. IN SECTION (m)
70
60
50
40
30
20
10
0
0
10
20
30
40
% ILLITE/SERICITE

Figure 24

Figure 25. Stratigraphic distribution of amorphous iron oxide/clay aggregates.

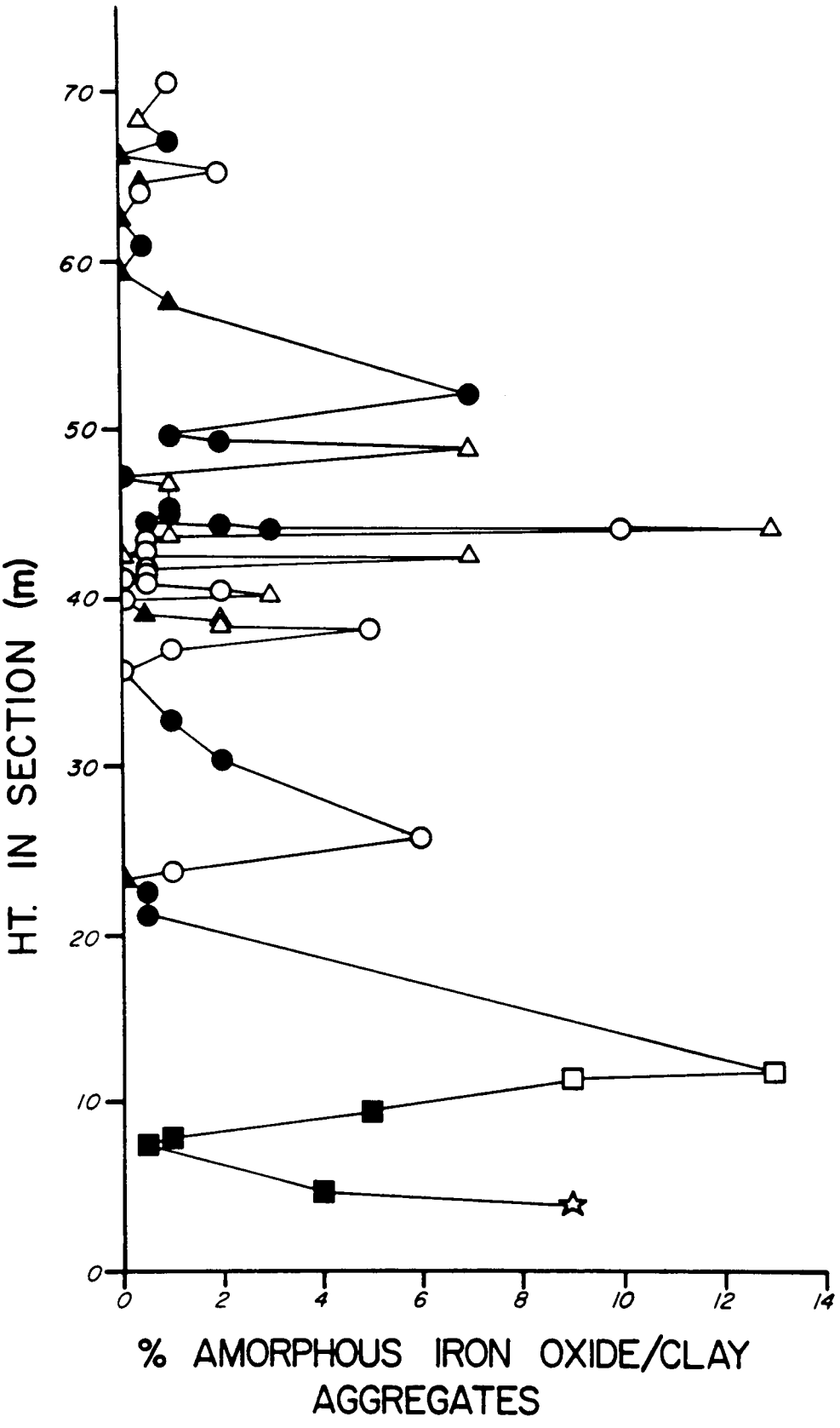
HT. IN SECTION (m)
0
10
20
30
40
50
60
70
0
2
4
6
8
10
12
14
% AMORPHOUS IRON OXIDE/CLAY AGGREGATES

Figure 25

Next most predominant mineral species after amorphous iron oxide-clay aggregates was polycrystalline quartz (Figure 26).

Following in abundance, yet occurring in relatively small amounts, are kaolinite and dickite (Figure 27) which are almost ubiquitous in the Clinch Sandstone. These two minerals are also difficult to petrographically resolve. When well-crystallized, kaolinite shows classic "book-like" morphology but more often than not, these two white to gray, low birefringent, fine-grained clays were only moderately well crystallized, and therefore were counted together. The distribution for kaolinite-dickite is slightly concentrated toward a maximum in the middle of the stratigraphic column.

Smectite is also present in the Clinch Sandstone (Figure 28). It is a fine-grained phyllosilicate, distinguishable from those listed previously by its high birefringence and its low relief (n<balsam). Smectite occurred in 26 of the 57 samples over most of the section but was most common in outcrop 2, Poor Valley Ridge Member samples.

Minerals with overall means of less than 0.5% are not graphed (see Appendix A for their point-count percentages and Table 5 for their means and ranges). Muscovite, biotite and chlorite, the other phyllosilicates present, occur in both Hagan Shale Member and Poor Valley Ridge Member rocks.

Plagioclase occurs in three Poor Valley Ridge Member samples and in all but one of the seven Hagan Shale Member samples. Michel-Levy measurements were made on satisfactory grains cut parallel to

Figure 26. Stratigraphic distribution of polycrystalline quartz.

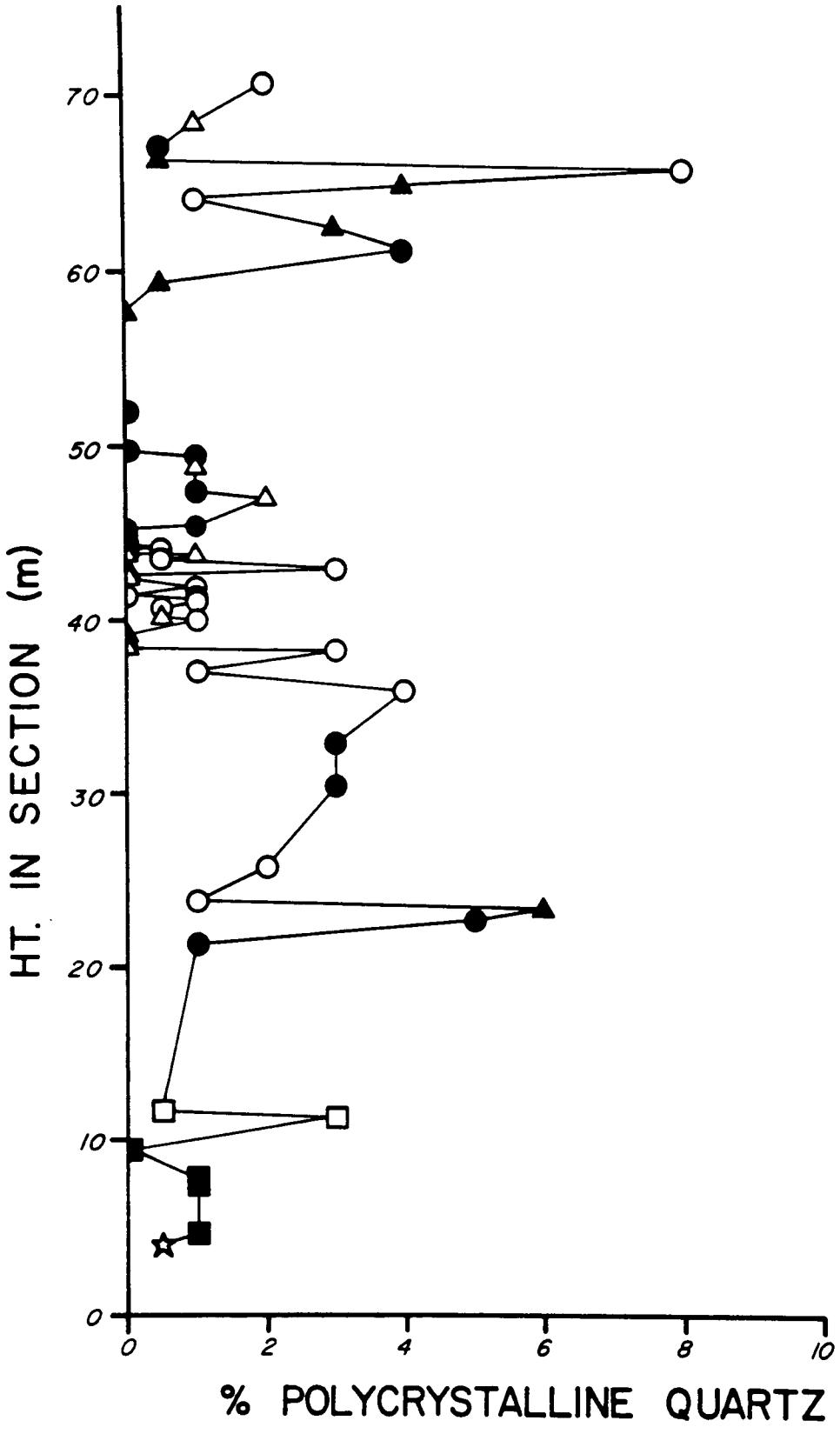
HT. IN SECTION (m)
0
10
20
30
40
50
60
70
0
2
4
6
8
10
% POLYCRYSTALLINE QUARTZ

Figure 26

Figure 27. Stratigraphic distribution of kaolinite/dickite.

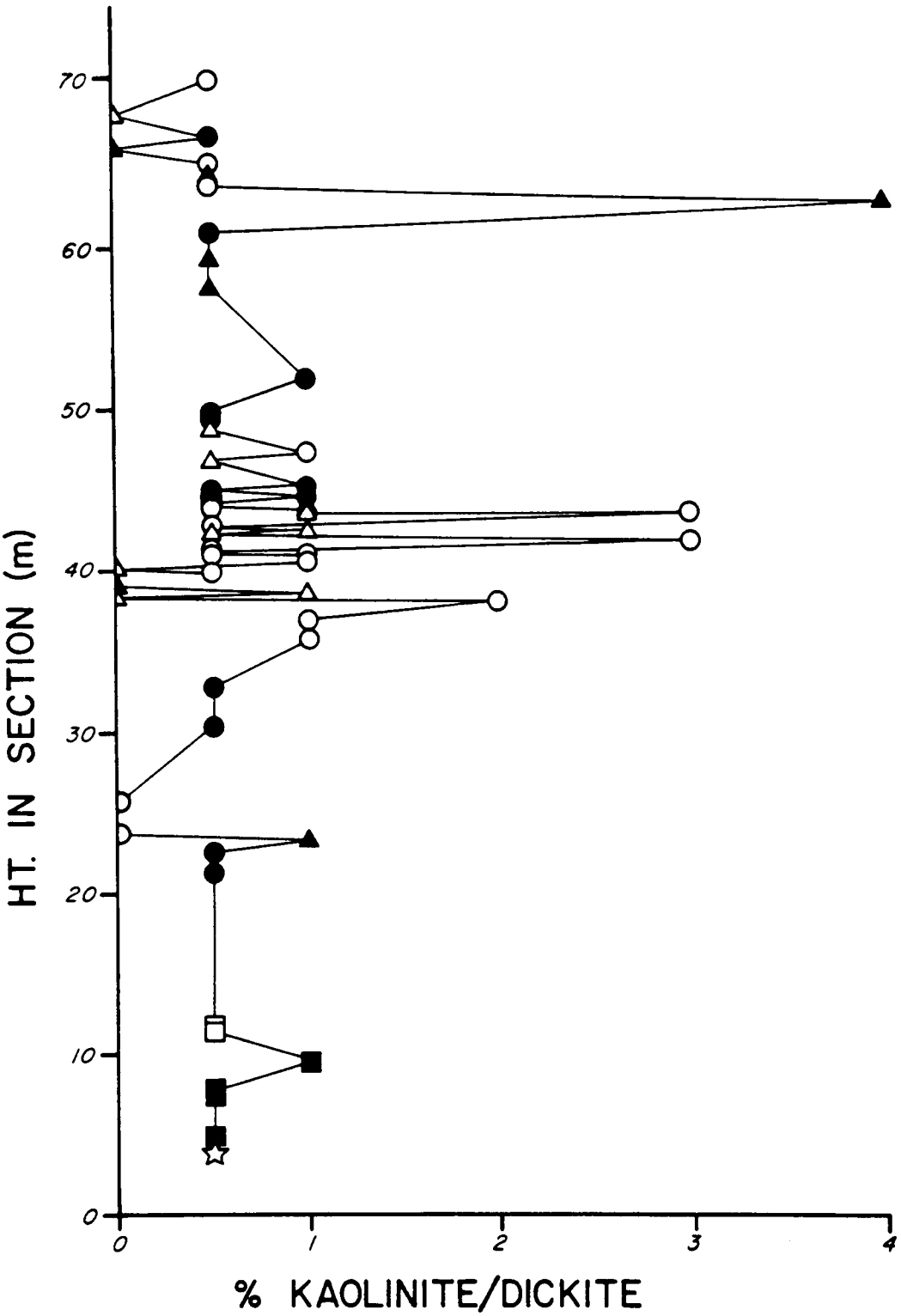

Figure 27

Figure 28. Stratigraphic distribution of smectite.

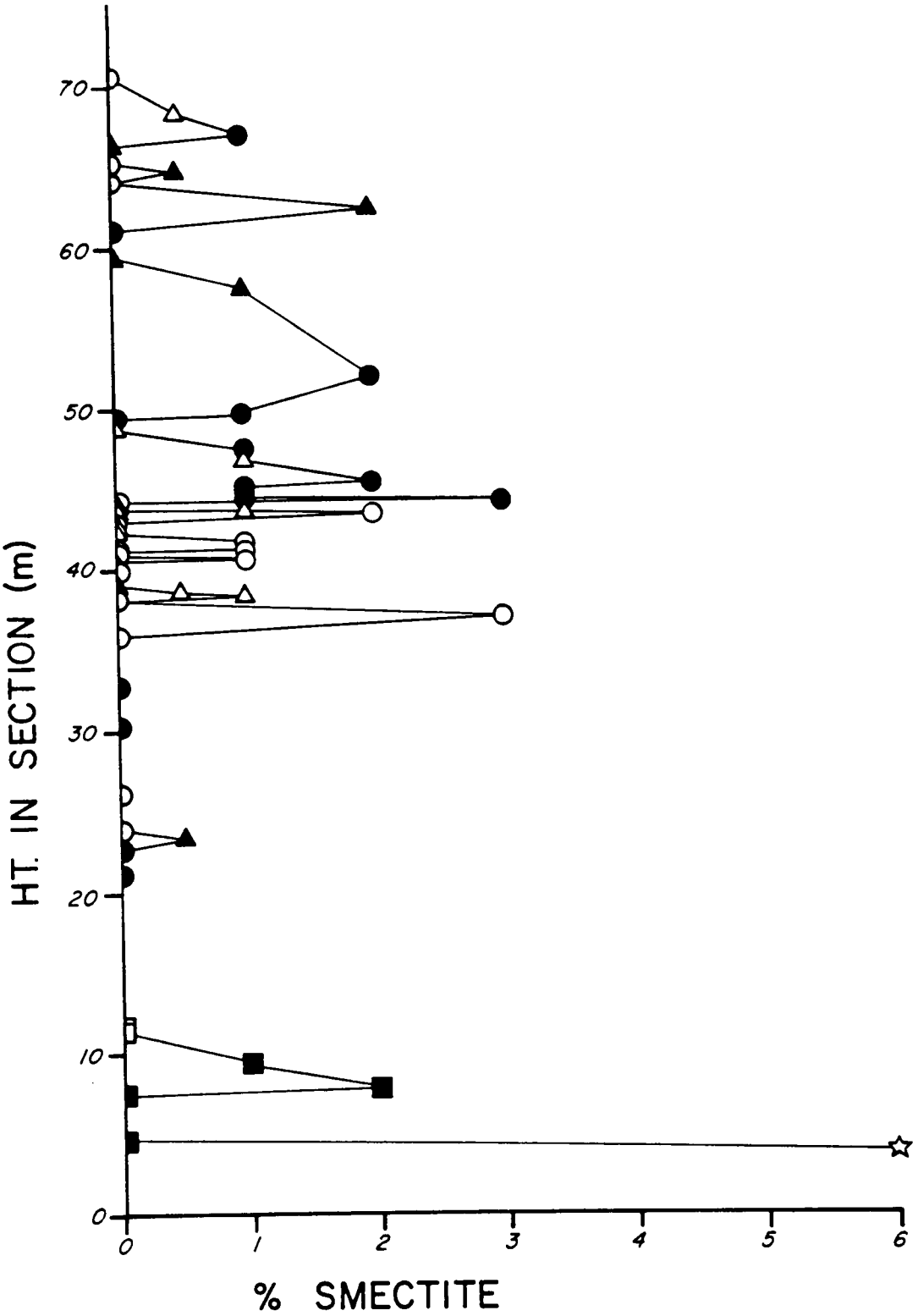

Figure 28

(010) (never enough to make this a valid determination of composition). These results suggested that andesine and oligoclase are the plagioclase species present in the Clinch Sandstone.

Biotite, though rate, was slightly concentrated toward the bottom of the stratigraphic column. Chert, difficult to distinguish from polycrystalline quartz, occurred only once higher than 30 m above the base of the Formation. Microcline occurred in all but 2 of the 7 Hagan Shale Member samples but only occurred in the lower 12 m of the section.

There is quite an extensive suite of heavy minerals present in the Clinch Sandstone on Clinch Mountain. Twelve heavy minerals are present in quantities of <1 to 1%. Tourmaline is the most widespread and is concentrated in the middle of the stratigraphic column. Zircon is also quite common in occurrence. Hornblende is third in abundance among heavy minerals. Garnet, ?epidote, ?apatite, rutile, and sphene are less common. Among opaque minerals ?hematite, ?pyrite, and ?magnetite are present but rare. These opaque mineral identifications are tentative because they were determined without the use of polished thin sections and reflected light.

In addition to these previously listed minerals, rock fragments (both sedimentary and metamorphic) are present in 3 of the lower Clinch Sandstone samples. The conglomerate, located 11.4 m above the contact with the Juniata Formation, contains 5% sedimentary rock fragments, specifically siltstone fragments. This sample is also the only one that contains body fossils. Two phosphatic brachiopod

fragments, either of the order Lingulida or Acrotretida (Clarkson, 1979) (both inarticulate brachiopods of the Lower Silurian) were identified in the conglomeratic sample. Two other samples from the lower Poor Valley Ridge Member contain rock fragments. Each contains <1% metamorphic rock fragments, in the form of foliated quartz aggregates.

Mineral Associations

Though a total of 25 mineral species were found in thin section, only seven will be presented here for analysis of trends and mineral-to-facies relationships. These are the minerals that average more than 0.5% in every sample. In order of decreasing abundance they are monocrystalline quartz, quartz overgrowths, illite-sericite, amorphous iron oxide-clay aggregates, polycrystalline quartz, kaolinite-dickite, and smectite.

The relationships that exist between minerals have been assessed on the basis of mineral pairs. Frequency distribution graphs depicting mineral quantities for the section have been compared and the relationships described. In the case of parallel trends for the two minerals, the relationship is described as positive (Figure 29). Where trends are opposite (as one increases, the other decreases), the relationship is considered negative (Figure 29). If parallel trends exist but they are separated by a some unknown period of time (represented as rock) then the minerals in question may have a postponed effect on each other. This

Figure 29. Classification for visual comparison of point-counted constituents and properties.

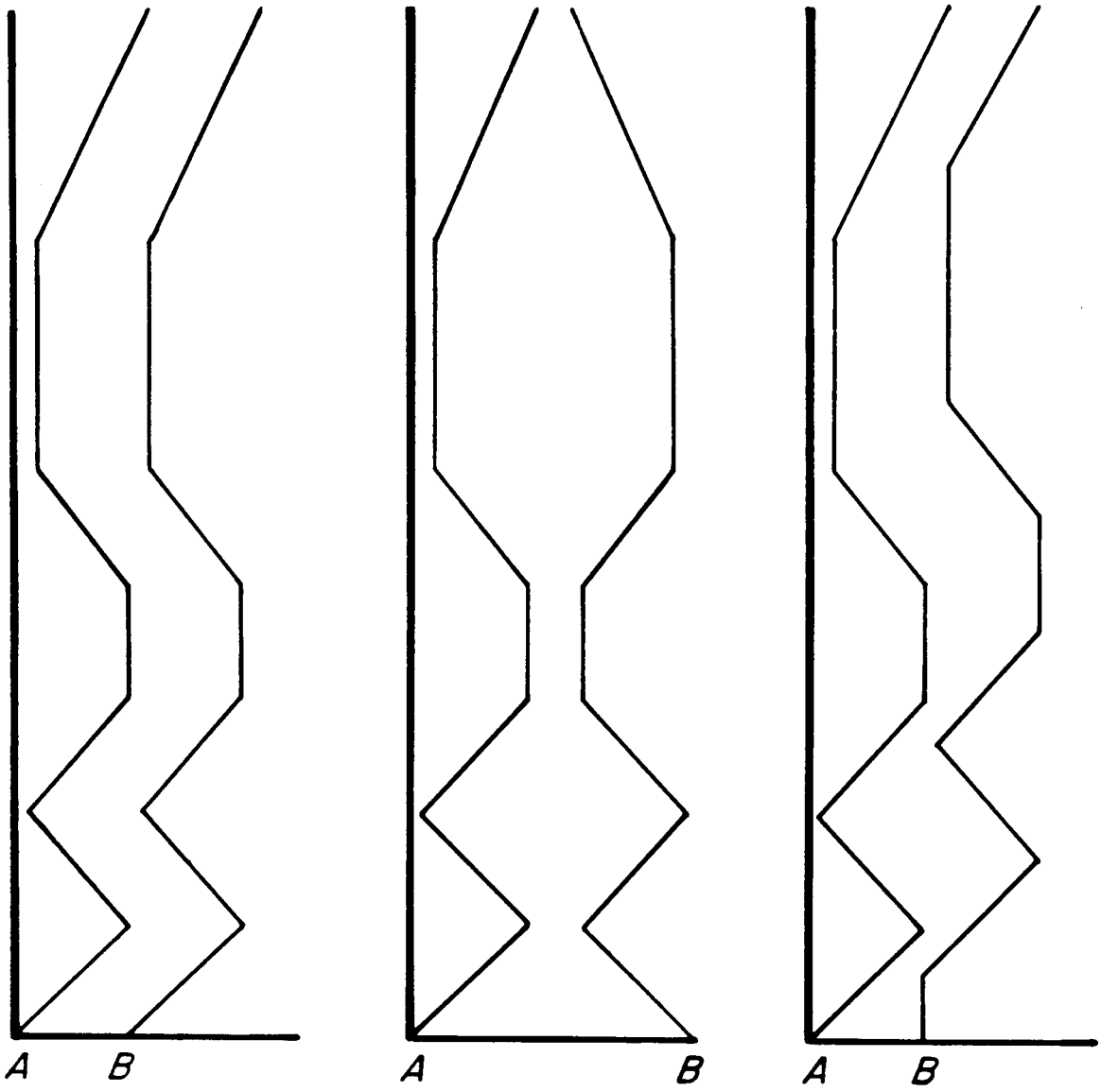

Figure 29

relationship is referred to as offset (Figure 29). These relationship relationships have been confirmed using correlation coefficients with a significance probability of $\alpha = 0.05$. This aids in evaluating the "offset" relationships as well as supporting positive and negative associations. Visual comparisons are shown in Table 6 and statistical tabulations in Table 7. The 95% significance level serves to eliminate several of the visually evaluated positive and negative relationships but did not prove any relationships valid that already had not been so interpreted.

Monocrystalline quartz, the dominant mineral in the Clinch Sandstone, shows a slight increasing frequency up section that coincides with decreasing variability. The texturally less mature Hagan Shale Member samples show less quartz, as would be expected. The Hagan Shale Member averages 74.4% monocrystalline quartz per sample with $\sigma = 6.37$, whereas the Poor Valley Ridge Member averages 84.1%, with $\sigma = 8.17$. This illustrates the upward increasing trend in compositional maturity that coincides with an overall increasing trend in textural maturity. Monocrystalline quartz content for each facies can be seen in Figure 22, p. 64, and the data are summarized in Table 8. Each of the Hagan Shale Member facies shows less monocrystalline quartz than the Poor Valley Ridge facies. Monocrystalline quartz content roughly follows the trend of textural maturity (Figure 30), further implying that compositional maturity is directly related to textural maturity in the Clinch Sandstone. Monocrystalline quartz also shows a direct correlation with grain size (Figure 31); as grain size increases, monocrystalline quartz content increases.

Table 6. Visually Estimated Correlations Between Constituents and Properties.

	Monocrystalline Quartz*	Quartz Overgrowths	Illite/ Sericite	Amorphous Iron Oxide/Clay Aggregates	Polycrystalline Quartz	Kaolinite/ Dickite	Smectite	Porosity	Textural Maturity	Rounding
Quartz overgrowths	NO									
Illite/ sericite	-	-								
Amorphous iron oxide/clay aggregates	-	-	NO							
Polycrystalline quartz	NO	-	+/-	NO						
Kaolinite/ dickite	-	NO	+	NO	NO					
Smectite	NO	NO	NO	+/o	NO	+				
Porosity	NO	NO	-	-	NO	+	o			
Textural maturity	+	+	NO	-	+	+	+	NO		
Rounding	NO	NO	NO	NO	NO	NO	NO	NO	NO	
Sorting	NO	NO	NO	NO	NO	NO/-	-/NO	+/-	+	NO

*+ Symbolizes a positive relationship

- Symbolizes a negative relationship.

NO Symbolizes no relationship discerned.

o Symbolizes an offset relationship.

x/x Symbolizes different relationships in the top part of the section and in the bottom part.

Table 7. Calculated Correlation Coefficients (r) Using $\alpha = 0.05$ to Determine Significance.

	Monocrystalline Quartz*	Quartz Overgrowths[a]	Illite/ Sericite	Amorphous Iron Oxide/Clay Aggregates	Polycrystalline Quartz	Kaolinite/ Dickite	Smectite
Quartz overgrowths	NO r = 0.138						
Illite/ sericite	- r = -0.817	- r = -0.380					
Amorphous iron oxide/clay aggregates	- r = -0.32	- r = -0.375	- r = 0.165				
Polycrystalline quartz	NO r = -0.08	NO r = -0.206	NO r = 0.060	NO r = -0.164			
Kaolinite/ dickite	NO r = -0.130	NO r = -0.253	NO r = 0.259	NO r = -0.106	NO r = 0.075		
Smectite	NO r = -0.25	NO r = -0.137	NO r = 0.063	NO r = 0.076	NO r = 0.226	NO r = 0.247	
Porosity	- r = -0.440	NO r = -0.109	NO r = 0.152	NO r = -0.086	NO r = 0.052	NO r = -0.186	NO r = 0.224

[a]Using 0.5 for all values between 0 and 1.

*NO symbolizes no statistically significant relationship. - Symbolizes a negative relationship.

Table 8. Ranges of Constituents and Properties for Each Facies.

	Hagan Shale Member			Poor Valley Ridge Member			
	A	B	C	1	2	3	4
Monocrystalline quartz	67%	65 - 82%	73 - 78%	74 - 92%	80 - 90%	80 - 93%	47 - 90%
Quartz overgrowths	4	<1 - 10	1 - 2	1 - 21	2 - 12	2 - 11	1 - 15
Illite/ sericite	0	1 - 23	6 - 7	0 - 4	0 - 4	0 - 5	0 - 40
Amorphous iron oxide/clay aggregates	9	<1 - 5	9 - 13	0 - 13	0 - 1	0 - 7	0 - 10
Polycrystalline quartz	<1	0 - 1	<1 - 3	0 - 2	0 - 6	0 - 5	0 - 8
Kaolinite/ dickite	<1	<1	<1	0 - 1	0 - 4	<1 - 1	0 - 3
Smectite	6	0 - 2	0 - 2	0 - 1	0 - 2	0 - 3	0 - 3
Rounding[a]	SR to R	SR to R	SA-R to R	SR-R to W	SR-R to R-W	SR-R to W	SA to R-W
Sorting[b]	W	P-M to W-VW	P-M to M	P to VW	P-M to W-VW	P to VW	P-M to W-VW
Textural maturity[c]	SM	IM to SUPM	IM	IM to SUPM	SM-M to SUPM	IM to M-SUPM	IM to SUPM
Porosity	10%	4 - 11%	1%	1 - 8%	3 - 7%	0 - 5%	0 - 16%
Number of samples	1	4	2	11	7	15	17

[a] SA = subangular; SR = subrounded, R = rounded; W = well-rounded.

[b] P = poorly sorted; M = moderately sorted; W = well-sorted; VW = very well-sorted.

[c] IM = immature; SM = submature; M = mature; SUPM = supermature.

Figure 30. Stratigraphic variation in textural maturity.

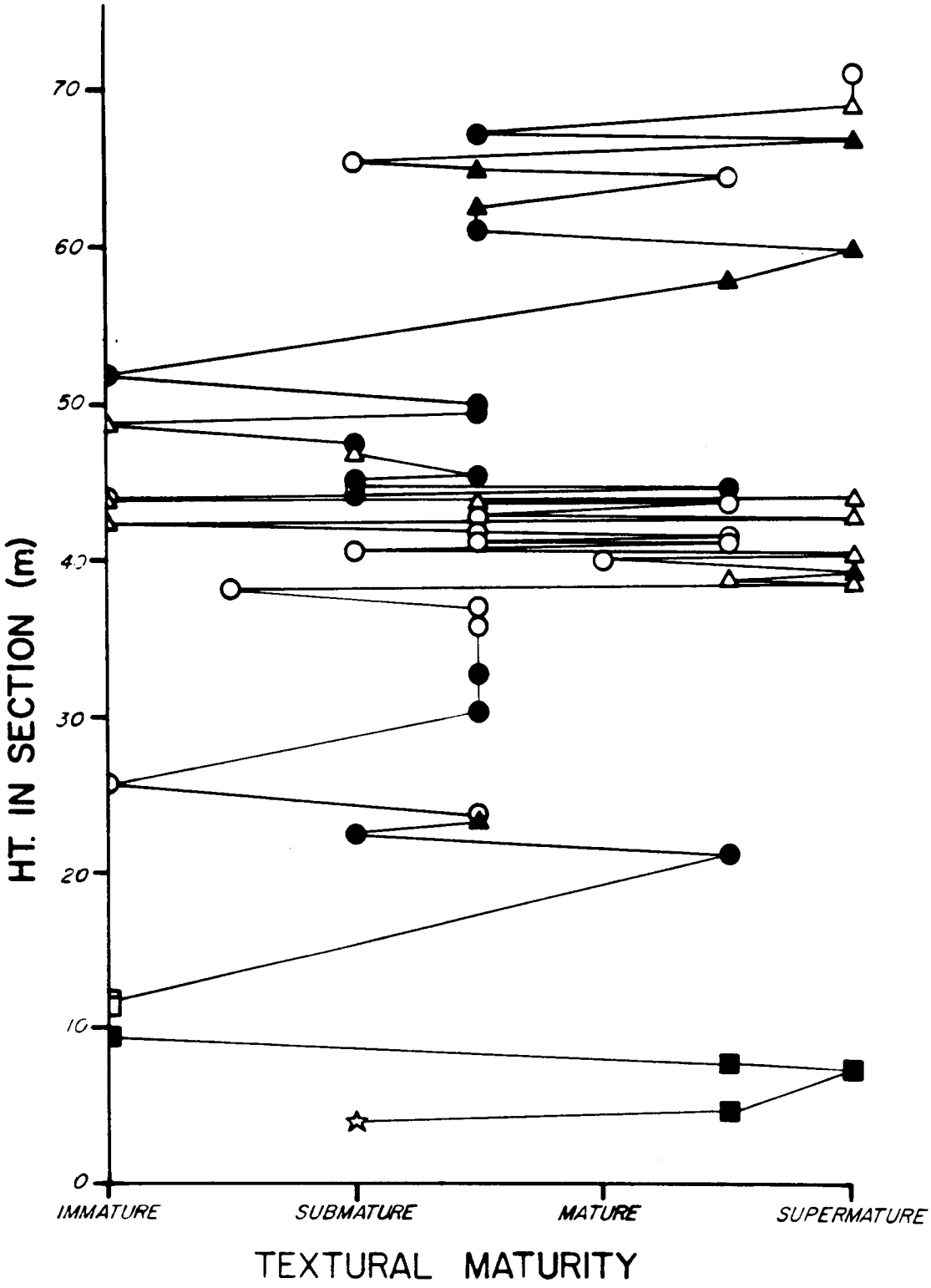
70
60
50
40
30
20
10
0
HT. IN SECTION (m)
IMMATURE
SUBMATURE
MATURE
SUPERMATURE
TEXTURAL MATURITY

Figure 30

Figure 31. Stratigraphic distribution of grain size.

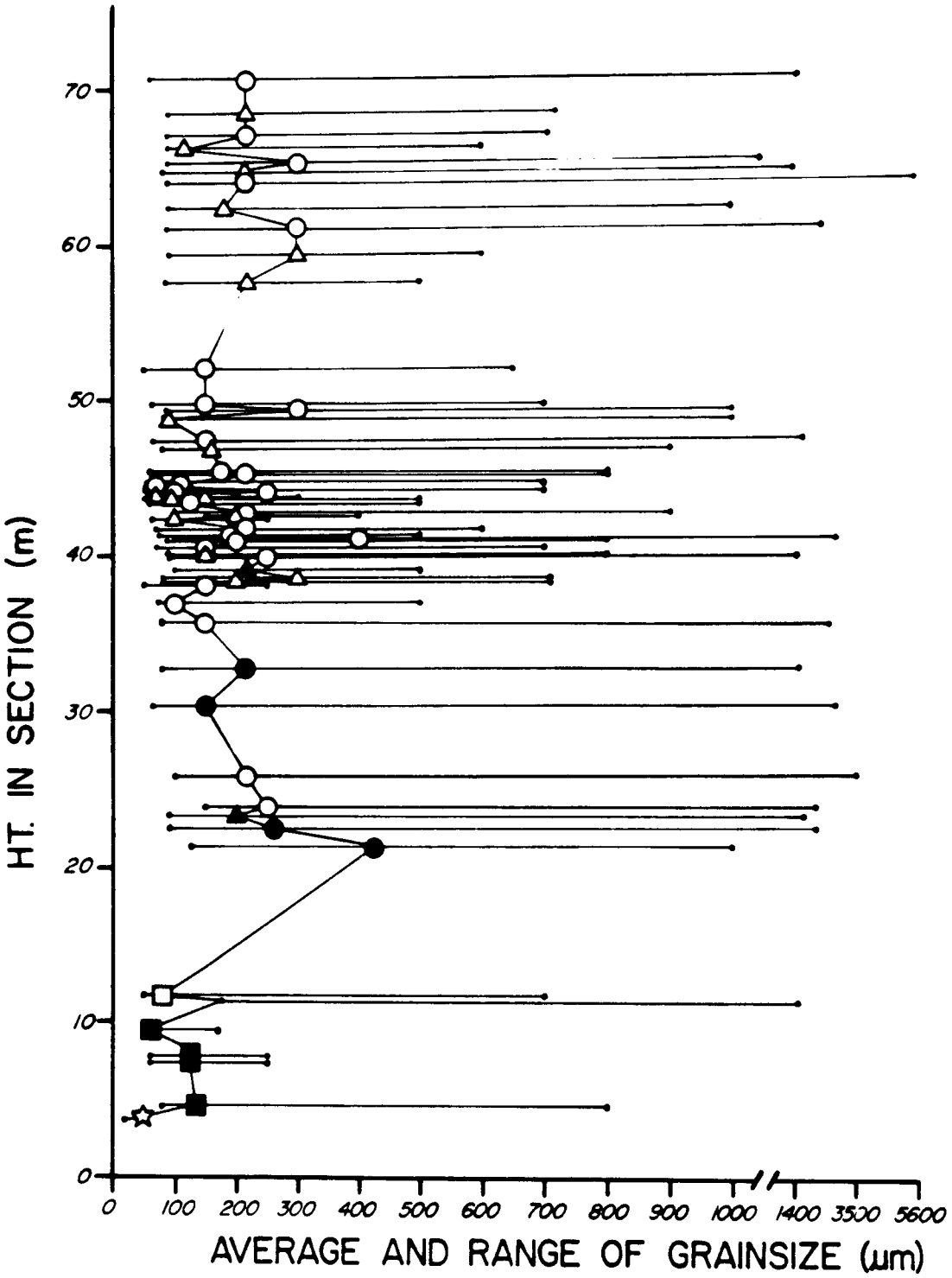
HT. IN SECTION (m)
0
10
20
30
40
50
60
70
0
100
200
300
400
500
600
700
800
900
1000
1400
3500
5600
AVERAGE AND RANGE OF GRAINSIZE (μm)

Figure 31

Important among mineral associations are the negative relationships that amorphous iron oxide-clay aggregates and illite-sericite exhibit with monocrystalline quartz. This may be due to the nature of the tabulation, where decreasing percentages of one mineral species result in apparent increases of another species. More likely, however, is that increasing amounts of monocrystalline quartz represent higher maturity whereas higher amounts of illite-sericite and amorphous iron oxide-clay aggregates represent immaturity.

Quartz overgrowths are quite variable in frequency for the lower 42 m of section, ranging from <1 to 21%, and averaging 6.05%, with σ = 4.97. The upper 28 m varies only between 2 and 10% and averages 5.63%, but more significantly, has a σ of only 2.2 (Figure 23, p. 66). The difference in standard deviation illustrates the variability in the lower portion of the section compared to the upper portion. Overall, however, the percentages remain relatively constant as shown by the similar means for the upper and lower part of the unit. The only exceptions to this are the low quantities between 25 and 38 m (1 to 5%). No significant trends can be seen in quartz overgrowths over the section.

Of the important relationships involving quartz overgrowths listed in Table 6, one of the most important is between quartz overgrowths and textural maturity. Overgrowths are positively associated with textural maturity, and are negatively related to illite-sericite and amorphous iron oxide-clay aggregates (Tables 6 and 7). Though the negative relationship may be a result of changing chemical

conditions, the similarity in their mode of occurrence may preclude coexistence. More overgrowths are present in the more mature Clinch Sandstone rocks, and fewer overgrowths in less mature rocks. Grain size, however, does not show an easily described relationship with overgrowths. For the most part, as grain size increases, overgrowths decrease, but there are several rare portions of the Formation in which this does not hold true and coarser sediments show more overgrowths (Figures 23 and 31, pp. 66 and 89).

Facies variations in overgrowth amount can be seen in Table 8. Facies A and C of the Hagan Shale Member contain the lowest quantities of quartz overgrowths. The other Clinch Sandstone facies vary.

Illite-sericite is the third most dominant component. Percentages are consistent over section except for a major peak at 38.2 meters. The Hagan Shale Member averages more illite-sericite, 6.7% (with σ = 7.97), than the Poor Valley Ridge Member. Above 38.5 m, illite-sericite only occurs in relatively limited amounts. There does not seem to be any overall trend, except for a decrease from the Hagan Shale Member into the Poor Valley Ridge Member. Illite-sericite does not seem related to textural maturity, alternating between a positive and negative relationship in different portions of the section. A negative relationship would be expected between illite-sericite and maturity because illite-sericite comprises a sizeable portion of existing matrix, and part of the textural maturity interpretations are based on overall percentage of matrix, yet they do not show a consistent (much less negative)

relationship. This may imply that most clays are diagenetic rather than depositional. A similar situation exists between illite-sericite and grain size; the two seem relatively independent, neither showing a positive nor negative relationship. The relationships between each facies and illite-sericite content do not exhibit any pattern and can be seen in Table 8.

All the clays examined in this study, when described as authigenic, show one or more of the criteria of Wilson and Pittman (1977) for recognizing authigenic clays. Most commonly used here were (1) the absence of impurities, (2) distinct crystal outlines, (3) delicacy of structure, (4) a high degree of crystallinity, (5) fracture-filling habit, (6) inward pore filling, and (7) a major break in grain size (no visible pelletization or flocculation in thin section).

Polycrystalline quartz and illite-sericite show a roughly positive relationship in the Poor Valley Ridge Member, and a largely negative relationship in the Hagan Shale Member (Table 6, p. 84). This phenomenon is probably related to immaturity. In the less mature Hagan Shale Member, presence of polycrystalline quartz coincides with absence of illite-sericite. In the more mature Poor Valley Ridge Member, amounts of each are reduced and the two minerals appear to coincide. This apparent correspondence may be due to the relatively low proportion (in relation to minerals like monocrystalline quartz). Overall, illite-sericite content shows no correlation (except for monocrystalline quartz and quartz overgrowths, already discussed).

The next most abundant mineral, amorphous iron oxide-clay aggregates, shows high variability, with many wide variations from the mean over the vertical extent of the unit (Figure 25, p. 70). The Hagan Shale Member at the base is very high in amorphous iron oxide-clay aggregates content but the amount decreases upward, until reversing its trend to reach another peak near the top of the member. The Poor Valley Ridge Member exhibits peaks in amorphous iron oxide-clay aggregates content throughout the unit at sporadic intervals. These peaks almost all show rapid appearances followed by much more gradual decreases. Presence of amorphous iron oxide-clay aggregates is negatively related to textural maturity (Table 6, p. 84). When amorphous iron oxide-clay aggregates content increases, textural maturity decreases. This relationship is in part due to the classification scheme used for determination of maturity, which is partially based on matrix content. Amorphous iron oxide-clay aggregates are an important part of the matrix in most cases. Grain size and amorphous iron oxide-clay aggregates also show a direct negative relationship over the entire section. Coarser sediments show a significantly lower amorphous iron oxide-clay aggregates content, whereas finer sediments have very high amorphous iron oxide-clay aggregates amounts.

Percentages of amorphous iron oxide-clay aggregates divided into facies are shown in Table 8 (p. 86). Facies 2 of the Poor Valley Ridge Member (trough cross-stratified) contains less amorphous iron oxide-clay aggregates than any of the other facies; facies A and

C of the Hagan Shale Member show the highest content. The other facies vary considerably.

Polycrystalline quartz shows two relatively high peaks, one at 22 m from the base of the section and one at 65 m (Figure 26, p. 73).

Polycrystalline quartz shows an apparent positive relationship with textural maturity but no relationships with other minerals (Tables 6 and 7, pp. 84 and 85). Monocrystalline quartz and textural maturity also show a positive relationship, as stated earlier, which means that compositional maturity and textural maturity coincide. Polycrystalline quartz is considered an indicator of immaturity (Pettijohn et al., 1973), yet in this study it shows a positive relationship with textural maturity. Relatively higher percentages of polycrystalline quartz are found in more mature samples. This phenomenon may be due to the quantities of the constituents under examination, because polycrystalline quartz occurs in such small amounts. Monocrystalline quartz occurs in very high percentages in the Clinch Sandstone, and therefore is closely tied with the classification scheme. Because Folk's (1974) textural maturity classification scheme does not take into account polycrystalline quartz or any other unstable framework grain (assuming polycrystalline quartz is unstable as suggested by Pettijohn et al., 1973), these unaccounted minerals (which occur in small amounts) may have even less effect on the textural classification. Of course, it may also mean polycrystalline quartz is one of the more stable of the unstable constituents and is, therefore, preserved in more mature sediments.

Polycrystalline quartz corresponds to coarser grain size, as well. In the coarser grain sizes, polycrystalline quartz quantities are high. When polycrystalline quartz percentages are low, grain size may be high or low. But when polycrystalline quartz is relatively high, the rock is typically coarse-grained. Quantities of polycrystalline quartz show no preferential occurrence for any of the facies (Table 8, p. 86).

Kaolinite is present in quantities over 1%, only 4 times in the Formation. These samples are spread through the extent of the unit. The quantity of kaolinite is highest in the middle portion of the section (at approximately 40 m above the base) (Figure 27, p. 75). Because quantities are so low there is little variance. The Hagan Shale Member is consistently low in kaolinite percentage, between <1 and 1. The Poor Valley Ridge Member fluctuates between 0 and 4%.

Kaolinite shows a rough positive correlation with textural maturity over the entire Formation, but its presence is not related to any other mineral except smectite, which defies explanation, except that these two occur in such small amounts it may be coincidence. Except for the interval between 38 and 41 m, peaks in kaolinite quantity correspond to higher maturity. The relationship between kaolinite and grain size, however, is complex. Most samples show a rough positive relationship between grain size and kaolinite content but this does not hold true for the entire section. There are short sporadic intervals which show a direct negative relationship. Kaolinite quantities are low in each facies (Table 8).

Smectite quantity shows an upward-increasing trend which has a peak between 44 and 49 m from the base of the unit (Figure 28, p. 77). Smectite content is very low at the base of the Poor Valley Ridge Member but increases upward.

Smectite shows a very rough positive relationship with textural maturity in the mid-portion of the section, but except for this occurrence there is no apparent relationship. Though smectite quantities are very low, they are higher in facies A than in the other Hagan Shale Member facies and lower in Facies 1 than the other Poor Valley Ridge Member facies (Table 8, p. 86). Relationships between smectite and the other minerals can be seen in Tables 6 and 7, pp. 84 and 85.

Textural Maturity

Rounding

Rounding was visually estimated in thin section by comparison with charts developed by Powers (1953). Samples with extensive authigenic quartz overgrowths were difficult to characterize. This problem is exemplified in Figure 32. For those samples the descriptions of rounding (and to some extent, sorting) are only approximations. Evaluations of rounding have been plotted over the stratigraphic column, assigning arbitrary values (equidistant along the abscissa) to each class (Figure 33). This is not meant to imply proportional intervals of rounding from one class to the next but to ease interpretation of the data. The same has been done for sorting and textural maturity.

Figure 32. Photomicrograph of quartz overgrowth (visible grain boundary on large, rounded monocrystalline quartz). Bar is 0.5 mm. Arrow shows up direction (crossed nicols).

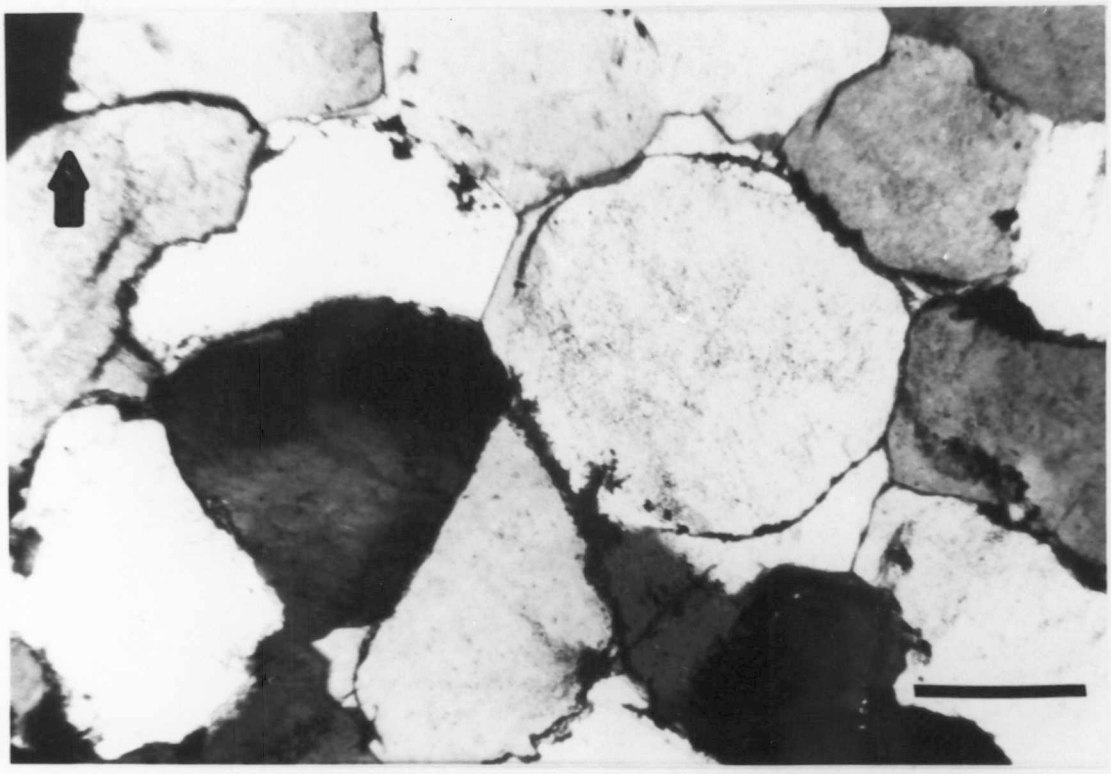

Figure 33. Stratigraphic variation in rounding.

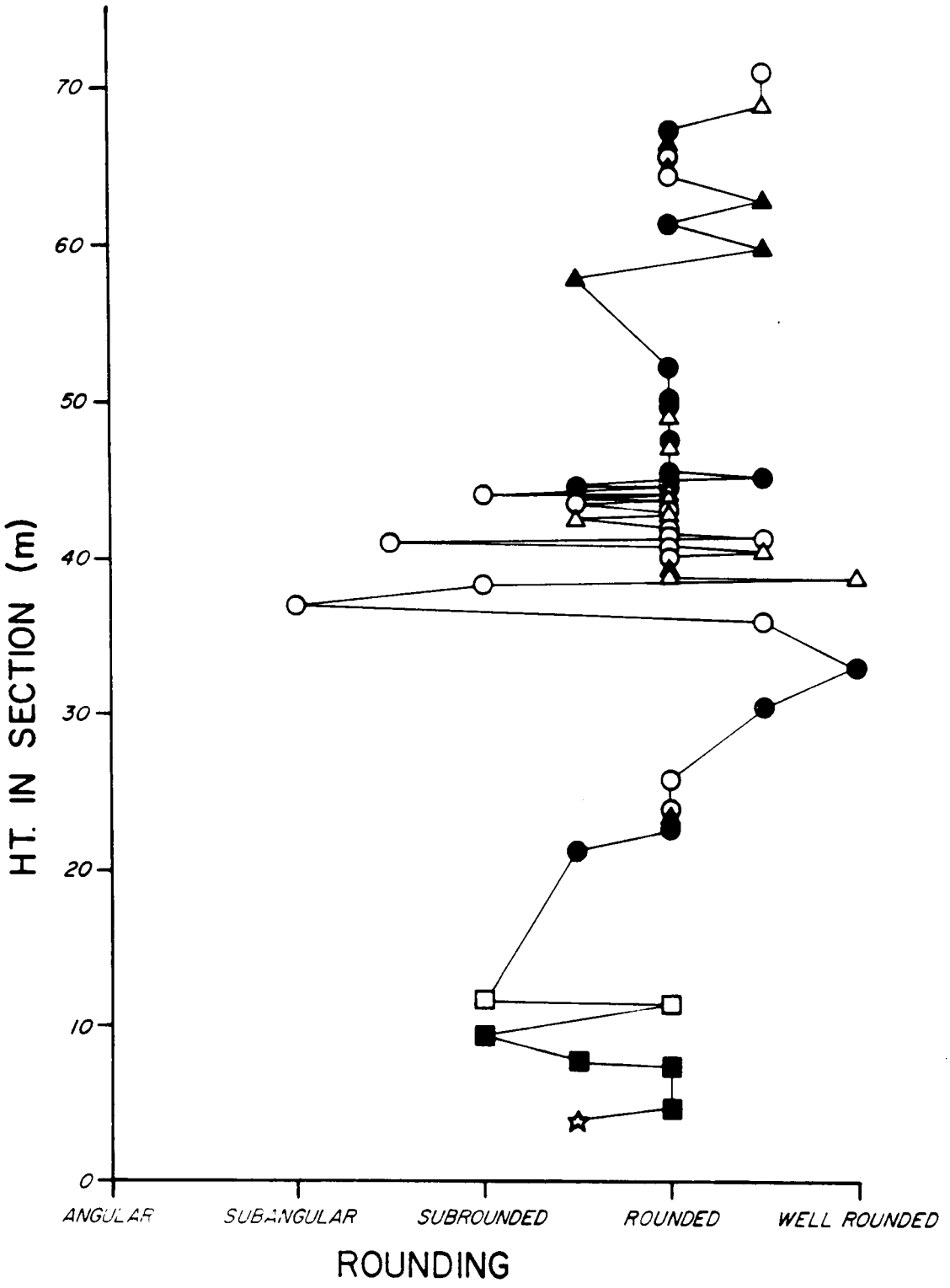
70
60
50
40
30
20
10
0
HT. IN SECTION (m)
ANGULAR
SUBANGULAR
SUBROUNDED
ROUNDED
WELL ROUNDED
ROUNDING

Figure 33

The Clinch Sandstone is characterized by consistently rounded sediments in the upper 41 m and variable and less well rounded in the lower 29.4 m. The Hagan Shale Member shows variable relationships between facies and rounding, averaging approximately subrounded to rounded. In the Poor Valley Ridge Member, rounding fluctuates as well. Facies 1 is the only one that shows a preferred amount of rounding (one degree of rounding occurs more than any other). It is somewhat better rounded, averaging rounded to well-rounded.

Sorting

Sorting is difficult to determine from a virtually two-dimensional planar surface such as that provided by a thin section. Sorting was estimated as best as possible from the thin sections using the sorting images included in Pettijohn et al. (1973).

Sorting is very consistent in the lower half of the Hagan Shale Member (Figure 34). Each sample is well sorted. The upper half is much less well sorted, ranging from poor to poor-moderate sorting.

The lower Poor Valley Ridge Member is quite variably sorted, fluctuating between poor, poor-moderate, and well-very well. In the interval between 38 and 45 m up in the Formation, sorting is improved, ranging from moderate to very well sorted. Above 45 m the Poor Valley Ridge Member is less well sorted but shows an upward-increasing trend with better sorting upwards in the section. The average for sorting in this interval is moderate.

Figure 34. Stratigraphic variation in sorting.

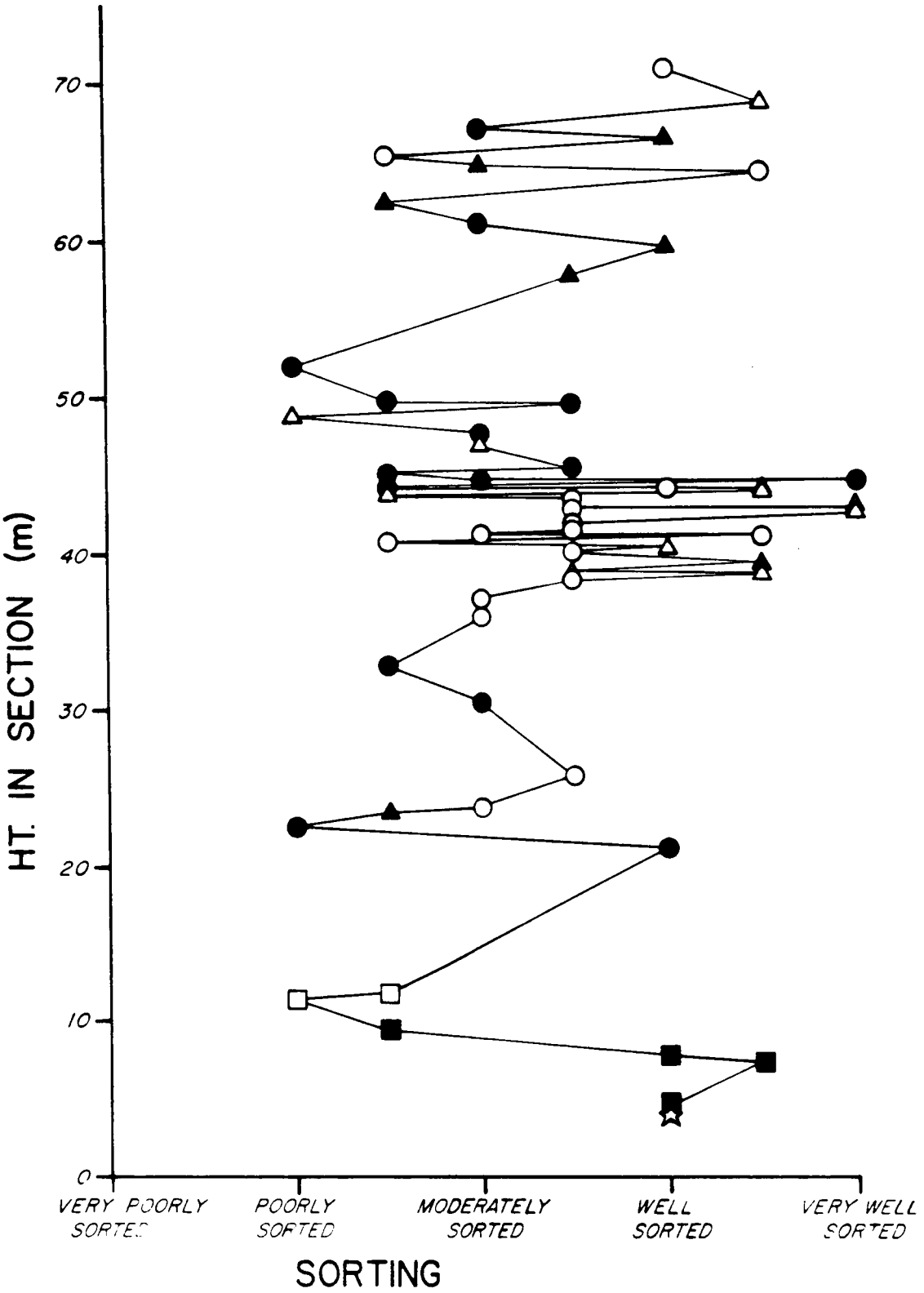
70
60
50
40
30
20
10
0
HT. IN SECTION (m)
VERY POORLY SORTED
POORLY SORTED
MODERATELY SORTED
WELL SORTED
VERY WELL SORTED
SORTING

Figure 34

Overall Textural Maturity

Overall textural maturity was evaluated using Scholle (1979, after Folk, 1974). This classification scheme takes into account clay matrix content, sorting and roundness to determine the degree of textural maturity. Correspondence between textural maturity and mineralogy has already been examined (see previous section). Independently, however, textural maturity shows a slight upward increasing trend. The upper portion of the Formation is more texturally mature, averaging mature to mature-supermature. Other than these two intervals and a submature-mature section in the middle of the Formation, the Clinch Sandstone overall is quite variable in textural maturity.

Post Burial Features

Cementation

Cementation in the Clinch Sandstone is commonly quite complete, occluding porosities to as low as 0, <1 and 1% in 18 of the 57 Clinch Sandstone samples. The most common cementing agent is authigenic quartz overgrowths. Also present but much less important are authigenic kaolinite and sericite which occur in 9 and 6 of the 57 samples, respectively. Post-depositionally squashed detrital grains also rarely serve to bind the particles together. The sources of silica used in the formation of authigenic minerals include altered feldspars, matrix and some altered quartz.

To distinguish authigenic overgrowths from original detrital quartz several lines of evidence were examined. Visible original

grain boundaries, clear vs. cloudy grain appearance, and crystalline growth characteristics such as enfacial angles and euhedral grain boundaries attest to the presence of grain growth after deposition. Cathodoluminescence was performed on several thin sections to substantiate the plane and polarized light identification. Original grain boundaries are also visible (petrographically) inside overgrowths in 28 samples concentrated in the mid portion of the stratigraphic column. In rare cases a substantial difference in grain clarity was noted between detrital grain and overgrowth (overgrowths were typically inclusion-free) but this only occurred locally on individual thin sections and, therefore, was not considered significant in determining the presence of overgrowths. Enfacial angles were observed in 34 of the 57 samples. Prismatic "saw-tooth" or "stair-step" growths also provide evidence for post-depositional grain growth. In these cases the quartz lattice is extended along crystallographic directions to ultimately form di-pyramidal terminations. "Stair-step" or rhombohedral projections which grow in the direction of the grain's c-axis and prismatic projections, which grow parallel to the c-axis (Waugh, 1970) are present in 19 samples and 6 samples, respectively, each concentrated in the upper portion of the column, from 44 m to 68 m above the contact with the Juniata Formation. The presence of phyllosilicate rims or rinds apparently inhibits precipitation of authigenic overgrowths (as was predicted by Lumsden et al., 1971). In localized areas of specific thin sections, the presence of clays coincides with a lack of overgrowths.

This is true in samples 1/2-1 and A-5. In totally contrary instances the presence of clays allows for observation of original grain, as the clays form rinds around detrital grains before authigenic overgrowths begin to form. In several examples (1/6-2A, 2/6-8 and 2/9-4) clays have formed rims around the authigenic overgrowths. Grain boundaries are visible, in these cases, due to subtle clarity differences between detrital grain (with sparse inclusions, especially near grain margins) and overgrowth (inclusion-free). Cathodoluminescence also suggested the presence of abraded overgrowths, which were unobserved under plane and polarized light.

In contrast to authigenic quartz overgrowths which are inhibited by the presence of clays, pressure solution (evidence of which is present in 34 of the 57 samples) is more abundant in the vicinity of clays, even on a millimeter-by-millimeter basis. Pressure solution is directly related to clays in 8 samples, in which sericite or amorphous iron oxide-clay aggregates serve to enhance pressure solution. Sutured grain boundaries, a sign of pressure solution (Pettijohn et al. (1973), are present in 21 samples, distributed throughout the Formation, but slightly more concentrated toward the top as are some of the other deformational features (Figures 35, 36 and 37). The majority of the thin sections that show sutures also exhibit other evidence of pressure solution as well. Microstylolitization, visible only in thin section in these rocks, is present in 10 samples. Contrary to Heald (1955), who stated that stylolites are common in clean sandstones but becomess less abundant as clay content increases, stylolites present in the Clinch Sandstone

Figure 35. Photomicrograph of pressure solution features: sutured grain boundary and stylolite. Bar is 0.05 mm. Arrow shows up direction (crossed nicols).

Figure 36. Photomicrograph of lateral elongation. Bar is 0.5 mm. Arrow shows up direction (crossed nicols)

Figure 37. Photomicrograph of squashed mica. Bar is 0.05 mm. Arrow shows up direction (transmitted light).

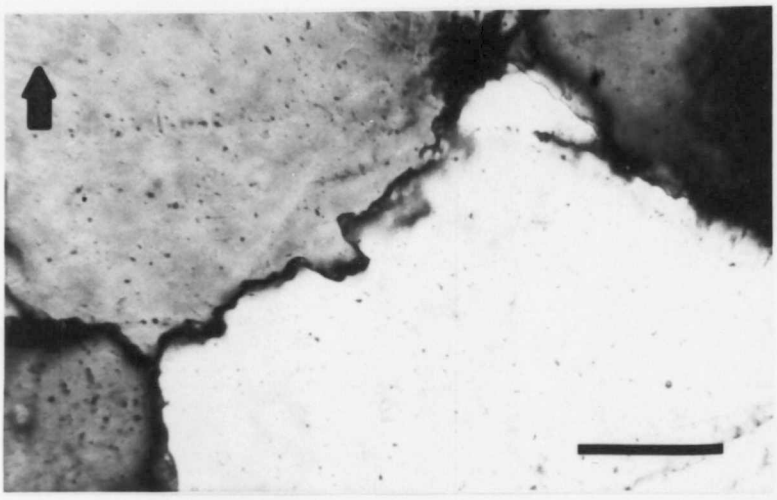

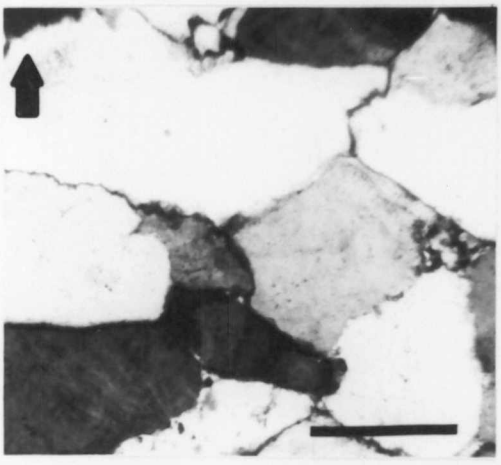

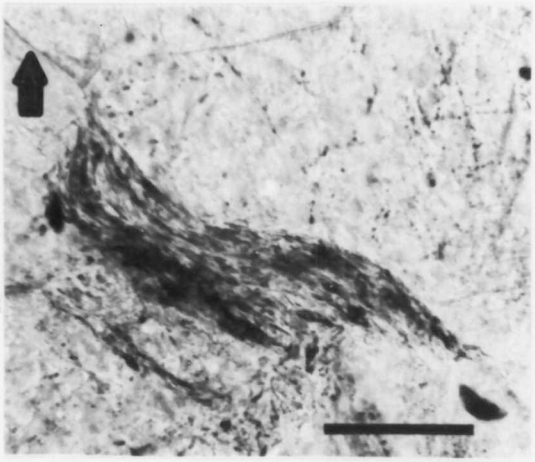

are very commonly associated with clays. A typical stylolite in the Poor Valley Ridge Member (there are none in the Hagan Shale Member samples examined) is associated with abundant heavy minerals, pore space and amorphous iron oxide-clay aggregates as stylocumulate. Immediately adjacent to the stylolite, amorphous iron oxide-clay aggregates are typically quite abundant.

Replacement and Alteration

Kaolinite is the major replacing mineral phase. In 40 of the 57 samples in which it is present, kaolinite occurs as a replacement mineral. Kaolinite replaces feldspars, both plagioclase and K-feldspar. Kaolinite also typically replaces the detrital matrix in wackes, as well as rarely replacing other clays (smectite and illite/sericite). Kaolinite also appears to replace monocrystalline and polycrystalline quartz. In the 15 samples that suggest this relationship, the grain being replaced is unequivocably quartz. The authigenic mineral exhibits low birefringence, relief greater than balsam and book-like crystal habit. The relationship between the two minerals appears to be one of replacement for several reasons. First, the kaolinite neither forms a rind nor coating on the quartz grain but instead appears to be part of the mineral. Also, kaolinite in these cases is present most commonly confined within the perimeter of the quartz grain, though in some cases the kaolinite may extend into adjacent pore space.

Sericite is a replacement product which occurs due to chemical alteration of silicates, especially feldspars (Potter et al., 1980;

Kerr, 1977). In the Clinch Sandstone, sericite replaces feldspars (in 5 samples) and detrital matrix (in 4 samples). There are also samples which exhibit apparent replacement textures between sericite and quartz, though this is rare and may only represent a clay coating or pitting filled with clays. Smectite is also present as a replacement mineral, occurring in 3 samples, most commonly replacing detrital matrix. In fine-grained lithologies, like those which compose the matrix in Clinch Sandstone wackes, these clays are commonly difficult to identify, especially with respect to original or replacement minerals. Amorphous iron oxide-clay aggregates also appear to replace original detrital grains (in 2 samples) but the proposed relationship is not without question because these clays are so fine-grained and their textural nature is difficult to evaluate.

In addition to diagenetic changes which affect mineralogy other changes affect the fabric of the sandstones. Deformation in the Clinch Sandstone is restricted to four major mechanisms: lateral elongation, squashing of ductile detrital grains, fracturing of framework grains and fracturing of the rock. Lateral elongation (Figure 36) partially qualifies as pressure solution and partially as authigenic overgrowths. Lateral elongation describes the fabric of a quartz-rich, matrix- and clay-poor sandstone which, under directed stress, has partially dissolved parallel to the direction of the stress and has grown in the direction perpendicular to stress (Riecke effect). This realigns a previously random fabric into one which appears laminated. Lateral elongation occurs in 23 Clinch

Sandstone samples (most commonly quartz arenites), distributed throughout the Formation.

Ductile framework grains, dominantly micas, may be bent around more rigid particles by compaction due to overburden (Figure 37). Squashed micas (primarily muscovite with some biotite) occur in 5 samples distributed throughout the unit.

Fracturing of grains and fracturing of the rock itself indicate a slightly higher degree of compaction which has caused more competent (yet more brittle) framework grains to break. Fracturing limited to individual grains can be observed in 9 samples (an example of which is shown in Figure 38). Rock fracturing has occurred in 5 samples, some of which have authigenic minerals precipitated in the fractures (kaolinite, for example, in Figure 39). Other samples, however, show unoccluded fractures which have been tentatively included as porosity.

Total Porosity

Porosity is present in the Clinch Sandstone in percentages from 0% in 2 samples to 16% in one atypical sample. The average is 3.5% with a σ of 3.4 (Table 5, p. 61). Porosity shows great variability over the vertical extent of the unit (Figure 40). It is relatively high between 0 and 5 m (10 to 11%), becoming more moderate and variable from 7 m to the top of the unit (0 to 16%) except for a very low interval between 41 and 44 m (0 to 2%). Porosity characteristics have been described for each facies and are listed in Table 8, p. 86.

Secondary porosity accounts for almost all porosity that is present in the Clinch Sandstone. Of Schmidt and McDonald's (1979)

Figure 38. Photomicrograph of grain fracturing present in large, oblong, monocrystalline quartz grain. Bar is 0.05 mm. Arrow shows up direction.

Figure 39. Photomicrograph of whole-rock fracture which has been occluded with authigenic kaolinite. Bar is 0.025 mm. Arrow shows up direction.

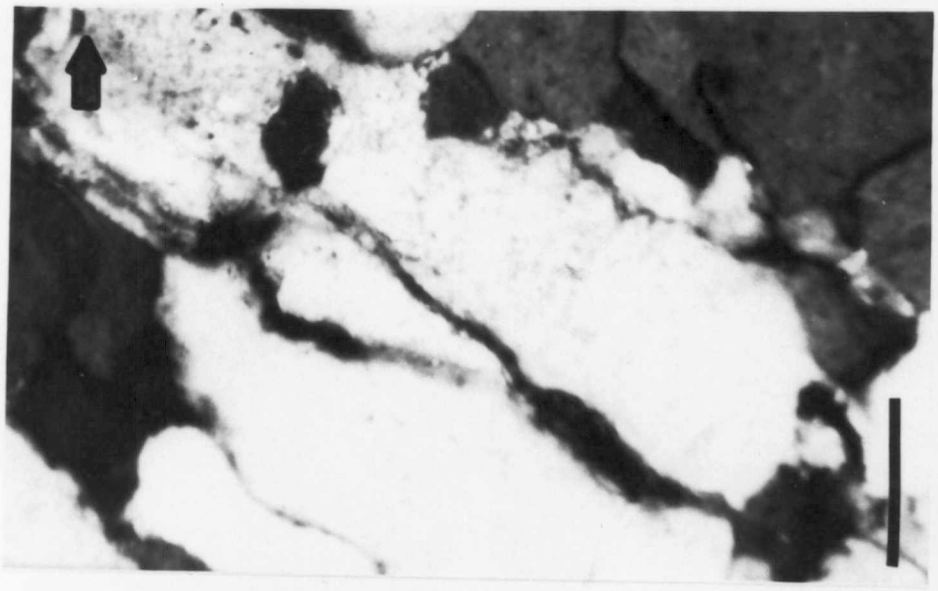

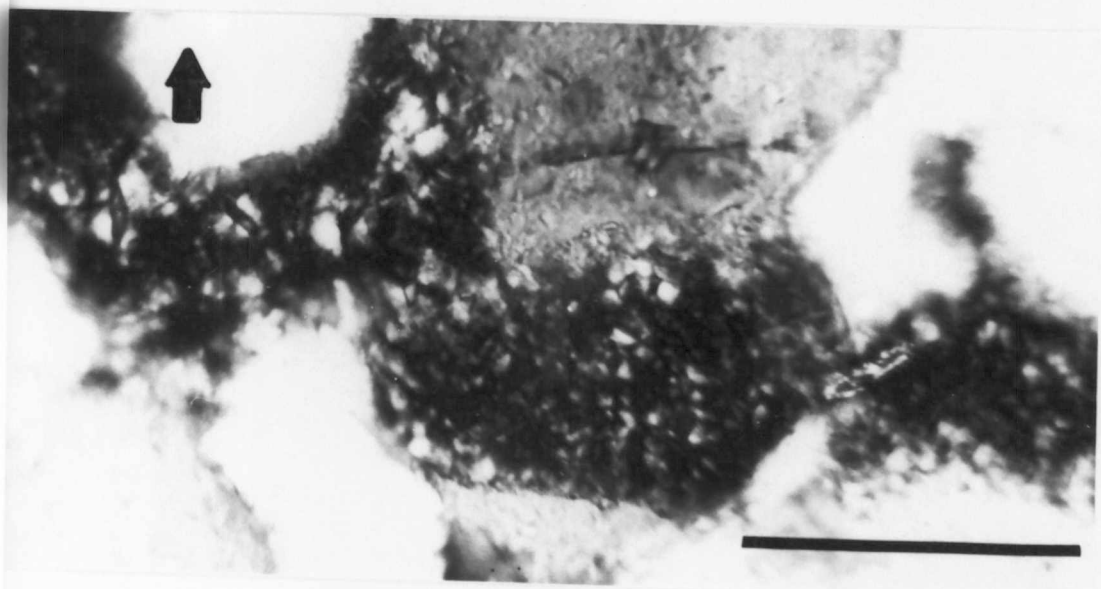

Figure 40. Stratigraphic distribution of porosity.

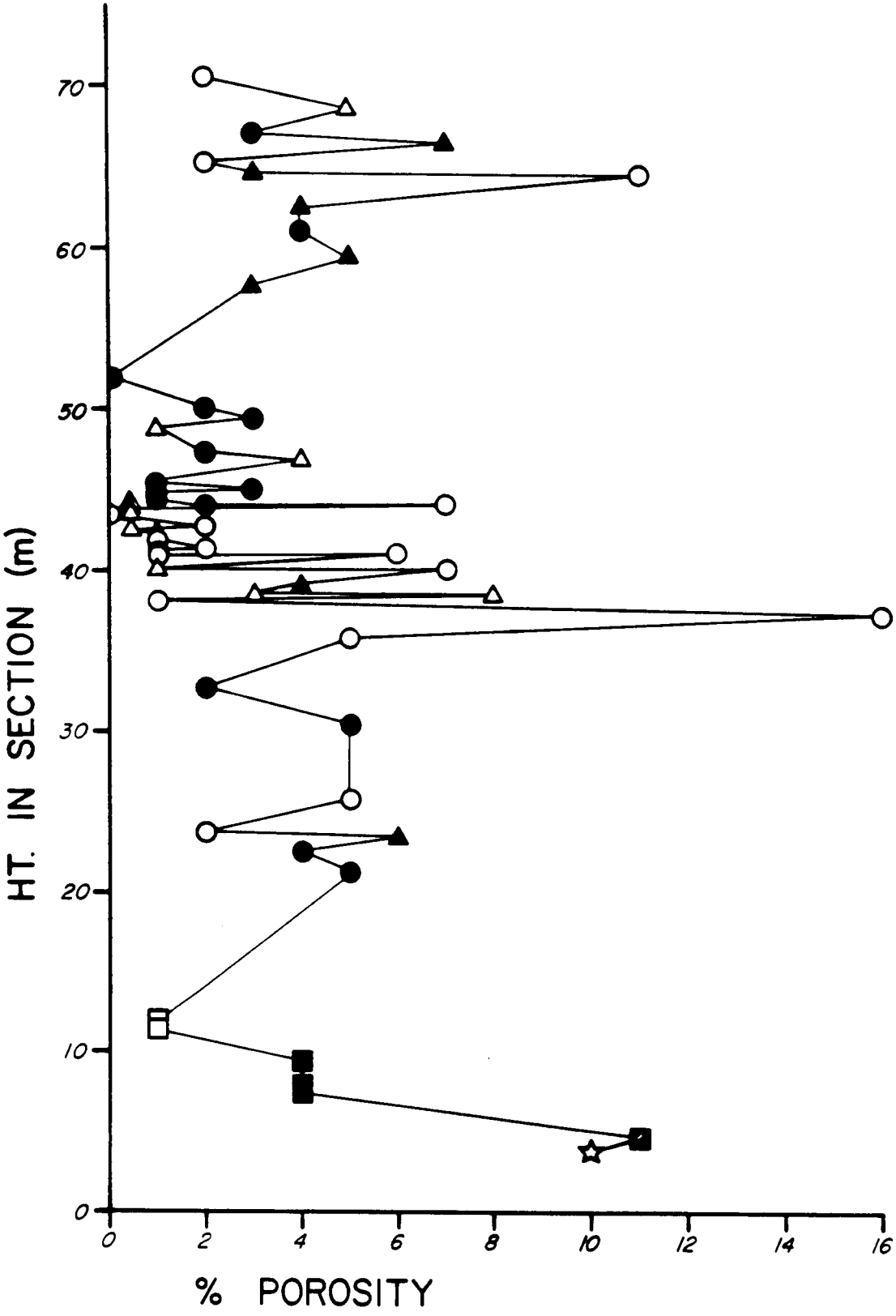

Figure 40

five recognized genetic classes of secondary porosity, three are present in the study area: (1) porosity created by fracturing, (2) porosity created by dissolution of authigenic cements, and (3) porosity created by dissolution of replacement minerals. Fracturing has taken place on two levels: individual grain and overall rock. Both of these are present in the Clinch Sandstone. Quantity and nature of porosity formed by dissolution is very difficult to evaluate in the Clinch Sandstone due to the arbitrary paragenetic relationships which do not offer much evidence for any particular pore genesis. Some of the porosity present now may be due to dissolution of former cements. In addition, J. Coleman (personal communication, 1984) has indicated that the Clinch Sandstone present in the same allocthon in the subsurface, shows virtually no porosity or permeability. With changes in pore water chemistry it is also highly probable that replacement minerals have been emplaced and subsequently dissolved in the past, leaving pore space which may have persisted to the present. There is also a high probability that the pores in the Clinch Sandstone are, for the most part, pores of hybrid origin and consist of both primary porosity and secondary porosity because authigenic minerals are ubiquitous, yet at the present only partially occlude some of the pores. Many pores in the Clinch Sandstone show overgrowths terminating into pore space, which may represent original depositional porosity that has never been completely occluded. A more logical explanation is that, with dissolution of unstable detrital framework grains, the resultant pores provided space for

the partial development of overgrowths, thus making these pores similar to hybrid pores.

Surprisingly, there is a relationship between porosity and outcrop locality. The two laterally extensive roadcuts, outcrop 1 and outcrop 2 (Figures 3 and 4, pp. 13 and 15), show trends that are not present in the other outcrops. In outcrop 1 eleven representative samples showed porosity decreases up section, whereas in outcrop 2 fourteen samples showed porosity increases up section. Because these two outcrops are almost laterally continuous, it seems strange that such a contradictory relationship exists. Similar trends would be expected in two equivalent stacks of rock that have been subject to the same amounts of exposure and weathering as have these two outcrops (Aycock, 1978). Relationships with other characteristics do not follow either of these trends. In fact porosity shows no relationship at all with textural maturity or grain size (Figures 30 and 31, pp. 87 and 89) except that very fine-grained rocks typically exhibit lower porosities, as is expected (Houseknecht, 1984). Porosity does show a positive relationship with sorting (Table 6, p. 84), as better-sorted sediments characteristically have higher porosities (Beard and Weyl, 1973; Blatt et al., 1980). This is to be expected as the potential interstitial pore space in poorly sorted sediments is commonly filled with fine-grained matrix (Blatt et al., 1980). Rounding and porosity conversely exhibit a negative relationship in the lower 40 m of the Clinch Sandstone (Table 6). In this interval, when rounding increases, porosity decreases. In more angular

sandstones porosity is high, and becomes low when grains show better rounding. Packing regime is probably a controlling factor in the high porosities of more angular lithologies as irregular packing may create more pore space. Porosity also shows a slight negative relationship with amorphous iron oxide-clay aggregates, illite/sericite, and kaolinite-dickite (Table 6, p. 84). Each of these is a matrix constituent or authigenic mineral. Increases in such interstitial components logically lead to decreases in preserved porosity. Smectite, the fourth most important fine-grained mineral, does not show any relationship with porosity. Total monocrystalline quartz shows a negative correlation with porosity that is probably due to the increased number of sites on which overgrowths can precipitate, which then serve to occlude pore space. Overgrowths, which occur in every sample as a major pore-occluding mechanism, do not have any apparent distinct relationship with porosity within the Formation (Tables 6 and 7, pp. 84 and 85). Matrix and authigenic phyllosilicates seem to be the most important factor in reducing porosity, as well as, to some extent, increased rounding. Sandstones with the highest porosities commonly display medium to coarse grain size, a subrounded to angular texture, little matrix and few authigenic phyllosilicates.

V. TRACE FOSSILS

The Clinch Sandstone is, for the most part, devoid of body fossils. With the exception of two fragments of phosphatic brachiopods found in a conglomeratic bed within the Hagan Shale Member, no body fossils have been recovered from outcrops at Beans Gap. At other localities of the Clinch Sandstone (or Clinch-equivalent rocks) in Tennessee (especially along Powell Mountain, Wallen Ridge and Poor Valley Ridge) a more diverse assemblage of brachiopods, gastropods, crinoids, bryozoans, cephalopods and pelecypods have been found (Nicholson, 1978). In Virginia, Miller and Fuller (1954) collected pelecypods, gastropods, trilobites and cephalopods, and later, Miller (1976) also found ostracods.

Thirteen ichnogenera have been identified from the Route 25E roadcuts over Clinch Mountain (Figure 9, p. 29). Nomenclature and identifications were made using descriptions and illustrations from Häntzschel (1962). Most common is the genus Arthrophycus. Found throughout the Clinch Sandstone, Arthrophycus occurs as sole markings in fine- to medium-grained sandstones commonly overlying a siltstone or shale. Its occurrence is typically quite dense, showing bunched, semi-circular to circular tubes with regularly spaced transverse ridges (Figure 41). A medial depression is rare. Lengths of tubes range from approximately 10-25 cm. This taxon is most closely related to facies 1, 3 and 4. Arthrophycus occurs in facies 1, in clay drape laminae that separate cross-sets and in facies 3, on the

Figure 41. Arthrophycus in Clinch Sandstone float. Scale is on left.



bases of massively burrowed beds. Arthrophycus is also commonly associated with Skolithos, because Skolithos and Diplocraterion are the primary ichnogenera responsible for massive reworking of facies 3 strata. In facies 4, Arthrophycus occurs on the bases of sandstone beds where interstratified with siltstone and shale.

Skolithos, a straight, cylindrical vertical tube, is the second most common ichnogenus present at Beans Gap (Figure 42). Two forms are present in the study area. Type A is the more robust form, 1.5-2.0 cm in diameter and up to approximately 1 meter long. Exact lengths are difficult to assign due to nonlinear burrows intersecting nonplanar outcrop faces. Type A, abundant at Beans Gap, is present as cross-sections coplanar with the outcrop face and occurs over most of the Formation. Type B is much more delicate, with tubes that range from 0.5-1 cm in diameter and measure up to only 15 cm in length (Figure 42). Lengths are difficult to determine with Type B as well as with Type A. Type B occurs as slightly curving tubes which stand out in relief from the outcrop face. Skolithos type A has been identified in all facies but is dominant in fine- to medium-grained facies 3 rocks where it is responsible for thorough burrowing. This extends the limited upper Tuscarora occurrence found in Virginia and West Virginia (Diecchio, 1973). Type B has only been found in the basal bedding unit at outcrop 1 and is associated with Skolithos type A and Diplocraterion.

Also common at Beans Gap is the trace fossil Planolites. Planolites is a cylindrical to subcylindrical, horizontal tube which

Figure 42. Skolithos type A and type B. Centimeter scales are present in each photograph.

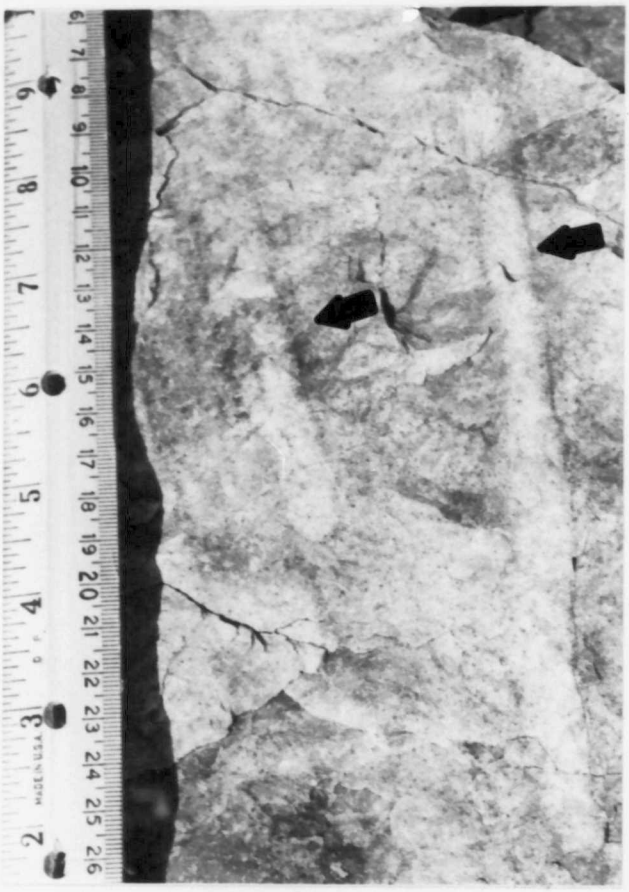

Type A



Type B

does not exhibit either transverse ridges or medial depressions (Figure 43). It averages 1 cm in diameter and may be up to 20 cm long. Planolites is the dominant ichnogenus of the Hagan Shale Member but also occurs near the very top of the Poor Valley Ridge Member. This trace fossil occurs in very fine- to fine-grained sandstone, most commonly associated with facies 4 horizontally laminated beds but also rarely with facies 2 cross-beds.

Also present at Beans Gap are excellent examples of Diplocraterion. This ichnogenus is present as U-shaped vertical burrows with well-developed spreite (Figure 44). Tubes are most commonly 1-2 cm in diameter, with 10-15 cm between branches, and may be 40 cm long. Diplocraterion is found in fine-grained sandstone restricted to outcrops 1 and 2, where it is most commonly associated with facies 3 massively burrowed beds and rarely with facies 4 horizontally laminated beds. Diplocraterion in the Clinch Sandstone most commonly exhibits a habit representative of life in an eroding environment (Goldring, 1964).

Rusophycus occurs less commonly at Beans Gap but is well preserved (Figure 45). Similar preservations (etched out surfaces) can be seen in Cruziana and Monocraterion (Figures 46 and 47). Rusophycus is bilobate, with transverse scratchmarks oriented at an acute angle to a deep medial groove. Rusophycus averages 10 cm in length and 7-8 cm in width, occurring on the bottom of sandstone beds. This trace fossil is most common in fine- to medium-grained lithologies, on the bases of facies 3 thoroughly burrowed beds or in Hagan Shale Member in facies B interbedded siltstone and sandstone.

Figure 43. Planolites (*) and Pelecypodichnus (+) in Clinch Sandstone float. Scale is on left.

Figure 44. Diplocraterion with spreite in Poor Valley Ridge Member. Bar equals approximately 10 cm.



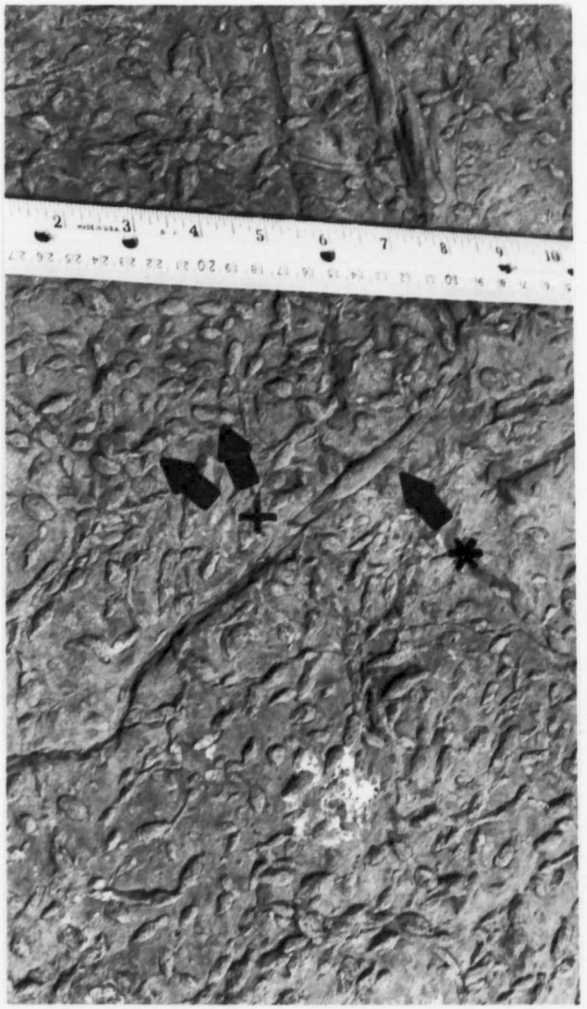

Figure 45. Rusophycus in Hagan Shale Member. Ruler is 30.5 cm long and is not in direct contact with outcrop.

Figure 46. Cruziana among Rusophycus in Hagan Shale Member. Bar equals approximately 5 cm.

Figure 47. Monocraterion in Clinch Sandstone float. Pencil is 8 mm in diameter.







Associated with Rusophycus is the trail Cruziana, which is limited in occurrence. Cruziana is elongated and bilobate, with transverse scratch marks, angled away from a deep medial groove (Figure 46). It also occurs on the bottom of fine- to medium-grained sandstone beds. Cruziana is 20-25 cm in length and 7-8 cm wide. It is only associated with facies 3 strata and has only been found in one horizon in the Poor Valley Ridge Member.

Also present at Beans Gap is the trace fossil, Monocraterion. It is another cylindrical, vertical, unbranching tube, very similar to Skolithos except that Monocraterion exhibits a cone-shaped termination at the top of the tube and upper bedding surface (Figure 47). Tube diameter is 1-2 cm, length is approximately 15-20 cm, and cone-shaped apertures are commonly about 5 cm in diameter. It is speculated that Skolithos may represent partial preservation of Monocraterion (in Skolithos the cone portion may have been eroded, leaving only the otherwise featureless cylindrical tube) (Goodwin and Anderson, 1974). Monocraterion occurs in fine- to medium-grained sandstone both in sandy interbeds of Hagan Shale facies B and in facies 3 of the Poor Valley Ridge Member.

Arenicolites is another vertical tube present in the Clinch Sandstone at Beans Gap. It is a U-shaped tube very similar to Diplocraterion but does not show spreite (Figure 48). The tubes are 1-2 cm in diameter, 20-30 cm long and commonly have about 10-15 cm between limbs. Arenicolites occurs in fine- to medium-grained sandstone, at the base of the Poor Valley Ridge Member. It is associated with Skolithos in thoroughly burrowed facies 3 strata.

Figure 48. Photograph tracing of Arenicolites in Clinch Sandstone. Scale is on right.

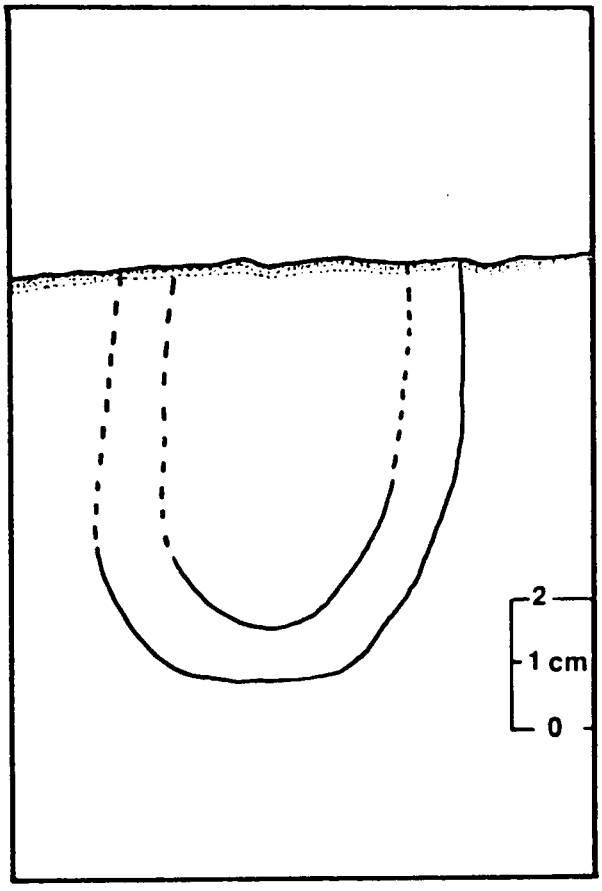

Figure 48

Possible Thalassinoides trace fossils occur at outcrop 1 on the base of a facies 4 horizontally laminated bed. This horizontal, cylindrical tube shows characteristic Y- and triangular-shaped, boxwork-branching patterns (Figure 49) but because it is exposed high above ground level, it is inaccessible and definite identification could not be made.

Chondrites (Figure 50) may also be present in the Hagan Shale Member, but identification is difficult due to complex overlapping relationships between it and associated trace fossils.

Examples of Paleophycus, Pelecypodichnus, and possible Corophioides (Figures 51; 43, p. 127; and 52) are present in Clinch Sandstone float. Paleophycus occurs as subcylindrical to ellipsoidal horizontal tubes, 1-2.5 cm in diameter and 5-10 cm long. Pelecypodichnus is gregarious, occurring as well-preserved, tapered pods, 1-2 cm long and 0.5-1 cm wide. Corophioides may be present as the bottoms of U-shaped tubes, protruding beyond horizontal bedding surfaces. Tubes are commonly 1-1.5 cm wide and 5-8 cm long, reentering the bedding plane at each extreme.

Figure 49. Photograph tracing of Thalassinoides(?) on underside of bed viewed from below. Bar equals 30 cm.

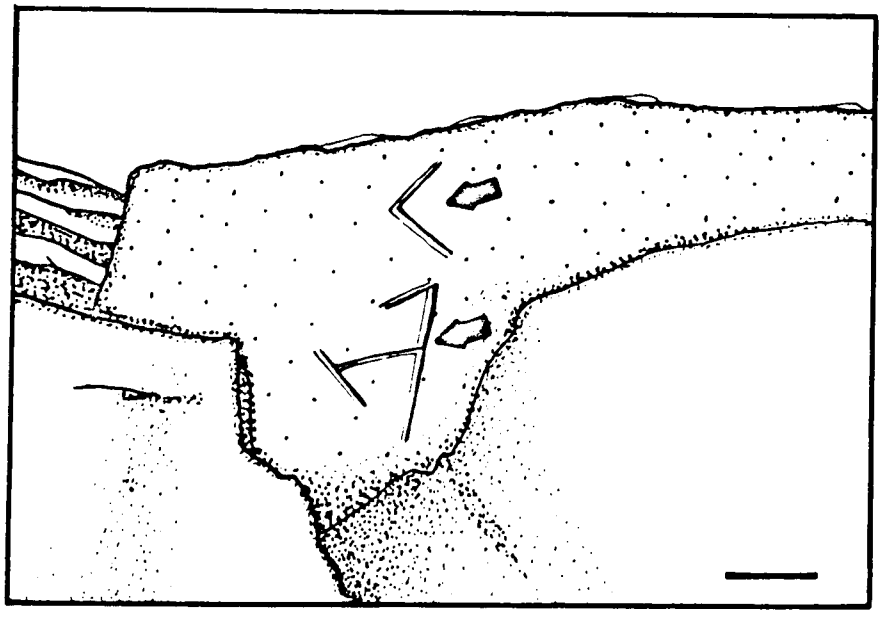

Figure 49

Figure 50. Possible Chondrites in Clinch Sandstone float. Scale is on left.

Figure 51. Paleophycus in Clinch Sandstone float. Scale is on left.

Figure 52. Corophioides (*) in Clinch Sandstone float. Scale is on right.


0 CM 1 2 3 4


4 5 6 7 8 9 1


4 5 6 7 8 9 10

VI. PALEOCURRENT ANALYSIS

Results

Paleocurrent orientation data were collected from all outcrops where suitable current indicators existed. Measurements were taken on planar-tabular cross-beds, trough cross-beds, ripple marks, channel axes, and subparallel- to parallel-oriented Rusophycus. In total 93 current indicators were measured, 82 of which were unambiguous unidirectional indicators. The small set of bidirectional indicators were graphed, but were not statistically analyzed due to the small sample size (Figure 53). Bidirectional indicators included 8 sets of oscillation ripple marks, an oriented group of Rusophycus, a channel axis with no discernible dip direction due to the trace geometry of the channel and outcrop surface, and possible flute casts. The latter do not align with the other measurements and, therefore, may be an invalid measurement. The most likely cause for an invalid measurement is the origin of these marks. The "current" direction was taken with care to ensure that the body of rock on which the measurement was taken had not moved. Accordingly, the most likely explanation for this anomalous reading is that the marks were not formed by current or a current-effected mechanism but represent the product of later structural deformation.

The 82 unidirectional measurements are composed of 62 measurements from planar-tabular cross-beds, 21 from trough cross-beds, and 1 channel axis. There is no perceivable difference in

Figure 53. Bidirectional paleocurrent indicators in Clinch Sandstone (length of wedges is proportional to number of observations).

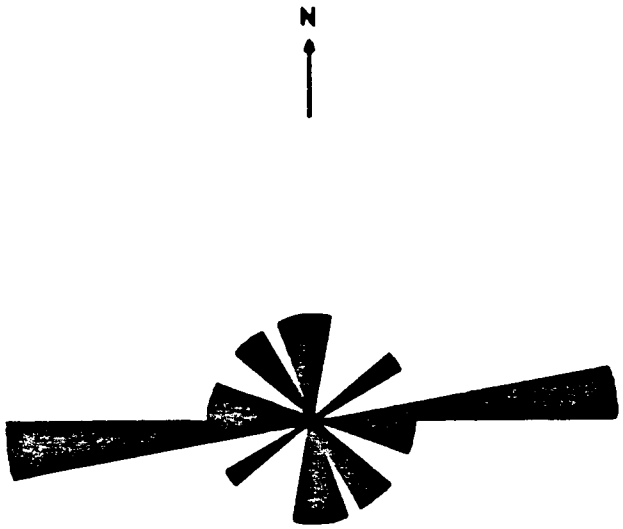

TOTAL BIDIRECTIONAL PALEOCURRENT INDICATORS

n = 11

Figure 53

paleocurrent directions derived from planar-tabular cross-beds and trough cross-beds (Figure 54). They are apparently part of the same population of measurements.

Four hypothetical subdivisions of the stratigraphic column were constructed to illustrate the changes in current direction through the Formation (Figure 55). Subdivisions were located solely on the basis of vertical groupings of the data which was dictated by the nature of the outcrops. Only 38 of the measurements can be placed on the stratigraphic column. They are grouped into the Hagan Shale Member, the lower Poor Valley Ridge Member, the middle Poor Valley Ridge Member, and the upper Poor Valley Ridge Member. Only one, the middle Poor Valley Ridge Member, is significantly ordered using α = .05 (sample size = 16). Vector mean for this subdivision is 293.9° (N66.1°W) and the magnitude of the vector mean (r) is .778.

When the unidirectional paleocurrent measurements for the entire section were analyzed, a strong unimodal vector mean of 329.9° (N30.1°W) was calculated. The distribution was significantly ordered, showing r to be 0.545 (Figure 56).

Interpretation of Data

Overall vector mean for the Clinch Sandstone is N30.1°W, which coincides with all previous paleocurrent measurements made on the Clinch Sandstone and equivalent units (Table 9). Inferred source direction for all of these localities is to the southeast. Alternatively, the source may have been east or northeast. Sediment may have

Figure 54. Comparison of planar-tabular vs. trough cross-bed paleocurrent indicators (length of wedges is proportional to number of observations).

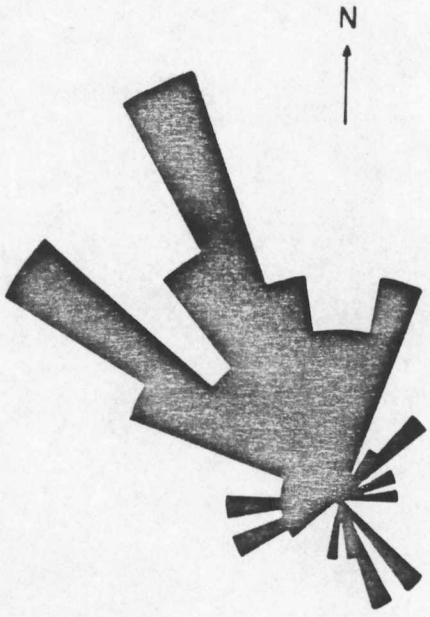

PLANAR-TABULAR
CROSS-BEDS
n=60



TROUGH
CROSS-BEDS
n=21

Figure 54

Figure 55. Stratigraphic breakdown of paleocurrent means in Clinch Sandstone.

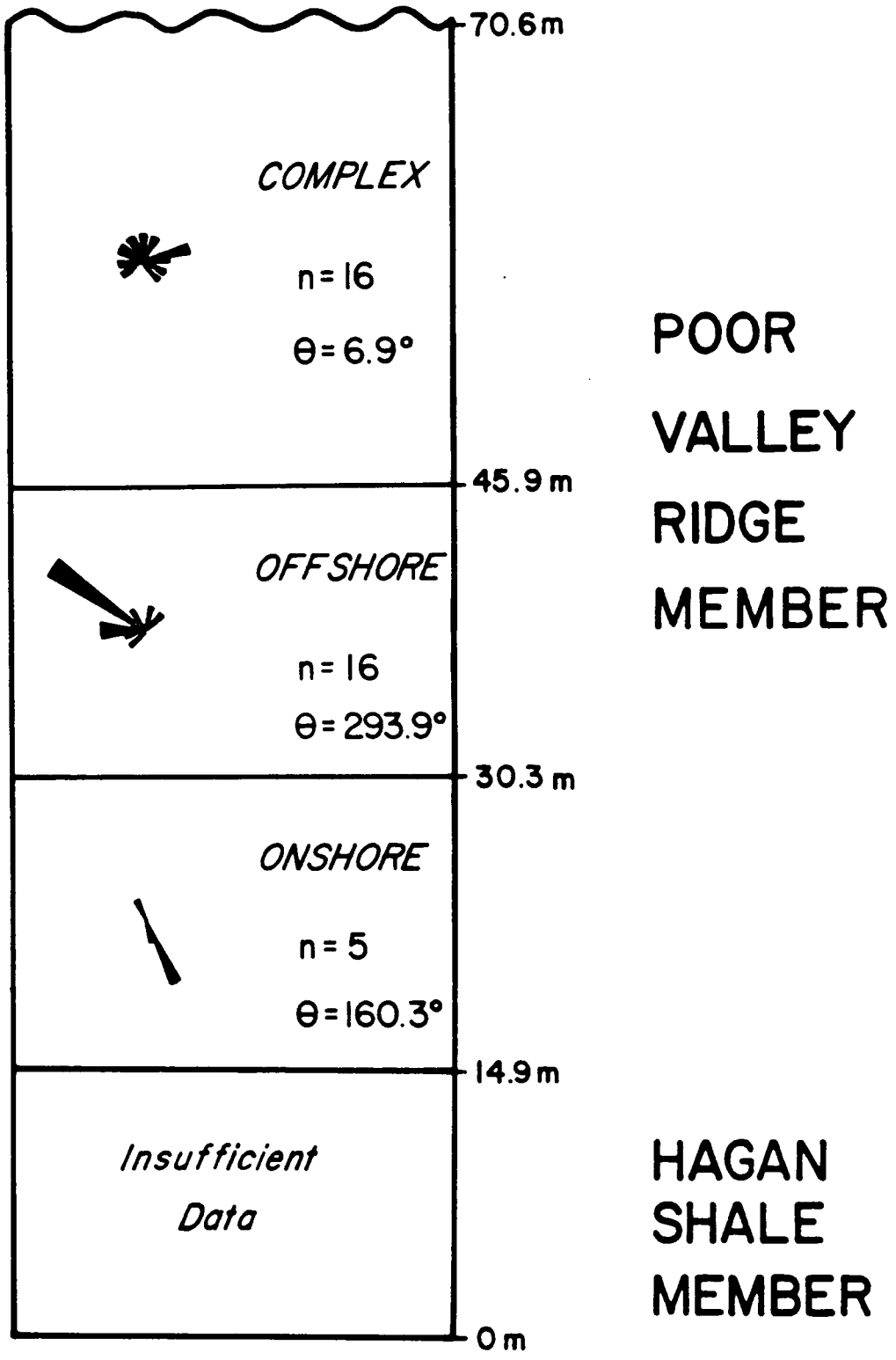
70.6m
COMPLEX
n=16
θ=6.9°
45.9m
OFFSHORE
n=16
θ=293.9°
30.3m
ONSHORE
n=5
θ=160.3°
14.9m
Insufficient
Data
0m
POOR
VALLEY
RIDGE
MEMBER
HAGAN
SHALE
MEMBER

Figure 55

Figure 56. Unidirectional paleocurrent indicators in Clinch Sandstone (length of wedges is proportional to number of observations).

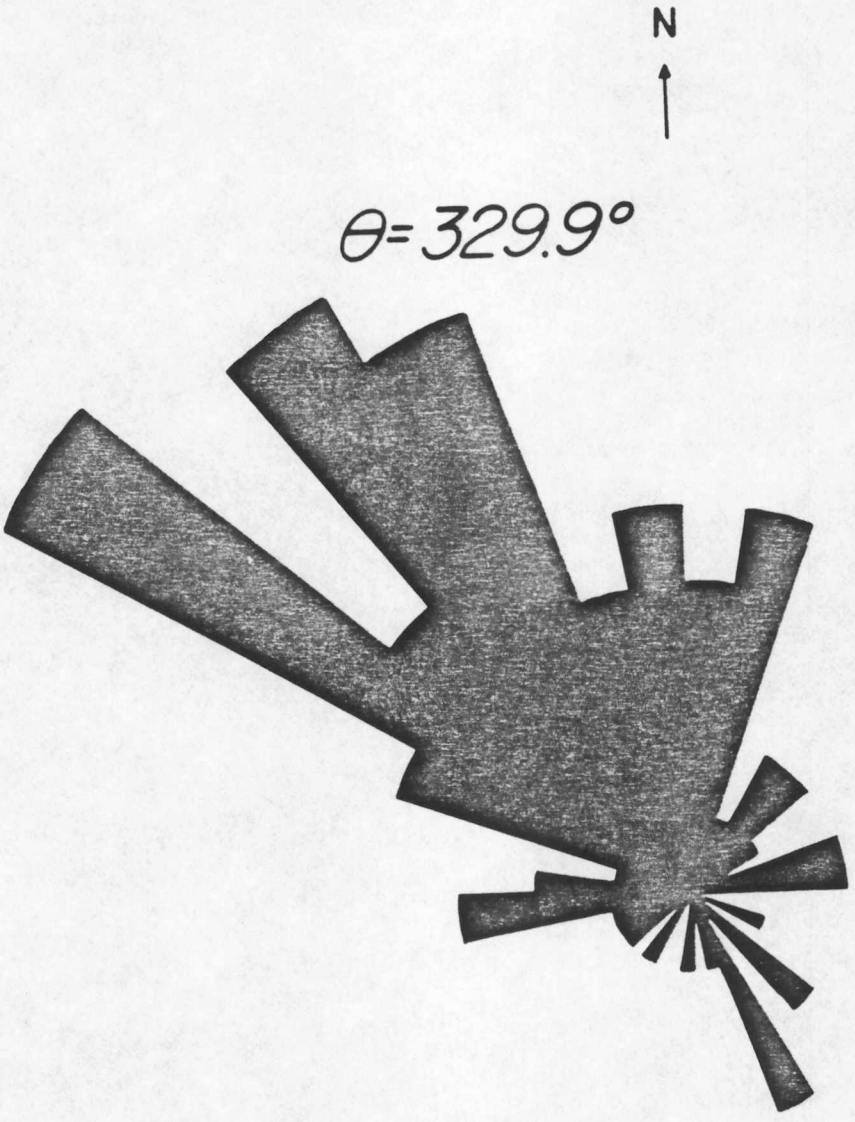

TOTAL UNIDIRECTIONAL PALEOCURRENT INDICATORS

$n=82$

Figure 56

Table 9. Paleocurrent Studies on Clinch Sandstone Lithostratigraphic Equivalents.

Author	Paleocurrent Vector Mean	Formation	Location
Yeakel (1962)	N38°W	Tuscarora	Central Appalachians
Martini (1971)	N34°W	Medina	New York and Ontario
Epstein and Epstein (1972)	N42°W N29°W	Shawangunk	Eastern Pennsylvania
Hayes (1974)	N29°W	Tuscarora	Southwestern Virginia
Whisonant (1977)	N48°W	Tuscarora	Western Virginia
Schoner (this study)	N30°W	Clinch	Northeastern Tennessee

been brought southwest by a longshore current and with reworking *in situ* by the tides, the cross-beds ultimately represent not source direction but prevailing ambient conditions. Mapping each value illustrates the parallel relationship between the means and supports the theory of a line source or linear depositional environment for Clinch Sandstone and equivalents (Whisonant, 1977) (Figure 57).

The linear nature of the Lower Silurian paleocurrents suggests a basin margin to the southeast of the study area. A major land area has been proposed to account for large aprons of Lower Silurian sediment (Dennison, 1970). This land area may have been of continental proportions (Whisonant, 1977). The likely source for these sediments is an uplift to the southeast which formed the Taconic highlands (Yeakel, 1962). The proposed mechanism for cross-bed formation (the most common paleocurrent indicator) is relatively slow piling up of water behind a barrier bar during flood tide. After reversal of the tidal phase, ebb tide and rip currents, especially intensified during high energy events such as storms, poured out through tidal inlets creating ebb-oriented planar cross-laminae (Reinson, 1979; Eliot, 1978). These cross-beds represent the migration of sand waves and dunes within the tidal inlets (Hunter et al., 1982). The parallel between shallow subtidal paleocurrents in east Tennessee and other proposed environments of Clinch Sandstone equivalents is probably a manifestation of coastal configuration and source location. Alluvial fan deposits, fluvial deposits and subtidal marine deposits are all represented in the northerly Tuscarora Formation outcrop belt (Cotter, 1982; 1983); all show northwesterly flow,

Figure 57. Map of paleocurrent vector means for Clinch Sandstone equivalents.



Figure 57

probably due to drainage off a SW-NE trending coastline. Measurements are needed from adjacent strike belts to determine the exact nature of all the Clinch/Tuscarora paleocurrents.

VII. LITHOLOGIC INTERPRETATION

Sedimentology

Facies

The lower Hagan Shale Member is a very slightly silty clayshale (facies A) which grades upward into interbedded clayshales and siltstones. This slight coarsening-upward trend continues into siltstones interbedded with fine sandstones (facies B) in the mid-section of the Member. Interstratified with this interval of sandstone-siltstone alternation are rare thicker siltstone to sandstone beds (facies C), which become more prevalent toward the top of the unit.

The nature of these lower Hagan Shale Member beds contrasts sharply with that of the underlying stratigraphic unit, the Upper Ordovician Juniata Formation. The upper Juniata Formation beds are maroon in color, with very thin- to medium-bedding, in contrast to the brown and green, irregular and thinly laminated lower Hagan Shale Member clayshales.

At Beans Gap, the Juniata Formation exhibits first a regressive, then a transgressive sequence (Ghazizadeh and Clement, 1985). This coincides with a significant glacioeustatic lowering of sea level in the Late Ordovician (Dennison, 1976) followed by a local slight deepening trend in the very Late Ordovician. A worldwide, rapid sea-level rise followed at the beginning of Silurian

time (Berry and Boucot, 1973; Leggett, 1978; McKerrow, 1979; Brenchley and Newall, 1980; Leggett et al., 1981).

These events are well documented in the uppermost Juniata Formation beds and lowermost Hagan Shale Member beds. The Juniata Formation has been interpreted elsewhere as an alluvial deposit (Yeakel, 1962; Meckel, 1970). The transgression that took place at the end of Juniata time is indicated by the change from continental and shallow marine characteristics (mudcracks, birdseye structures, and bryozoans) to slightly more open marine conditions near the top of the Juniata Formation (disappearance of the previously listed features and increase in bioturbation) (Ghazizadeh and Clement, 1985). A rapid increase in rate of transgression is postulated for the beginning of Hagan Shale Member deposition. This resulted in deposition of clayey to silty muds, characteristic of outer and, to some extent, inner marine shelf environments (Potter et al., 1980).

The most likely setting for Hagan Shale Member deposition is that of the so-called "transition zone," which includes sediments transitional between coastal sands and shelf muds (Reineck and Singh, 1980).

The trace fossils contained in the Hagan Shale Member allow for at least some environmental generalities to be stated. Present in the Hagan Shale Member are Arthrophycus, Skolithos, Rusophycus, Planolites, Monocraterion, and ?Chondrites. Arthrophycus is interpreted to be feeding burrows of arthropods or worms (Häntzschel, 1962). Skolithos is interpreted to be the dwelling burrows of worms, phoronids or crustaceans (Häntzschel, 1962; Diecchio, 1973; Frey,

1978). Rusophycus is a typical trilobite resting trace (Häntzschel, 1962; Frey, 1978). Planolites, created presumably by worms (Häntzschel, 1962), represents deposit-feeding traces (Heinberg and Birkelund, 1984). Monocraterion is interpreted similarly to and may represent the tops of uneroded Skolithos (Goodwin and Anderson, 1974; Heinberg and Birkelund, 1984). ?Chondrites is a dwelling or deposit-feeding burrow (Häntzschel, 1962; Frey, 1978). The presence of deposit-feeders (Arthrophycus, Planolites, and Chondrites) and suspension feeders (Skolithos and Monocraterion) indicates a changing energy environment, in which sediment and organic matter was agitated periodically so the suspension feeders could exist. Otherwise deposit feeders mined finer material which settled during times of quiescence.

The lowermost Hagan Shale Member deposits are predominantly clay (with interbedded silt layers) which were probably deposited as shelf muds. Such shelf mud deposits typically contain layers of coarse silt or fine sand which originate during intense storms (Hayes, 1967; Reineck et al., 1967; Gadow and Reineck, 1969). The degree of bioturbation is quite variable in these shelf muds. In the Gulf of Gaeta, Italy, even though the animal population is sparse, the amount of bioturbation is extreme (Reineck and Singh, 1980). Modern North Sea shelf muds contain very high animal populations and a high degree of bioturbation. Only storm sand layers show little bioturbation (Reineck and Singh, 1980). A deep sea or slope-rise paleoenvironment is not likely for the Hagan Shale Member

for the following reasons: (1) the sediments are not the characteristic dark gray to black color of deep ocean sediments, (2) the thickness of the Hagan Shale Member is relatively limited (14.9 m compared to hundreds of meters expected in stable slope-rise or deep ocean deposits), (3) no so-called "deep marine" trace fossils are present (such as Zoophycus or Nereites), and (4) the clayshales at the base of the member (the finest grained rocks present) are intercalated with beds that contain some silt, which may preclude a deep-sea depositional site. A shallow beach or deltaic environment is also not likely for the Hagan Shale Member because the typical high energy conditions of a beach or delta front system would tend to keep fine-grained material in suspension and produce a well-sorted sandstone deposit (Clifton, 1969). The Hagan Shale Member also shows no evidence for subaerial exposure. The depositional environment was, therefore, relatively far offshore because there is also no evidence for high-energy tractional currents as might be expected in the nearshore environment.

The outer North Sea shelf, then, seems to represent a possible modern analog for lower Hagan Shale Member deposition. Muddy sediment was deposited at the very base. Upward through the unit, increasing amounts of silt are present in the muddy layers. These silty clay layers commonly show a high degree of burrowing, which is visible as burrow mottling. Silt layers are intercalated with sandy layers, probably of storm origin (suggested by their sharp bases), which show less bioturbation. Upward in the section more

definitive traces appear (Rusophycus, Cruziana, Skolithos, Planolites, Monocraterion, possible Chondrites, etc.). This represents a shift from more distal outer shelf deposits to shoreface deposits upward through the Hagan Shale Member as continental influx becomes more dominant. There are rare, thin, problematic cross-beds in the Hagan Shale Member which indicate that some type of tractional flow affected the sediment. Klein (1977) stated that sandstone deposited on tidally reworked shelves commonly exhibit medium- to large-scale cross-sets. His tidally-influenced shelf model suggests that the medium-scale cross-beds in the Hagan Shale Member represent bed forms (sand waves and ripples) which migrated across sand sheets. A slight increase in energy upwards in the Hagan Shale may also be indicated by the upward increase in suspension-feeding burrows (Skolithos and Monocraterion) and may support a slight shoaling-upward origin. Even harder to explain is a conglomerate lens which occurs 12 m from the base of the Member, among the sandy siltstones of facies C. This conglomerate, which is limited in lateral extent, may represent a scour lag deposit of some kind deposited during a very high-energy storm, or the granule lag at the base of a small turbidity current, both of which are not common in the transition zone. No suitable origin fits the transitional environment model.

An alternative depositional model for Hagan Shale Member deposition would indicate that there was no rapid transgression at the Upper Ordovician/Lower Silurian boundary. Deposition instead continued in a marginal environment with only a slight deepening of

the water. The reason for the dramatic change in color from the deep maroon and buff of the Juniata Formation to the gray-green of the Hagan Shale Member remains unknown and may be due to a local undetermined chemical change. Nonetheless, with a slight deepening trend, the tidal flat of Late Ordovician time (Ghazizadeh and Clement, 1985) may have been flooded to form a lagoonal environment. The Skolithos and Monocraterion present in the Hagan Shale Member are most commonly associated with intertidal settings like those associated with a lagoon. The sandy layers and rare thin cross-beds may be the preserved portions of washover deposits. This lagoonal model also may better explain the conglomerate in the Hagan Shale Member. The pebble-sized sediment may be a beach lag (Blatt et al., 1980) that was carried into the lagoonal environment by a washover. The conglomerate is composed of some unstable rock fragments (siltstones), however, that are not representative of a common beach lag (Blatt et al., 1980). Also, there are no signs of subaerial exposure in the Hagan Shale Member, which are commonly associated with lagoonal/tidal flat deposits (Reinson, 1979). Apparently there is not a perfect fit for any Hagan Shale Member depositional model.

The Hagan Shale Member becomes coarser upwards and grades into the sandier beds of the Poor Valley Ridge Member. In these sandier beds a similar assemblage of trace fossils occurs. Diplocraterion, Monocraterion, Rusophycus, Cruziana, and abundant Arthrophycus are present in the lower sections of the Poor Valley

Ridge Member. Diplocraterion represents dwelling burrows in a similar environment to Skolithos (Narbonne, 1984) but the habit of many of the Diplocraterion examples in the Clinch Sandstone also suggests ongoing erosion (Goldring, 1964) coinciding with a higher energy environment of substantial sediment movement. Cruziana represents trilobite crawling traces (Seilacher, 1970) in the offshore, neritic environment (Rhoads, 1975; Crimes, 1975). Thalassinoides, a dwelling structure produced by crustaceans or similar organisms (but commonly found in younger rocks as stated by Häntzschel, 1962), is present in one similar bedding unit. It probably existed in the same high-energy nearshore environment as Skolithos (Crimes, 1975). Skolithos dominates at the top of the section.

Interpretations based on trace fossils have been very conservative and purposely vague in this study because there is not much substantiation for many of the interpretive claims made in past literature. Traces are best used for environmental interpretations when grouped in assemblages, because in bathymetric interpretations, the specifically named genera need not actually be present or may overlap into other assemblages (Frey, 1975).

Deposition of Hagan Shale Member transition zone clays and silts was followed by an uplift in the source area (the "Taconic Highlands") that contributed much coarser (sand-sized) material. Uplift initiated development of a progradational sequence, such that coarser Poor Valley Ridge Member sandstones were deposited over the finer Hagan Shale Member clayshales. During the initial stages of

progradation coarser sediments were seldom carried out onto the distal portions of the shelf by storm currents. As time passed and progradation continued, coarser material was carried further out onto the shelf. In the shallow-water alternative model the coarser material may represent shoreface or foreshore sands "backing over" the lagoonal fine-grained sediments. This coarsening-upward sequence can be seen in the lower Poor Valley Ridge Member rocks. The coarser quartz sand fraction may have been derived from a source terrain of uplifted Cambrian Chilhowee Group or Precambrian Ocoee Supergroup rocks. Bioturbation and deposition of interbedded clays and silts occurred during periods of quiescence between distal storm pulses (probably responsible for transport of sands). Storm-generated currents were also the likely mechanism by which older Juniata Formation intraclasts were scoured, ripped up and reworked into the younger Hagan Shale Member depositional environment.

In the Poor Valley Ridge Member of the Clinch Sandstone, the four delineated facies represent four different sets of environmental conditions (Driese et al., 1984). Facies 1 (trough cross-beds) represents migration of megaripples during very high-energy flow events. Flow depths of 3 to 5 m and velocities of 70 to 90 cm per second are estimated for the largest sets using the methods of Allen (1970) and Harms et al. (1982). Bedform migration was episodic, interrupted by suspension deposition of clays and bioturbation. Shale intraclasts up to 1.5 cm in diameter and rare deeply incised channel surfaces attest to periodic strong scour. Facies 2 (planar-tabular cross-beds) represents migration of sand waves during

high-energy flow events. Flow depths of 10-11 m and velocities of 60-80 cm per second are estimated for the largest sets using the methods of Allen (1970) and Harms et al. (1982). Bedform migration was somewhat more continuous than for Facies 1. Smaller bedforms (ripples) were typically superimposed upon, and migrated across the larger sand waves. Quartz pebble lags, with pebbles up to 2 to 3 cm in diameter, indicate some current velocities in excess of 150 cm per second (Hjulström, 1935), which scoured and reworked sand wave tops. Facies 3 (densely bioturbated sandstone) represents periods of very low-energy and reduced sediment influx; bioturbation was able to continually keep pace with physical sedimentation processes (Howard, 1978). However, at least moderate agitation seems indicated by the prevalence of suspension-feeding types of trace fossils. Facies 4 represents deposition characterized by alternating high-energy events (horizontally laminated and rippled sandstones) and low-energy events (suspension deposition of clays followed by bioturbation). All of these Poor Valley Ridge Member deposits represent deposition in a subtidal, marine environment with probable water depths between approximately 3 and 20 m. An increase in the energy of the Poor Valley Ridge Member environment relative to the Hagan Shale Member is indicated by the predominance of larger-scale bedforms (from 50 cm thick in the Hagan Shale Member and the lower 20 m of the Poor Valley Ridge Member to 150-200 cm thick cross-sets in the upper part of the Poor Valley Ridge Member), gravel lags, and large (up to 2-3 cm in diameter) clayshale intraclasts. Poor Valley

Ridge Member deposition was more continuous than that of the Hagan Shale, yet there were many interruptions, represented by clay drapes and zones of increased bioturbation.

Depositional Setting

These facies, which are so intimately interstratified and intertonguing in outcrop, describe an environment of high-energy and low-energy fluctuation. Rare reactivation surfaces and abundant clay drape laminae suggest a nearshore, tidally-influenced setting (Kumar and Sanders, 1974; Klein, 1977; deMowbray and Visser, 1984). Of the environments characterized by mature, quartz-rich, cross-bedded sandstones that contain marine trace fossils, the following are most likely: an estuary, a delta, a tidal flat/beach complex, an open-marine shelf and a barrier-bar system. Fluvial, eolian, alluvial fan, and lacustrine settings are impractical due to the abundance of marine trace fossils in the Clinch Sandstone. Continental slope and submarine fan settings are also improbable because the Clinch Sandstone is a well-sorted, mature, quartz sandstone.

An estuarine model, however, is unlikely because marine trace fossils are present almost throughout the entire unit and marine forms are commonly present only in estuarine lower reaches (Clifton, 1982). The Clinch Sandstone is also probably not a result of estuarine deposition as Clifton (1982) stated that estuaries are areally limited (which the Clinch Sandstone is not) and commonly exhibit herringbone cross-strata and bimodal paleocurrents (which the Clinch Sandstone does not). The strong unimodality of the Clinch

Sandstone current directions also precludes a subaqueous deltaic depositional environment, because deltaic sediments, though river-dominated, are typically affected by waves and tides and, therefore, commonly show bimodal paleocurrents (Coleman and Prior, 1982). Channel and channel-fill structures are also far more abundant in recognized ancient deltaic deposits than in the Poor Valley Ridge Member of the Clinch Sandstone, where they are very sparse (Coleman and Prior, 1982).

The marine trace fossils present in the Poor Valley Ridge Member, however, partially suggest a marginal marine environment, such as a tidal flat. In the tidal flat environment abundant trace fossils are well preserved, commonly showing low diversity and high abundance (Weimer et al., 1982). Skolithos and other vertical tubes, abundant in the Poor Valley Ridge Member, typify tidal flat trace fossils (Rhoads, 1975). Except for similarity between trace fossil assemblages, though, only a very small portion of the Poor Valley Ridge Member actually might consist of tidal flat deposits. The thinly laminated siltstone interval, between 37 and 40 m up from the base of the Formation, Horizon C (Figure 58) may represent a tidal flat deposit, even though it shows no signs of subaerial exposure. Even more likely is that the siltstone represents deposition in a back bay or lagoon environment fed by periodic washover fans. Parts of the washover fans were preserved in surrounding horizontally laminated beds (facies 4); planar subhorizontal to horizontal beds are associated with washover fans (McCubbin, 1982).

Figure 58. Portion of thinly laminated siltstone interval (2.46 m thick) in Poor Valley Ridge Member. Ruler is 30.5 cm long.



The two most probable depositional environments for the Poor Valley Ridge Member of the Clinch Sandstone are sandy, tidally-influenced continental shelves and asymmetric, tidally-influenced barrier-bar systems. The former commonly contain large-scale bedforms such as megaripples and sandwaves (Klein, 1977), which form large-scale cross-stratification. Planar horizontal laminations and interbedded silts and clays, with high amounts of bioturbation, are typical shallow-marine shelf characteristics (Klein, 1977; Walker, 1979; Bouma et al., 1982) found in the Poor Valley Ridge Member. There are, however, several important attributes of sandy continental shelves which are not present in the Clinch Sandstone. Most important of these is hummocky cross-stratification, which is produced by storm waves (Walker, 1979). Though there are several styles of cross-stratification present in the Clinch Sandstone none can be classified as hummocky cross-stratification. To produce the large-scale cross-beds present in the Poor Valley Ridge Member a strong current of some kind must have influenced the marine shelf bottom at least episodically. Deep-reaching tidal currents and/or storm currents may have been responsible for the deposition of the Poor Valley Ridge Member, but their geometric relationships and strongly unimodal paleocurrents preclude either tides or storms as the dominant origin. Tides, even when distinctly asymmetrical, produce herringbone cross-stratification and/or reactivation surfaces (Klein, 1977). Storms approach from multiple directions, most influenced by seasonal weather track shifts (Fox and Davis, 1976). These variably oriented storms and their associated currents would

produce a complex paleocurrent pattern in continental shelf deposits (Bouma et al., 1982).

The strongly unimodal Clinch Sandstone paleocurrents, predominantly large-scale cross-beds, abundant marine traces and rare oscillation ripple marks suggest a nearshore, high-energy and low-energy, mesotidal to macrotidal rip channel/tidal inlet sequence cutting a barrier-bar system. Table 10 lists modern barrier and associated environments and the characteristics they have in common with the Poor Valley Ridge Member. A meso- to macro-tidal system is inferred because microtidal environments do not contain the channels or inlets which serve to generate and ultimately preserve large-scale structures (Hill and Hunter, 1976). A generalized profile is illustrated and shows the location of offshore bars (Figure 59).

Unimodality of paleocurrents in these examples is still not as strong as that of the Clinch Sandstone but ebb-oriented structures (as these would be assuming a NE-SW trending shoreline; Section VI on paleocurrents) are the major result of rip current flow. Offshore dipping cross-beds are more commonly associated with barred nearshore sequences than nonbarred (Hunter et al., 1979). "Ebb-oriented," "seaward-dipping" or "offshore-facing" cross-stratification has been described from numerous modern rip channel/tidal-inlet barrier-bar sequences (Davidson-Arnott and Greenwood, 1976; Kumar and Sanders, 1974; Hunter et al., 1979). The setting was likely one in which flood tide came in gradually, building water up behind the bar until ebb flow began. As the water level fell at a faster rate than it

Table 10. Similarities Between the Clinch Sandstone and Modern Bar and Associated Environments.

Author	Location	Setting	Product	Depositional Process
Davidson-Arnott and Greenwood (1976)	Kouchibouguac Bay, New Brunswick	almost totally submergent bars off barrier island (2 bars parallel to beach)	seaward-dipping cross-beds (up to 20 cm thick) in rip current channels (vel=75+ cm/sec) or over bars	megaripple migration influenced by rip currents
Hill and Hunter (1976)	Padre Island, Texas (microtidal - 51.8 cm diurnal range)	submerged bar trough system	planar laminae (commonly bioturbated)	high waves, upper flow regime (?)
Hunter et al. (1982)	NE Bering Strait (inner shelf)	edge of Yukon Delta, seaward of delta plain	asymmetric ripples on flanks of subaqueous distributary channels; sand waves in channels, seaward-facing	high flow velocities due to high discharge
McCubbin (1982)	Generalized from: Howard and Reineck (1979) Ventura Oxnard coast, Calif.; Bernard et al. (1962) Galveston Island, Texas	upper shoreface	high angle tangential cross-strata in trough shaped sets in rip current channels	oscillation motion (shore-normal)
		lower shoreface	parallel laminated fine sand and coarse silt interbedded with bioturbated muds	river flood-nearshore sediments are redistributed offshore by storm-induced waves
Kumar and Sanders (1974)	Fire Island, New York	Tidal inlet deep channel	ebb-oriented cross-laminae with gently dipping flood-oriented reactivation surfaces	ebb-oriented large sandwaves (ebb>flow)
		shallow channel	plane-parallel beds	upperflow (ebb>flow)
		Spit platform bottomset	ebb-oriented cross-laminae	ebb-oriented megaripples (ebb>flow)
		Beachface	steeply, gently dipping laminae; wide range of directions	swash and backwash (upper flow regime)
Hunter et al. (1979)	Southern Oregon coast	partially submerged oblique bars with longshore trough and rip channel	seaward-facing tough cross-beds, seaward-facing tabular cross-beds (vel=40-80 cm/sec)	lunate megaripples sand waves (20-50 cm high)

Figure 59. Generalized profile of a nearshore marine environment (after Reinson, 1979).

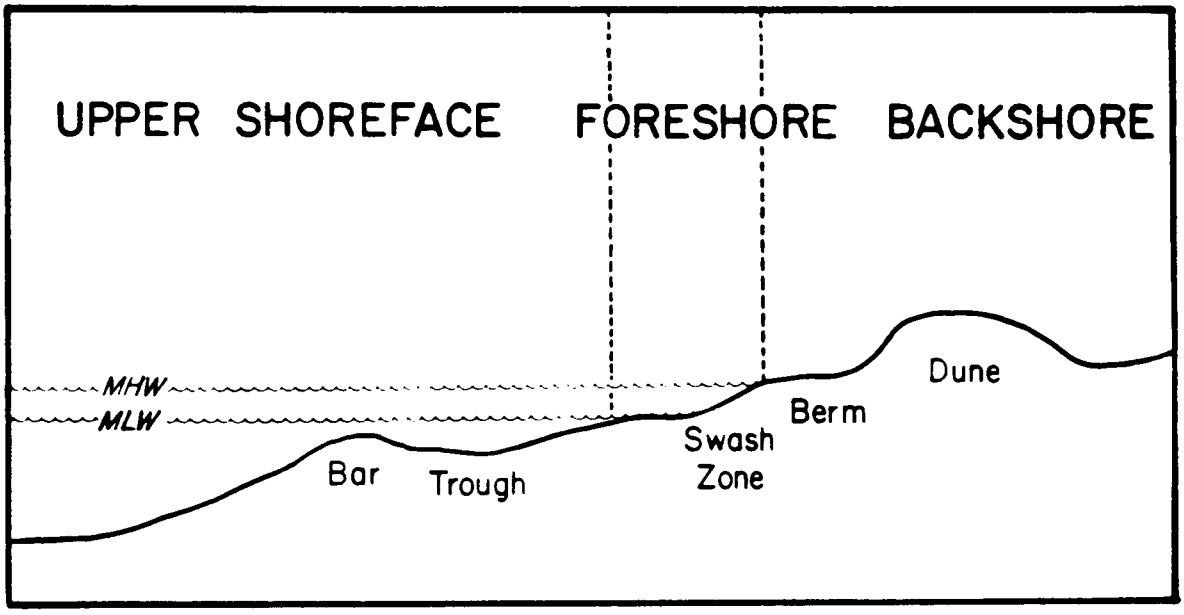
UPPER SHOREFACE
FORESHORE
BACKSHORE
MHW
MLW
Bar
Trough
Swash
Zone
Berm
Dune

Figure 59

rose, strong rip currents rushed out through the permanent tidal channels. Predicted speeds from Poor Valley Ridge Member sedimentary structures range from 60 to 90 cm per second. Documented velocities in modern tidal channels of 40 to 90 cm per second (Hunter et al., 1979) and 75 cm per second (Davidson-Arnott and Greenwood, 1976) correspond to those reflected in Poor Valley Ridge Member cross-beds.

The cross-bedding found in barrier-bar tidal channels may be trough or planar-tabular and is formed by migration of megaripples and sandwaves (Davidson-Arnott and Greenwood, 1976; Kumar and Sanders, 1974; Hunter et al., 1979). These are common in the geologic record as products of channelized rip current flow (Eliot, 1978). Small-scale ripple marks, which are less common than large-scale cross-beds in the Poor Valley Ridge Member, represent oscillation and current ripple bedforms. Ripples may form in trough regions landward of the submerged bars (Davidson-Arnott and Greenwood, 1976), on the seaward bar slope (Hill and Hunter, 1976; Davidson-Arnott and Greenwood, 1976), in the shoreface (Reinson, 1979), or in the foreshore (Eliot, 1978). Very rare reactivation surfaces are preserved in the Poor Valley Ridge Member. They represent reversing current direction which may occur in the deep channel (Kumar and Sanders, 1974). Clay drapes preserved on foresets like those in facies 1 trough cross-beds are common in tidal channels (Eliot, 1978; deMowbray and Visser, 1984). These fine-grained drapes are formed during the periods of time, at the turn of the tide, when velocities in the channels are close to zero (deMowbray and Visser, 1984). Fine-grained sediment falls out of

suspension and is deposited on the surface of exposed foresets. Cases in which the reverse current is very weak show no erosion of the mud drape, only thin sand deposited over it, which is, in turn, buried by sand from the next tide reversal (deMowbray and Visser, 1984). Bioturbation is also common in tidal channels where burrowing organisms destroy physical sedimentary structures (Hill and Hunter, 1976) and may leave abundant traces in the lower shoreface (Howard, 1972) or on the seaward bar slope (Davidson-Arnott and Greenwood, 1976). Alternating bioturbation (low energy) and high energy, as seen in facies 4 and to some extent in facies 1, has been described in modern barrier sequences (Howard and Reineck, 1972a and b). The quartz-rich nature of the Clinch Sandstone also fits a migrating barrier sequence model (Eliot, 1978), in which surprisingly, progradation of a rip channel/tidal inlet complex preserves little or none of the bar facies itself (Hunter et al., 1979). In a barrier-bar depositional environment, rip channels, the bar trough, and lowermost extreme bar slope are most likely to be preserved (Davidson-Arnott and Greenwood, 1976). It is the previously mentioned progradation of the entire beach to offshore facies including rip channel/tidal inlets that produces coarsening-upward sequences like that of the Clinch Sandstone (Hunter et al., 1979; Eliot, 1978; Davidson-Arnott and Greenwood, 1976). An ideal sequence can be seen in Figure 60 in which bioturbated offshore silt, emplaced by slow deposition with rare periods of higher energy, is overlain by lower shoreface, bioturbated silty sand and sand. The lower shoreface deposits are commonly parallel laminated and are

Figure 60. Ideal prograding beach-to-offshore sequence (modified from Howard and Reineck, 1979; and McCubbin, 1982).

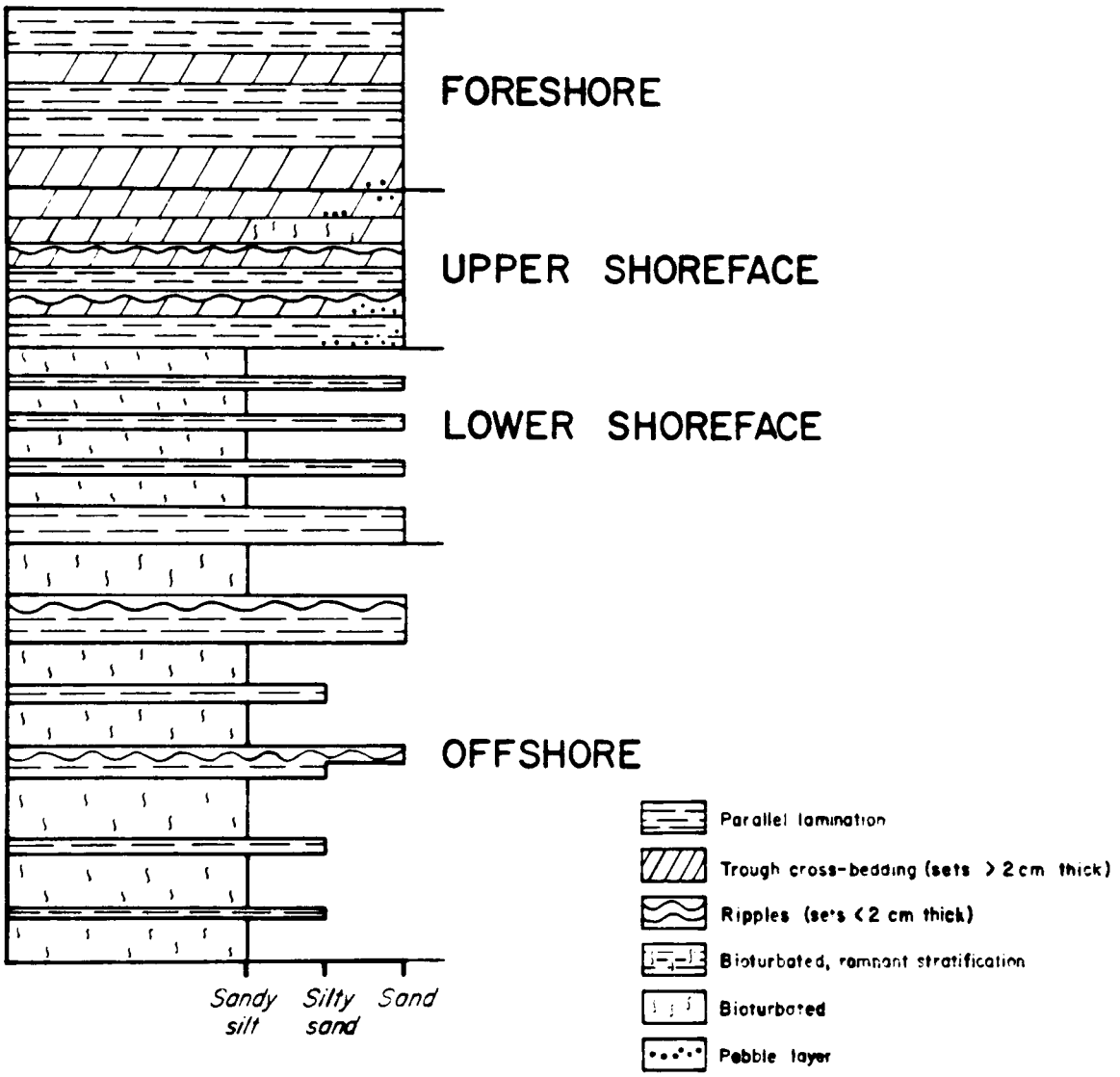
FORESHORE
UPPER SHOREFACE
LOWER SHOREFACE
OFFSHORE
Sandy silt
Silty sand
Sand
Parallel lamination
Trough cross-bedding (sets > 2 cm thick)
Ripples (se's < 2 cm thick)
Bioturbated, remnant stratification
Bioturbated
Pebble layer

Figure 60

produced by storm surge and slow gravitation deposition. These beds are overlain by fine- to medium-grained, sandy upper shoreface deposits containing isolated pebbles. The upper shoreface is subtidal and dominated by wave surge and wave currents, producing trough cross-stratification, ripples and parallel lamination. Some bioturbation is present. Foreshore deposits cap this prograding barrier sequence and are low-angle seaward-dipping laminae and some trough cross-stratification produced by intertidal wave swash processes (McCubbin, 1982).

The overall vertical sequence of the Clinch Sandstone shows numerous environmental shifts. Extensive lithologic descriptions can be found in Appendix D. From the outer shelf to the more prominant inner shelf (Hagan Shale Member rocks), storm events rarely produced small- to medium-scale bedforms. Overall quiescence is indicated, however, by the abundance of trace fossils (Figure 61). At the Hagan Shale Member-Poor Valley Ridge Member contact a substantial increase in the proportion and scale of physical sedimentary structures occurs. Oscillation ripples in Poor Valley Ridge Member horizon A (Figure 55, p. 145, and 61) suggest that progradation had reached the point that the depositional environment was affected by more day-to-day wave and tidal processes. Horizon A represents a higher-energy environment than the Hagan Shale Member, as is signified by the presence of onshore-directed cross-beds, although the data are somewhat sparse (Figure 55), intraclasts, a coarse sand lag and a clayey rip-up lag. Horizon A represents shoreface deposition (Figure 61) similar to that found at Fire Island, New York: basal gravel→evenly laminated sand→

Figure 61. Proposed paleoenvironments for Clinch Sandstone at Beans Gap (adapted from Reinson, 1979).

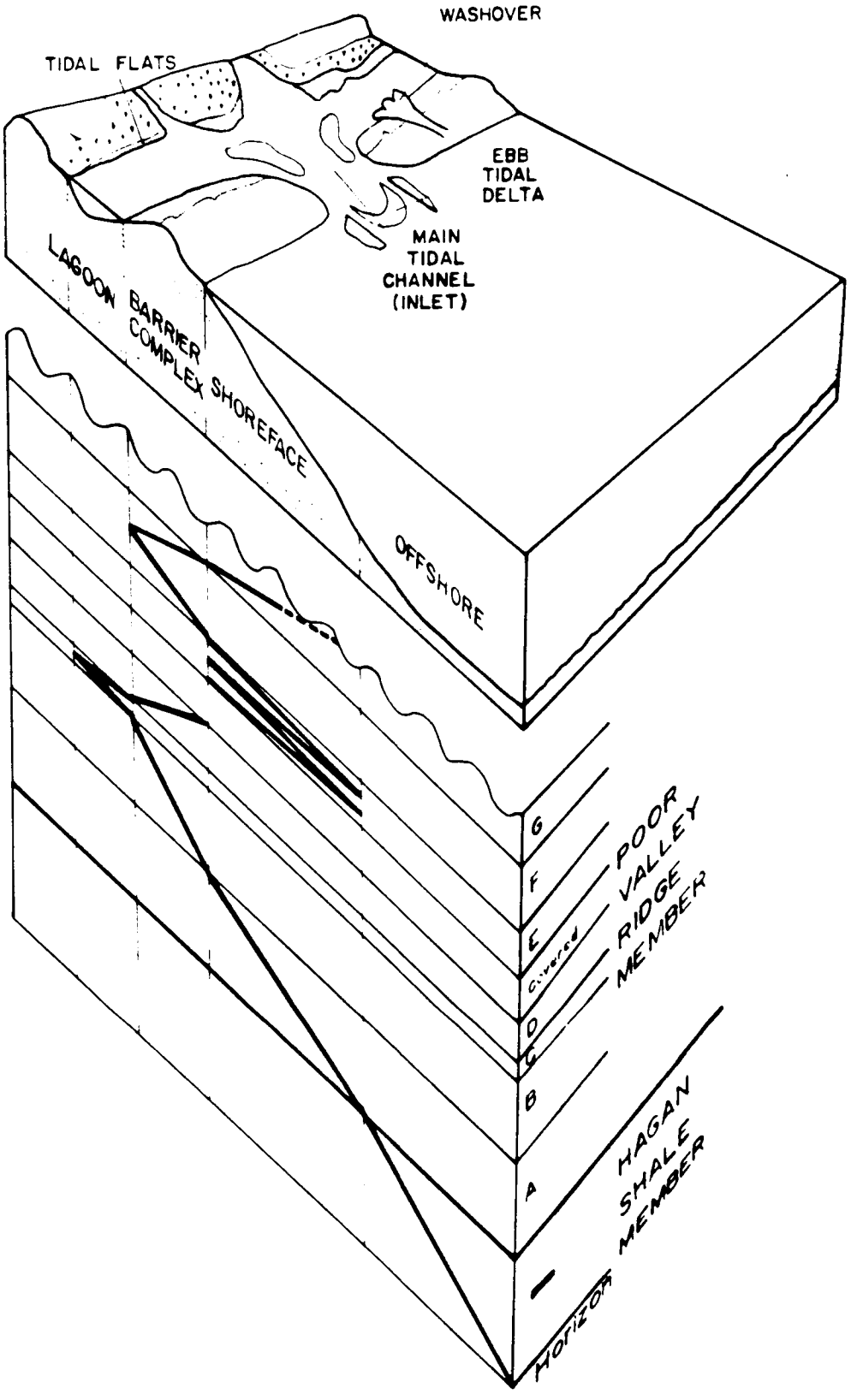
WASHOVER
TIDAL FLATS
EBB TIDAL DELTA
MAIN TIDAL CHANNEL (INLET)
LAGOON
BARRIER COMPLEX
SHOREFACE
OFFSHORE
G
F
E
Covered
D
C
B
A
POOR VALLEY RIDGE MEMBER
HAGAN SHALE MEMBER
HORIZON

Figure 61

bioturbated or wave rippled laminae (Kumar and Sanders, 1976). Upward in the Clinch Sandstone, in horizon B, however, paleocurrents reverse (Figure 55, p. 145) and are directed offshore, silt layers become more predominant as does cross-stratification. This portion (horizon B) of the Formation (Figure 61) represents rip channel/tidal inlet deposition characterized by megaripple and sand wave migration, scour episodes, and low-energy periods of deposition and bioturbation of silty sediment. The inlets cut barriers which were probably almost always submerged. This is supported by the lack of subaerial exposure features in the Clinch Sandstone. The barriers may have been exposed briefly, however, at times of very low tide. Horizon B is overlain by the extensive siltstone section (horizon C), discussed previously, which was probably deposited in a protected back-bay or lagoonal environment of lower energy.

Overlying the fine-grained deposits of horizon C are more rip channel/tidal inlet beds (horizon D) with ebb-oriented planar-tabular and trough cross-beds, pebbles and a thin siltstone layer. A thin section (horizon E) overlies these rip channel/tidal inlet deposits (the sequence is interrupted by a covered section) which may represent lower shoreface and upper shoreface fluctuations. Oscillation ripples, multidirectional paleocurrents, some bioturbation, cross-beds and fine pebbles may represent a return to a more wave-influenced environment in horizon E. An increase in siltstone layers and a predominance of planar-tabular cross-beds indicates a return to the rip channel/tidal inlet environment where bioturbation again becomes abundant

(horizon F). The top of the section (horizon G) is characterized by well-sorted sands, commonly planar bedded. Horizon G likely is the result of deposition in a wave-dominated setting characterized by oblique wave approach to shore as indicated by the polymodal paleocurrents (Figure 55, p. 145).

An Early Silurian transgression is recorded at Beans Gap which placed the Clinch Sandstone in a marine shelf environment. Shelf deposition, which accounts for a major part of the Tuscarora Formation in Pennsylvania (Cotter, 1982; 1983), persisted for only a relatively short time in the southern Appalachians. A "major (sediment) input center" in western Pennsylvania, proposed by Cotter (1982), may explain the rapid progradation recorded in Clinch sediments that is not present in the central and northern Appalachians. Progradation then dominated throughout the earlier half of southern Appalachian Clinch time. The deposits record a shoaling-upward sequence which is overlain by a back bay/lagoonal siltstone (Figure 61). The shoaling event was then followed by shifts in environments ending in a return to a slightly deeper, higher-energy environment (the shoreface) at the present top of the Formation.

Distinct differences exist between the uppermost Clinch Sandstone deposits and the uppermost Tuscarora Formation deposits. Cotter (1982, 1983) proposed a reduction in sediment influx coinciding with sea-level lowering for the cause of fine sediment deposition in the uppermost coastal sand and mudflat rocks (the Castanea Member). The high-energy shoreface deposits which cap the Clinch Sandstone at Beans Gap do not record this reduction in sediment influx or

regression. The last regression of Tuscarora/Clinch time, if it occurred in the Southern Appalachians, therefore, has not been preserved along Clinch Mountain. Erosion may have removed up to 30 m of Clinch Sandstone (Dennison and Boucot, 1974; Miller and Fuller, 1954). Beds resembling the Castanea Member are, however, present in roadcuts at the Clinch Sandstone/Rose Hill Formation contact near Abingdon, Virginia. It is these missing rocks which may record a fining-upward segment in the regressive sequence as is displayed in Pennsylvania. The southern equivalent to the overlying marine Rose Hill Formation of the Northern and Central Appalachians may also have been eroded at Clinch Mountain, removing the evidence for the Lower Silurian-Middle Silurian transgression seen in Pennsylvania and in southwestern Virginia.

Petrography

The dominant mineral in the Clinch Sandstone is undulose monocrystalline quartz showing neither mineral nor fluid inclusions. Undulose extinction was noted in each sample but not measured with a universal stage, thus interpretations based upon degree of undulosity may be less than valid. The undulose nature of the monocrystalline quartz does indicate that the grains have been deformed either during crystallization or after deposition (by tectonic processes) (Blatt and Christie, 1963). Scarcity of inclusions suggests an igneous origin but is not conclusive (Scholle, 1979). Polycrystalline quartz is uniformly coarsely crystalline, commonly with more than 5 crystallets per quartz grain. It is present in quantities up to 8% and may

be derived from igneous or metamorphic rocks, sandstones and cherts (Pettijohn et al., 1973), although chert is classified separately in this study. In Folk's (1974) classification the Clinch Sandstone varieties are either plutonic (with few inclusions) or recrystallized metamorphic (straight boundaries between equant interlocking crystallets).

Several varieties of feldspar are present in the Clinch Sandstone. The plagioclase feldspars are composed of andesine and oligoclase. These sodic feldspar varieties are most common in sandstones (Pettijohn et al., 1973). The only identified potassium feldspar is microcline, though some untwinned orthoclase (resembling quartz) may also be present. Proportions of feldspar varieties are controlled by two factors: source mineralogy and the characteristics of the transport and depositional environments. The feldspars in the Clinch Sandstone comprise a suite that reflects both source composition and stability, because sodic feldspars are not only more common but also more stable than calcic feldspars (Pettijohn et al., 1973). Potassium feldspars are the chemically most stable of the feldspars (Blatt et al., 1980; Leeder, 1982), which is reflected here to some degree in the prevalence of microcline. Due to low feldspar quantities (<1%) in the Clinch Sandstone there is little substantive evidence for source interpretation of any kind. Micas are also present in very low amounts (1% or <1%) and are ambiguous with respect to interpretation of origin. Muscovite occurs more commonly than biotite or chlorite in the Clinch Sandstone, but these

occurrences are probably not related to source, because muscovite is much more resistant to chemical weathering than either biotite or chlorite (Scholle, 1979; Pettijohn et al., 1973). Biotite, when abundant, may indicate a volcanic source, but when present in low amounts may be derived from all types of igneous and metamorphic terrains (Scholle, 1979).

The Clinch Sandstone detrital matrix is composed of smectite and illite/sericite, with kaolinite occurring more commonly as a replacement mineral. These phyllosilicates are considered unstable due to the exchangeable nature of the interlayer position. Ions move into and out of these interlayer positions and structural changes occur in response to ambient chemical composition, thus creating mineral changes in the phyllosilicates (Pettijohn et al., 1973).

The rock fragments present in the Clinch Sandstone are very limited in quantity and diversity and only include siltstone fragments in one Hagan Shale Member sample and rare metamorphic rock fragments in the Poor Valley Ridge Member. Rare occurrences of rock fragments may be attributable to their tendency to disaggregate (Scholle, 1979), whereas higher rock-fragment quantities are typically associated with coarse sediments (Hunter, 1967; Blatt et al., 1980). Evidence for this is present in the Clinch Sandstone where the highest quantity of rock fragments occurs in the conglomeratic bed within the Hagan Shale Member. Other than to say the siltstone rock fragments were derived from a siltstone and the metamorphic rock fragments from a metamorphic terrain, little can be concluded from examining rock

fragments as analogies are rare to nonexistent (Pettijohn et al., 1973). Heavy minerals do not show any significant trends through the section as would reflect substantial source area changes (e.g., unroofing a pluton). Zircon and tourmaline, dominant heavy minerals in the Clinch Sandstone, occur primarily in igneous rocks, particularly granites (Lindsay, 1981) but can also be found in metamorphic rocks. The shape and nature of the zircon grains present in the Clinch Sandstone most closely represents those of migmatitic or gneissic origin (Pupin and Turco, 1983). Zircon's hardness and lack of cleavage make it very stable and characteristic of mature sandstones (Blatt et al., 1980). Tourmaline is almost as hard and also lacks good cleavage (Kerr, 1977). Both minerals occur in very low quantities in igneous (Scholle, 1979) and metamorphic rocks but their amounts become enriched during transport and deposition as detrital components because they are quite stable. Hornblende, present in 22 samples, is typically green, the most common color in detrital rocks, and may represent a metamorphic-granitic source (Scholle, 1979).

The fossils found in the Hagan Shale Member of the Clinch Sandstone were probably washed in from an adjacent environment, because they are so rare and breakage and abrasion is apparent (some of which may have occurred in situ). These phosphatic brachiopods are postulated to have lived in brackish, intertidal environments, but they have also been found living in a variety of other environments. Thus, their interpretive value is limited (Clarkson, 1979).

The maturity of the quartz arenites, quartz wackes and the subarkosic wacke that comprise the Clinch Sandstone shows great

variation over time. The textural maturity does not imply any progressive change in source or depositional environment such as Hayes (1974) found in the Tuscarora Formation in southwestern Virginia. Most of the quartz grains are rounded, showing a slight increase in angularity upwards that may be attributable to a change in environment or source. Much of the Clinch Sandstone at Beans Gap has been characterized in this study as well-rounded or rounded to well-rounded, which is slightly more mature than the Virginia equivalents (Hayes, 1974). This and abraded overgrowths suggest a multicyclic nature for the Clinch Sandstone and, hence, a sedimentary source (Friedman and Sanders, 1978).

Sorting also varies over the section but shows no pattern or trend, similar to the sorting in the Tuscarora Formation to the northeast (Hayes, 1974). A possible explanation for the poorly sorted nature of many sediments is the likelihood of framework grain alteration creating fine-grained replacement products, which appear to be matrix (especially after slight deformation has occurred).

The mineralogic maturity of the Clinch Sandstone is high when presence of matrix and replacement products is ignored. The source terrain probably included quartz-rich sedimentary rocks such as the Cambrian Chilhowee Group (as has also been proposed by Folk, 1960, and Hayes, 1974).

The Clinch Sandstone at Beans Gap is characterized by a much more limited mineral suite than the Tuscarora Formation to the

northeast (Folk, 1960; Laughrey and Donahue, 1983; Cotter, 1983), except for Hayes' (1974) study in southwestern Virginia in which matrix constituents were only noted, but not quantified. Folk (1960) and Hayes (1974) did find much more variation to the quartz types present in the Tuscarora Formation in West Virginia and Virginia, however, than is present in the Clinch Sandstone in Tennessee. In the Clinch Sandstone of east Tennessee, almost all of the monocrystalline quartz is strained and of a plutonic origin. The Tuscarora Formation (Virginia) rocks show vein and pressure quartz in addition to plutonic (Hayes, 1974), which are not present in appreciable amounts in the Clinch Sandstone at Beans Gap. Folk's (1960) division of the Tuscarora Formation in West Virginia into three parts, the red Tuscarora, lower white Tuscarora and upper white Tuscarora, immediately suggests a different depositional environment, source, or both of these two equivalent stratigraphic units. In east Tennessee there is no equivalent to his lowest subdivision, the red Tuscarora, which is characterized by well-developed unimodal cross-bedding, clay and silt matrix, clay galls, an abundant suite of metamorphic rock fragments and an absence of shale interbeds. The lower white Tuscarora shows sparse metamorphic rock fragments, moderate to poor sorting and moderate and variable rounding (Folk, 1960). The lower part of the Poor Valley Ridge Member (approximately 14 m to 20 m above the Hagan Shale Member) shows similar moderate to poor sorting and variable rounding. These two subdivisions may be stratigraphically equivalent. The upper part of the Tuscarora Formation, described as containing only rare chert and metamorphic rock fragments, with high

rounding and sorting seems to be similar (mineralogically) to the upper Poor Valley Ridge Member in east Tennessee. The upper Poor Valley Ridge Member is rounded to well-rounded, yet shows variable sorting. These two segments, the upper white Tuscarora and the Upper Poor Valley Ridge Member may be lithostratigraphic equivalents as well. The variable nature of the sorting in the Poor Valley Ridge Member is probably due to two major factors: (1) tidal processes acting on the sediments subjected them to continuous changes in velocity, resulting in considerable mixing and (2) the lateral shifting of the environments through time, some of which reworked the sediment better than others. The fluvial origin proposed for part of the Tuscarora Formation to the northeast (Folk, 1960; Yeakel, 1962; Cotter, 1983) is unlikely in Tennessee because the composition of the Clinch Sandstone is quite mature; framework grains are almost totally quartz and the matrix may be totally authigenic. A beach interpretation for the Clinch Sandstone (as proposed by Nicholson (1978) is suggested by the very mature mineralogy but is rejected on the basis of significant sedimentolgic characteristics, most specifically, unimodal paleocurrents and water depths of at least 3 to 5 m for much of the Poor Valley Ridge Member. A nearshore, shallow-marine origin is more likely. It is in this environment of high and low energy alternation (due to tidal influence) that rounding would be high but sorting would vary, like that found in the Poor Valley Ridge Member.

Rounding remains constant throughout the majority of the unit, not only because the energy of the environment was high, but also because the source remained constant. To deposit mineral suites with such limited variety either a uniform igneous or metamorphic terrain was eroded, a pre-existing sandstone was eroded, or substantial reworking and chemical and physical weathering occurred. Because metamorphic rock fragment quantities are low and no igneous minerals (rock fragments or straight extinction quartz) are present, the first possibility is unlikely. Reworking has occurred to a rather high degree, and post-depositional chemical weathering has altered the few unstable framework grains to phyllosilicates. Undoubtedly the source rock characteristics and high-energy depositional environment are the primary causes for the constant rounding and for the detrital mineralogy present in the Clinch Sandstone. Folk (1960) suggested a Cambrian quartzite as a possible source for the Tuscarora Formation but then dismissed the possibility. He proposed a source history for the Tuscarora Formation in West Virginia which included erosion of a metamorphic blanket (responsible for high percentages of metamorphic rock fragments in the red Tuscarora) to uncover a quartz-rich pluton below (the source for straight extinction quartz above). Hayes (1974), working to the southwest of Folk, claimed the source for the Tuscarora Formation was progressively higher amounts of metamorphic and some plutonic rocks mixed with recycled Cambrian and Late Precambrian sedimentary rocks. The rocks apparently become more mature to the south and terminate in a pinch out of the Lower Silurian sand sheet to the south. This increasing maturity, when coupled with the

paleocurrent data, suggests transport from the northeast along a coastline which ultimately deposited and reworked the most mature sediment farthest to the south. This is supported in that in the Beans Gap area the sediments contain less metamorphic and plutonic rock fragments, and the lithic component is almost entirely sedimentary. The Lower Silurian rocks on Clinch Mountain were most likely derived from a moderately mature sandstone, which underwent extensive transport. This allowed partially rounded sediments to become rounded to well-rounded in the second cycle of deposition. Because degree of rounding is constant, the sediment was either derived from one source with consistent rounding or underwent abrasion in transport or at the site of deposition.

Diagenetic History

After deposition of the Clinch Sandstone, compaction was probably the first event to occur leading to lithification. This caused a loss of water from the sediment arising from overlying sediment deposition (Berner, 1971). Original porosity was also affected by the initial compaction.

The first authigenic minerals to form in the Clinch Sandstone varied, to some extent, depending on the grain size and, more importantly, on the sorting and mineralogy of the sediment. Cementation patterns commonly relate most closely to detrital mineralogy than to any other factor (Carrigy and Mellon, 1964). No set pattern of paragenesis can be defined for the Clinch Sandstone, which may be a result of the variations in accessory detrital mineralogy.

Precipitation/dissolution successions can be determined in so few thin sections and so seldom do they describe the same or corresponding sequence that only an approximate paragenesis can be proposed (Figure 62). The most common and most likely first stage in diagenesis (after early burial compaction) was formation of authigenic quartz overgrowths (as occurred in the equivalent Medina Group in Pennsylvania as mentioned by Laughrey in 1982). Fine-grained matrix, where present, commonly inhibited overgrowths. The nature of many Clinch Sandstone quartz grains (floating in overgrowths) implies precipitation of authigenic quartz occurred soon after deposition and at a relatively shallow depth (Blatt, 1979). Because the quantity of overgrowths does not relate to quantity of detrital monocrystalline quartz (Section IV) and overgrowths are ubiquitous, it is apparent that overgrowths occur on most monocrystalline quartz regardless of other controlling factors. The only requirements for secondary quartz precipitation are a pH below 9 and low temperatures combined with supersaturated solutions (Pettijohn et al., 1973). These conditions are easily met as clay and K-feldspar decomposition liberates silica and potassium to the porewater (Pettijohn et al., 1973). This first precipitation of quartz overgrowths occluded a great deal of the pore space, although no easily recognizable correlation exists to dictate that abundant overgrowths mean less porosity (even though this is certainly logical and expected) (Table 6, p. 88). The lack of such a relationship may indicate that there has been subsequent dissolution of overgrowths (and some localized pressure solution). It also suggests that the authigenic phyllosilicate minerals smectite,

Figure 62. Approximate composite paragenetic sequence for Clinch Sandstone at Beans Gap.

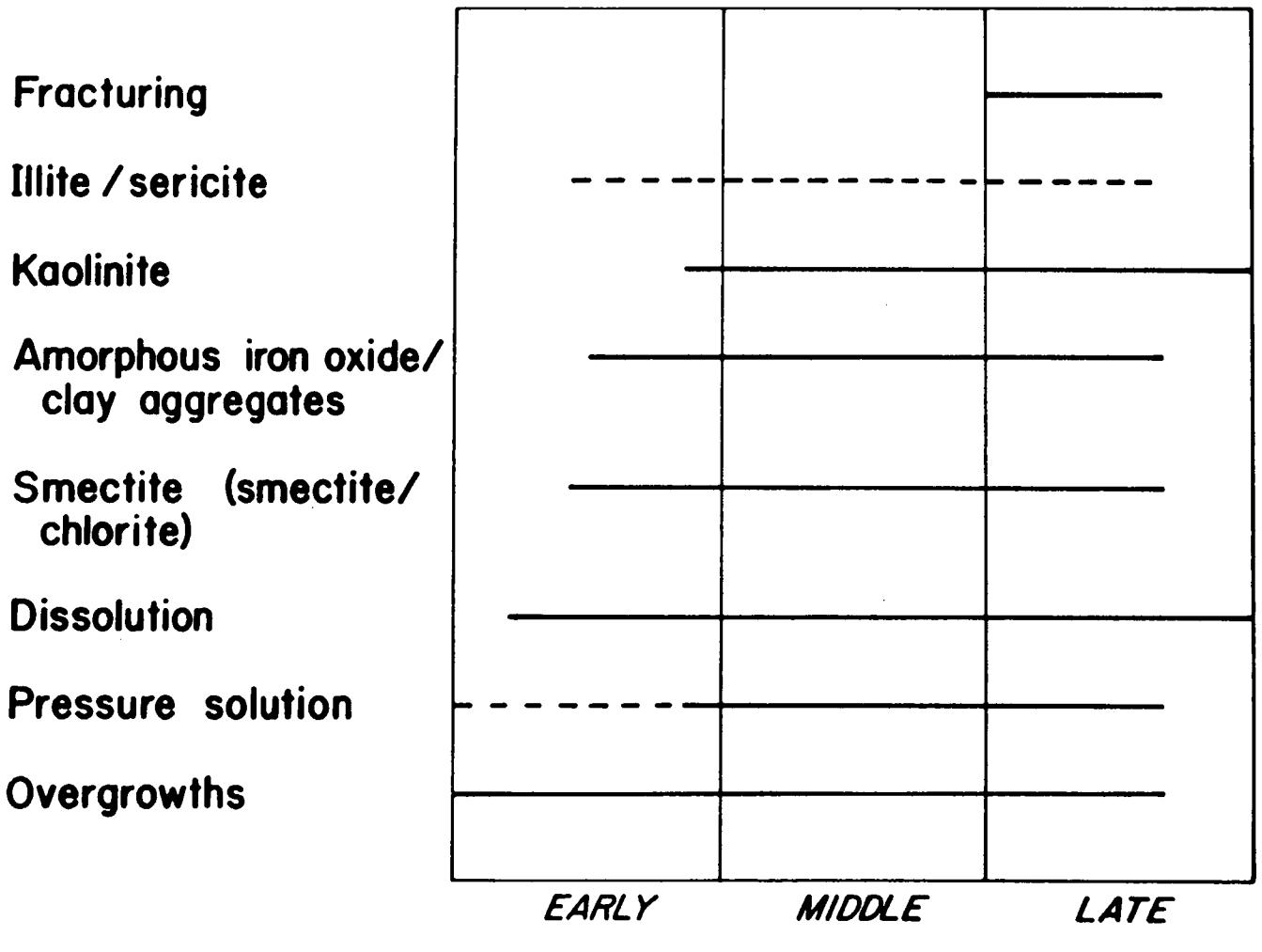
Fracturing
Illite / sericite
Kaolinite
Amorphous iron oxide/ clay aggregates
Smectite (smectite/ chlorite)
Dissolution
Pressure solution
Overgrowths
EARLY
MIDDLE
LATE

Figure 62

smectite/chlorite, kaolinite, possible amorphous iron oxide-clay aggregates and sericite are the most significant pore space occluders. This is especially true because the last three show a negative relationship with porosity. Authigenic smectite or smectite/chlorite appears to have been the first clay to develop. Smectite is not a commonly precipitated mineral, more often deposited as detrital matrix in the Clinch Sandstone. In the few cases where it appears authigenic its presence may be explained by direct formation "from igneous minerals in potassium-poor mafic rocks," according to Blatt et al. (1980), which may be derived from a subjacent source. Smectite, typically, is later altered to illite, with increases in ambient aluminum and potassium, which result from decomposition of K-micas and K-feldspars (Hower, 1982; Blatt et al., 1980). This creates interlayered smectite and illite, which ultimately becomes pure illite (Blatt, 1979).

Kaolinite appears to have been the next to form in those thin sections in which a paragenetic sequence could be ascertained. It shows somewhat positive relationships with smectite and polycrystalline quartz (Section IV), which may indicate a less compositionally mature suite of detrital minerals. From this less mature group K-feldspar may have provided the necessary aluminum and silica for kaolinite precipitation. Kaolinite may be the last authigenic mineral to have been precipitated because it alone fills fractures that cut earlier-formed or -deposited minerals (Figure 39, p. 113). Kaolinite develops more readily in marine rocks (Carrigy and Mellon,

1964), but is probably controlled more by original composition because fewer unstable minerals are deposited in the marine environment (Blatt et al., 1980).

Fracturing may have preceded kaolinite formation. Fracturing was probably due to tectonism.

Pressure solution accounts for a great deal of the final porosity occlusion which occurs in the Clinch Sandstone. Quartz overgrowths are compressed against adjacent grains and, because solubility increases with pressure, grain boundaries dissolve (Berner, 1971). This process is commonly promoted by the presence of a clay film on the grains (Waugh, 1970), as is exhibited in several of the Clinch Sandstone thin sections. This dissolution, upon reduction of pore pressure, may lead to immediate quartz precipitation, typically on adjacent grains (Pettijohn et al., 1973; Waugh, 1970). When this occurs on the lateral boundaries of a grain stressed from above, as it commonly does in the Clinch Sandstone, a pseudo-laminated texture appears, which, in this study is referred to as lateral elongation (Riecke effect). Stylolites, though not very common, are also present in the Clinch Sandstone, and indicate localized areas where more extensive dissolution of silicate framework grains has occurred. Heavy minerals and amorphous iron oxide-clay aggregates are abundant along stylolites, indicating their lower solubilities. Stylolites are related to late pressure solution in clean sandstones (Heald, 1955) and are commonly formed in the deep subsurface (Blatt et al., 1980).

Sericite is an important authigenic mineral whose timing is hard to determine. Sericite replaces detrital matrix, feldspars, and quartz. Where sericite is present in matrix, it is commonly due to alteration. Sericitization of feldspars is common in humid environments (James et al., 1981) which may indicate a similar setting for alteration of feldspars in the Clinch Sandstone. Sericite also seems to be growing on or corroding identifiable quartz grains. This is a reaction that does not have any logical explanation but is seen in several places in the Clinch Sandstone. Perhaps temperature and pH became very high causing quartz to become slightly unstable. Under these conditions sericite may have precipitated on the quartz grain or replaced part of the reacting grain itself.

The diagenesis of the Clinch Sandstone is admittedly complex and difficult to interpret. In the study area, paragenesis clearly took several paths depending on the nature of the rock itself (sorting, grain size and mineralogic composition). Secondary porosity has formed by dissolution in most of the Clinch Sandstone, and it is this very late stage diagenesis (weathering?) which further complicates the paragenetic sequence. Thus, there is no overall sequence proposed here but some preferred diagenetic relationships are suggested instead.

VIII. SUMMARY AND CONCLUSIONS

The Clinch Sandstone source and depositional environment proposed here differ from some of those previously proposed for lithostratigraphic equivalents to the northeast. The Clinch Sandstone in east Tennessee is composed of a shale-siltstone Member and a quartz arenite-quartz wacke Member. The lower fine-grained beds of the Hagan Shale Member represent a transgressive sequence in which rapid deepening occurred, resulting in deposition of the early Hagan Shale Member sediments on the outer marine shelf. Shelf sedimentation deposited less material in Tennessee than northern equivalents. Fine-grained outer marine shelf deposits (clayshale) are overlain by fine-grained, yet coarser lithologies (siltstone), which exhibit an upward increase in bioturbation by suspension feeders and medium-scale cross-beds. These upward trends indicate the beginning of upward shoaling in the marine environment. Significant as well are the storm sand layers, rare in the bottom and middle of the Member but more common upward. Shoaling within the environment is suggested by these sand layers, characteristic of the transition zone where coarser terrigenous clastics are interstratified with fine pelagic sediments. The constant upward increase in coarse-grained terrigenous clastics attests to increasing proximity to source. Depths for any part of the Hagan Shale Member are difficult to estimate due to the scarcity of diagnostic physical sedimentary structures.

Deposition of the Poor Valley Ridge Member began with an uplift in the source area (the Taconic Highlands) which caused coarser

sediment to be carried further out onto the shelf. Uplift and proximity to source may explain the abbreviated shelf sequence seen in the southern Appalachians, whereas a more complete sequence is present in the central and northern Appalachians. The exact source lithology for the Clinch Sandstone sediments is not known but is most likely quartzose sedimentary rocks. The Cambrian Chilhowee Group sediments in the southern Appalachians are less mature than the Clinch Sandstone (Whisonant, 1974; Mack, 1980; Cudzil, 1985) but bear a mineralogic resemblance and have been proposed elsewhere as a likely source (Folk, 1960; Hayes, 1974). The source had to be extensive because the sediments carried into the Clinch Sandstone depositional area remained rather constant in mineralogic nature throughout the deposition of the upper Member. Progradation of the shoreline continued as sediment influx outweighed subsidence and/or sea-level rise. A barrier-bar system, including shoreface, lagoonal and tidal channel deposits, prograded over the transition zone (shelf) sediments. During the progradational and local shoaling events, shoreface sediments were deposited over the transition zone sediments at the base of the Poor Valley Ridge Member. Continued progradation was joined by migration of the tidal channels which resulted in large-scale bedforms and unimodal paleocurrents (directed offshore due to strong ebb flow). The original shoaling-upward sequence is capped by a unique siltstone unit, which may have been deposited in a back bay or lagoonal environment. Fluctuations between shoreface and tidal channel settings continued up to the erosive top of the Formation. Neither a regression

nor reduction in sediment influx is preserved in the uppermost Clinch Sandstone in east Tennessee, as is exemplified in the fine-grained Castanea Member of the Tuscarora Formation in Pennsylvania. Erosion may have removed a substantial portion of the top of the Clinch Sandstone, which possibly recorded a regressive sequence equivalent to that in Pennsylvania. The overlying Middle Silurian unit(s) may also have been eroded in Tennessee, thus removing the evidence for a Lower Silurian-Middle Silurian transgression as is seen in Pennsylvania. This "complete" sequence may be represented at the outcrop in Abingdon, Virginia, where the Middle Silurian Rose Hill Formation overlies the Clinch Sandstone and a Castanea Member (Tuscarora Formation)-like lithology intervenes (Miller, 1976).

To test this model several avenues (which are beyond the scope of this study) need to be investigated: (1) extensive cathodoluminescence and scanning electron microscope work will provide more data on the petrologic relationships and phyllosilicate identifications, (2) coring for the Clinch Sandstone at depth may yield more unequivocal information about the Formation's petrology, (3) evaluating outcrops along other strike belts will aid in ascertaining depositional environment and position in the regional picture, (4) investigations along strike may find the transitional areas between marine and continental deposits and the exact nature of the southernmost uneroded top of the Clinch Sandstone, and (5) detailed study of the underlying Upper Ordovician Juniata Formation will definitely aid in setting the stage for Silurian deposition in the

southern Appalachians. In the local area bidirectional current indicators, marine trace fossils, and mature quartz sandstones will substantiate the proposed nearshore marine environment. Further evidence in the area for tidal channels, tidal deltas, washover fans, lagoonal and eolian deposits will add support to the proposed barrier-bar environment for the Clinch Sandstone at Beans Gap.

REFERENCES

REFERENCES

Allen, J. R. L., 1970, Physical Processes of Sedimentation: New York, American Elsevier, 248 p.

Beard, D. C., and Weyl, P. K., 1973, Influence of texture on porosity and permeability of unconsolidated sand: Am. Assoc. Petroleum Geologists Bull., v. 57, p. 349-369.

Berner, R. A., 1971, Principles of Chemical Sedimentology: New York, McGraw-Hill, 240 p.

Berry, W. B. N., and Boucot, A. J., 1970, Correlation of the North American Silurian rocks: Geol. Soc. America Spec. Paper 102, 289 p.

Berry, W. B. N., and Boucot, A. J., 1973, Glacio-eustatic control of Late Ordovician-Early Silurian platform sedimentation and faunal changes: Geol. Soc. America Bull., v. 84, p. 275-284.

Blatt, H., 1979, Diagenetic processes in sandstones, in Scholle, P. A., and Schluger, P. R., eds., Soc. Econ. Paleontologists and Mineralogists Spec. Pub. no. 26, p. 141-151.

Blatt, H., and Christie, J. M., 1963, Undulatory extinction in quartz of igneous and metamorphic rocks and its significance in provenance studies of sedimentary rocks: Journal Sed. Pet., v. 30, p. 559-579.

Blatt, H., Middleton, G., and Murray, R., 1980, Origin of Sedimentary Rocks: Englewood Cliffs, New Jersey, Prentice-Hall, 782 p.

Bouma, A. H., Berryhill, H. J., Knebel, H. J., and Brenner, R. L., 1982, Continental shelf, in Scholle, P. A. and Spearing, D., eds., Sandstone Depositional Environments: Am. Assoc. Petroleum Geologists Mem. 31, p. 281-328.

Brenchley, P. J., and Newall, G., 1980, A facies analysis of Upper Ordovician regressive sequences in the Oslo Region, Norway—a record of glacioeustatic changes: Palaeogeog., Palaeoclimat., Palaeoecol., v. 31, p. 1-38.

Carr, T. R., 1982, Log-linear models, Markov chains and cyclic sedimentation: Journal Sed. Pet., v. 52, p. 905-912.

Carrigy, M. A., and Mellon, G. B., 1964, Authigenic clay mineral cements in Cretaceous and Tertiary sandstones of Alberta: Journal Sed. Pet., v. 34, p. 461-472.

Chowns, T. M., 1972, Molasse sedimentation in the Silurian rocks of northwest Georgia, in Chowns, T. M., ed., Sedimentary Environments in the Paleozoic Rocks of Northwest Georgia: Georgia Dept. of Natural Resources, Geol. Surv. of Georgia, p. 13-44.

Clarkson, E. N. K., 1979, Invertebrate Palaeontology and Evolution: London, George Allen and Unwin, 321 p.

Clifton, H. E., 1969, Beach lamination: nature and origin: Marine Geology, v. 7, p. 553-559.

_____, 1982, Estuarine deposits, in Scholle, P. A. and Spearing, D., eds., Sandstone Depositional Environments: Am. Assoc. Petroleum Geologists Mem. 31, p. 179-190.

Coleman, J. M., and Prior, D. B., 1982, Deltaic environments, in Scholle, P. A. and Spearing, D., eds., Sandstone Depositional Environments: Am. Assoc. Petroleum Geologists Mem. 31, p. 139-178.

Colton, G. W., 1970, The Appalachian Basin—its depositional sequences and their geologic relationships, in Fisher, G. W. et al., eds., Studies in Appalachian Geology: Central and Southern: New York, Interscience, p. 5-47.

Cotter, E., 1982, Tuscarora Formation of Pennsylvania: Soc. Econ. Paleontologists and Mineralogists Eastern Section Field Trip Guidebook, 105 p.

_____, 1983, Shelf, paralic, and fluvial environments and eustatic sea-level fluctuations in the origin of the Tuscarora Formation (Lower Silurian) of central Pennsylvania: Journal Sed. Pet., v. 53, p. 25-49.

Crimes, T. P., 1975, The stratigraphical significance of trace fossils, in Frey, R. W., ed., The Study of Trace Fossils: New York, Springer-Verlag, p. 109-130.

Cudzil, M. R., 1985, Sedimentology of the Cambrian Chilhowee Group: Master's thesis, University of Tennessee, Knoxville, Tennessee (in preparation).

Davidson-Arnott, R. G. D., and Greenwood, B., 1976, Facies relationships on a barred coast, Kouchibouguac Bay, New Brunswick, Canada, in Davis, R. A. and Ethington, R. L., eds., Beach and Nearshore Sedimentation: Soc. Econ. Paleontologists and Mineralogists Spec. Pub. no. 24, p. 149-168.

Deer, W. H., Howie, R. A., and Zussman, J., 1966, An Introduction to the Rock Forming Minerals: New York, Wiley and Sons, 528 p.

de Mowbray, T., and Visser, M. J., 1984, Reactivation surfaces in subtidal channel deposits, Oosterschelde, Southwest Netherlands: Journal Sed. Pet., v. 54, p. 811-824.

Dennison, J., 1970, Silurian stratigraphy and sedimentary tectonics of southern West Virginia and adjacent Virginia, in Silurian stratigraphy, central Appalachian basin: Charleston, West Virginia, Appalachian Geol. Soc., p. 2-33.

_____, 1976, Appalachian Queenston delta related to eustatic sea-level drop accompanying Late Ordovician glaciation centered in Africa, in Bassett, M. G., ed., The Ordovician System: Cardiff, Univ. Wales Press, p. 107-120.

Dennison, J., and Boucot, A. J., 1974, Little War Gap at Clinch Mountain provides standard reference section for Silurian Clinch Sandstone and most nearly complete Devonian section in Eastern Tennessee: Southeastern Geology, v. 16, p. 79-95.

Diecchio, R. J., 1973, Lower and mid-Silurian ichnofacies and their paleoenvironmental significance, central Appalachian Basin of the Virginias: Master's thesis, Duke University, North Carolina, 100 p.

Driese, S. G., Schoner, A. E., and McDonald, C. J., 1984, Sedimentology of the Poor Valley Ridge Member of the Clinch Sandstone (Lower Silurian), northeastern Tennessee and southwestern Virginia: Appalachian Basin Industrial Associates Program, v. 6, p. 47-75.

Eliot, T., 1978, Clastic shorelines, in Reading, H. G., ed., Sedimentary Environments and Facies: New York, Elsevier, p. 143-177.

Epstein, J. B., and Epstein, A. G., 1972, The Shawangunk Formation (Upper Ordovician (?) to Middle Silurian) in eastern Pennsylvania: U.S. Geological Survey Prof. Paper 744, 45 p.

Epstein, A. G., Epstein, J. B., and Harris, L. D., 1977, Conodont color alteration—an index to organic metamorphism: U.S. Geological Survey Prof. Paper 995, 27 p.

Folk, R. L., 1960, Petrography and origin of the Tuscarora, Rose Hill, and Keefer Formations, Lower and Middle Silurian of eastern West Virginia: Journal Sed. Pet., v. 30, p. 1-58.

_____, 1974, Petrology of Sedimentary Rocks: Austin, Texas, Hemphill's Bookstore, 170 p.

Fox, W. T., and Davis, R. A., Jr., 1976, Weather patterns and coastal processes, in Davis, R. A., Jr. and Ethington, R. L., eds., Beach and Nearshore Sedimentation: Soc. Econ. Paleontologists and Mineralogists Spec. Pub. no. 24, p. 1-23.

Frey, R. W., 1975, The realm of ichnology, its strengths and limitations, in Frey, R. W., ed., The Study of Trace Fossils: a Synthesis of Principles, Problems and Procedures in Ichnology: New York, Springer-Verlag, p. 13-38.

_____, 1978, Behavioral and ecological implications of trace fossils, in Basan, P. B., ed., Trace Fossil Concepts: Soc. Econ. Paleontologists and Mineralogists Short Course No. 5, p. 43-66.

Friedman, G. M., and Sanders, J. E., 1978, Principles of Sedimentology: New York, Wiley and Sons, 792 p.

Gadow, S., and Reineck, H. E., 1969, Ablandinger Sandtransport bei Sturmfluten: Senckenbergiana Marit, v. 1, p. 63-78.

Ghazizadeh, M., and Clement, C. R., 1985, Depositional environment interpretation of the Juniata Formation of a measured section at Clinch Mountain near Bean Station, Tennessee, in Walker, K. R. and Byerly, D. W., eds., Paleozoic Section along Rt. 25E (Thorn Hill section) Grainger County, east Tennessee: A field excursion: Studies in Geology, no. 9, Dept. Geol. Sciences, University of Tennessee, Knoxville (in press).

Goldring, R., 1964, Trace fossils and the sedimentary surface in shallow water marine sediments, in van Straaten, L. M. J. U., ed., Deltaic and Shallow Marine Deposits: Amsterdam Elsevier, p. 136-143.

Goodwin, P. W., and Anderson, E. J., 1974, Associated physical and biogenic structures in environmental subdivision of a Cambrian tidal sand body: Journal of Geology, v. 82, p. 779-794.

Häntzschel, W., 1962, Trace Fossils and Problematica, in Moore, R. C., ed., Treatise on Invertebrate Paleontology, Pt. W, Miscellanea, Lawrence, Kansas, Geol. Society of America and Univ. Kansas Press, p. W177-W245.

Hardeman, W. D., 1966, Geologic map of Tennessee: Tennessee Division of Geology, 1: 250,000.

Harms, J. C., Southard, J. B., and Walker, R. G., 1982, Structures and sequences in clastic rocks: Soc. Econ. Paleontologists and Mineralogists Short Course No. 9, 249 p.

Harms, J. C., Southard, J. B., Spearing, D. R., and Walker, R. G., 1975, Depositional environments as interpreted from primary sedimentary structures and stratification sequences: Soc. Econ. Paleontologists and Mineralogists Short Course No. 2, 161 p.

Harris, A. G., 1979, Conodont color alteration, an organo-metamorphic index, and its application to Appalachian Basin Geology, in Scholle, P. A. and Schluger, P. R., eds., Aspects of Diagenesis: Soc. Econ. Paleontologists and Mineralogists Spec. Pub. no. 26, p. 3-16.

Hayes, A. W., 1974, Origin of the Tuscarora Formation in Southwestern Virginia: Ph.D. dissertation, Virginia Polytechnic Institute and State University, Blacksburg, Virginia, 162 p.

Hayes, M. O., 1967, Hurricanes as geological agents, south Texas coast: Am. Assoc. Petroleum Geologists Bull., v. 51, p. 937-942.

Heald, M. T., 1955, Stylolites in sandstone: Journal of Geology, v. 63, p. 101-114.

Heinberg, C., and Birkelund, T., 1984, Trace-fossil assemblages and basin evolution of the Vardekloft Formation (Middle Jurassic, Central East Greenland): Journal of Paleontology, v. 58, p. 362-397.

Helgeson, H. C., Brown, T. H., and Leeper, R. H., 1969, Handbook of Theoretical Activity Diagrams Depicting Chemical Equilibria in Geologic Systems Involving an Aqueous Phase at One Atm and 0° to 300°C: San Francisco, Freeman, Cooper and Company, 253 p.

Hill, G. W., and Hunter, R. E., 1976, Interaction of biological and geological processes in the beach and nearshore, northern Padre Island, Texas: Soc. Econ. Paleontologists and Mineralogists Spec. Pub. No. 24, p. 169-187.

Houseknecht, D. W., 1984, Influence of grain size and temperature on intergranular pressure solution, quartz cementation, and porosity in a quartzose sandstone: Journal Sed. Pet., v. 54, p. 348-361.

Howard, J. D., 1972, Trace fossils as criteria for recognizing shorelines in the stratigraphic record, in Rigby, J. K, and Hamblin, W. K., eds., Recognition of Sedimentary Environments, Soc. Econ. Paleontologists and Mineralogists Spec. Pub. No. 16, p. 215-225.

_____, 1978, Sedimentology and trace fossils, in Basan, P. B., ed., Trace Fossil Concepts: Soc. Econ. Paleontologists and Mineralogists Short Course No. 5, p. 13-47.

Howard, J. D., and Reineck, H. E., 1972a, Georgia coastal region, Sapelo Island, U.S.A.: Sedimentology and biology. IV. Physical and biogenic sedimentary structures of the nearshore shelf: Senckenbergiana Marit, v. 4, p. 81-123.

Howard, J. D., and Reineck, H. E., 1972b, Georgia coastal region, Sapelo Island, U.S.A.: Sedimentology and biology. VIII. Conclusions: Senckenbergiana Marit, v. 4, p. 217-222.

Howard, J. D., and Reineck, H. E., 1979, Sedimentary structures of a "high-energy" beach to offshore sequence; Ventura-Port Heuneme area California (abs.): Am. Assoc. Petroleum Geologists, v. 63, p. 468-469.

Hower, J., 1982, Clay mineral reactions in clastic diagenesis: Am. Assoc. Petroleum Geologists Bull., v. 66, p. 1444-1445.

Hunter, R. E., 1967, The petrography of some Illinois Pleistocene and Recent sands: Sedimentary Geology, v. 1, p. 57-75.

Hunter, R. E., Clifton, H. E., and Phillips, R. L., 1979, Depositional processes, sedimentary structures, and predicted vertical sequences in barred nearshore systems, southern Oregon coast: Journal Sed. Pet., v. 49, p. 711-726.

Hunter, R. E., Thor, D. R., and Swisher, M. L., 1982, Depositional and erosional features of the inner shelf, northeastern Bering Sea: Geologie en Mijnbouw, v. 61, p. 49-62.

James, W. C., Mack, G. H., and Suttner, L. J., 1981, Relative alteration of microcline and sodic plagioclase in semi-arid and humid climates: Journal Sed. Pet., v. 51, p. 151-164.

Kerr, P. F., 1977, Optical Mineralogy: New York, McGraw-Hill, 492 p.

Klein, G. D., 1977, Clastic Tidal Facies: Champaign, Illinois, Continuing Education Publication Company, 149 p.

Kumar, N., and Sanders, J. E., 1974, Inlet sequence: a vertical succession of sedimentary structures and textures created by the lateral migration of tidal inlets: Sedimentology, v. 21, p. 441-532.

Laughrey, C. D., 1982, Diagenesis and secondary porosity in Medina reservoir sandstones, Athens and Geneva fields, Crawford County, Pennsylvania: Am. Assoc. Petroleum Geologists Bull., v. 66, p. 1171.

Laughrey, C. D., and Donahue, J., 1982, Diagenetic trends within the Tuscarora-Medina sequence in the northern Appalachians: Appalachian Basin Industrial Associates Program, v. 3, p. 49-59.

Leeder, M. R., 1982, Sedimentology: Process and Product: London, George Allen and Unwin, 344 p.

Leggett, J. K., 1978, Eustasy and pelagic regimes in the Iapetus Ocean during the Ordovician and Silurian: Earth and Planetary Science Letters, v. 41, p. 163-169.

Leggett, J. K., McKerrow, W. S., Cocks, L. R. M., and Richards, R. B., 1981, Periodicity in the early Paleozoic marine realm: Jour. Geol. Soc. London, v. 138, p. 167-176.

Lindsay, C. G., 1981, Heavy mineral analysis of various Pennsylvanian sandstones in Webster County, Iowa: Geol. Soc. America Abstracts with Program, v. 13, p. 286.

Lowe, D. R., and LoPiccolo, R. D., 1974, The characteristics and origins of dish and pillar structures: Journal Sed. Pet., v. 44, p. 484-501.

Mack, G. H., 1980, Stratigraphy and depositional environments of the Chilhowee Group (Cambrian) in Georgia and Alabama: Amer. Jour. Science, v. 280, p. 497-517.

Martini, I. P., 1971, Regional analysis of sedimentology of Medina Formation (Silurian), Ontario and New York: Am. Assoc. Petroleum Geologists Bull., v. 55, p. 1249-1261.

McCubbin, D. G., 1982, Barrier-island and strand plain facies, in Scholle, P. A. and Spearing, D., eds., Sandstone Depositional Environments: Am. Assoc. Petroleum Geologists Mem. 31, p. 247-280.

McKerrow, W. S., 1979, Ordovician and Silurian changes in sea level: Jour. Geol. Soc. London, v. 136, p. 137-145.

Meckel, L. D., 1970, Paleozoic alluvial deposition in the central Appalachians: a summary, in Fisher, G. W. et al., eds., Studies in Appalachian Geology: Central and Southern, New York, Interscience, p. 49-67.

Miller, R. L., 1976, Silurian nomenclature and correlations in southwest Virginia and northeast Tennessee: U.S. Geological Survey Bull. 1405-H, 23 p.

Miller, R. L., and Fuller, J. O., 1954, Geology and Oil Resources of the Rose Hill District: Virginia Geological Survey Bull., v. 71, p. 140-150.

Narbonne, G. M., 1984, Trace fossils in Upper Silurian tidal flat to basin slope carbonates of Arctic Canada: Journal of Paleontology, v. 58, p. 398-415.

Nicholson, F. H., 1978, Sedimentology of the Clinch Sandstone; northeastern Tennessee and southwestern Virginia: Master's thesis, University of Kentucky, Lexington, Kentucky, 65 p.

Pettijohn, F. J., Potter, P. E., and Siever, R., 1973, Sand and Sandstone: New York, Springer-Verlag, 618 p.

Potter, P. E., Maynard, J. B., and Pryor, W. A., 1980, Sedimentology of Shale: New York, Springer-Verlag, 310 p.

Powers, M. C., 1953, A new roundness scale for sedimentary particles: Journal Sed. Pet., v. 23, p. 117-119.

Pupin, J-P., and Turco, G., 1983, Le zircon, mineral commun significatif des roches endogenes et exogenes: Bulletin de Mineralogie, v. 104, p. 724-731.

Ragan, D. M., 1973, Structural Geology, An Introduction to Geometrical Techniques: New York, Wiley and Sons, 217 p.

Reineck, H. E., Gutmann, W. F., and Hertweck, G., 1967, Das Schlickgebiet südlich Helgoland als Beispiel rezenter Schelfablagerungen: Senckenbergiana Lethaea, v. 48, p. 219-275.

Reineck, H. E., and Singh, I. B., 1980, Depositional Sedimentary Environments: New York, Springer-Verlag, 439 p.

Reinson, G. E., 1979, Barrier island systems, in Walker, R. G., ed., Facies Models: Toronto, Ontario, Geoscience Canada Reprint Series 1, p. 57-74.

Rhoads, D. C., 1975, The paleoecologic and environmental significance of trace fossils, in Frey, R. W., ed., The Study of Trace Fossils: New York, Springer-Verlag, p. 147-160.

Rodgers, J., 1953, Geologic map of East Tennessee with explanatory text: Tennessee Division Geology Bull., v. 58, 168 p.

Scholle, P. A., 1979, A Color Illustrated Guide to Constituents, Textures, Cements, and Porosities of Sandstones and Associated Rocks: Am. Assoc. Petroleum Geologists Mem. 28, p. 201.

Seilacher, A., 1970, Cruziana stratigraphy of non-fossiliferous Paleozoic sandstones, in Crimes, T. P. and Harper, J. C., eds., Trace Fossils: Geol. Jour. Spec. Issue, v. 3, p. 447-476.

Selley, R. C., 1970, Studies of sequence in sediments using a simple mathematical device: Quat. Jour. Geol. Soc. London, v. 125, p. 557-581.

Smith, N. D., 1970, The braided stream depositional environment: Comparison of the Platte River with some Silurian clastic rocks, north-central Appalachians: Geol. Soc. America Bull., v. 81, p. 2993-3014.

_____, 1972, Some sedimentological aspects of planar cross-stratification in a sandy braided river: Journal of Sed. Pet., v. 42, p. 624-634.

Swanson, R. G., 1981, Sample Examination Manual: Tulsa, Oklahoma, Am. Assoc. of Petroleum Geologists Publishing, 117 p.

Walker, R. G., 1979, Shallow marine sands, in Walker, R. G., ed., Facies Models: Toronto, Ontario, Geoscience Canada Reprint Series 1, p. 75-90.

Waugh, B., 1970, Formation of quartz overgrowths in the Penrith Sandstone (lower Permian) of northwest England as revealed by scanning electron microscope: Sedimentology, v. 14, p. 309-320.

Weimer, R. J., Howard, J. D., and Lindsay, D. R., 1982, Tidal flats, in Scholle, P. A. and Spearing, D., eds., Sandstone Depositional Environments, Am. Assoc. Petroleum Geologists Mem. 31, p. 191-246.

Whisonant, R. J., 1974, Petrology of the Chilhowee Group (Cambrian and Cambrian(?)) in central-eastern and southern Tennessee: Journal of Sed. Pet., v. 44, p. 228-241.

_____, 1977, Lower Silurian Tuscarora (Clinch) dispersal patterns in western Virginia: Geol. Soc. of America Bull., v. 88, p. 215-220.

Yeakel, L. S., 1962, Tuscarora, Juniata, and Bald Eagle paleocurrents and paleogeography in the central Appalachians: Geol. Soc. of America Bull., v. 73, p. 1515-1540.

APPENDICES

APPENDIX A

TOTAL POINT-COUNT DATA

Table A-1. Total Point-Count Data.

Sample	mQ*	pQ	cht	over	plag	micro	musc	bio	chl	clay	i/s	smec	kao	heav's[a]	opaq[b]	RF's	fossils	φ	ave gr. size	range gr. size	sort[c]	roun[d]	textural maturity[e]
A-10	88	2		7			-	-		1	-		-	T	P			2	215 um	60-1500 um	M	R-W	S
A-8	87	1		7						-		-		ZH				5	215	90- 720	W-VW	R-W	S
A-7	89	-		6						1		1	-	TZ				3	250	88- 710	M	P	s-M
4-1	84	-		8							-			Z				7	125	88- 600	W	P	S
4-2	85	8		3						2	-		-	TZ				2	300	90-2400	P-M	P	s
A-9	86	4		6			-			-	1	-	-	Z				3	215	80-1400	M	P	s-M
A-6	80	1		6						-	-		-	Z				11	215	88-5500	W-VW	R	M-S
A-5	80	3		2			1	-			4	2	4	TZH				4	180	90-1000	P-M	R-W	s-M
A-4	83	4	-	9						-	-		-	Z				4	300	88-2300	M	P	s-M
A-3	90	-		5			-				-		-	TZ				5	300	90- 600	W	R-W	S
C-5	86			9					-	1	-	1	-	T	PH?			3	215	88- 500	M-W	s-P	M-S
2/10-2	80			5			-	-		7	5	2	1	TZG					150	50- 650	P	R	I
2/9-3	90			6					-	1		1	-	TZ				2	150	62- 700	M-P	P	s-M
2/9-6	86	1		8						2	-		-	TH				3	300	88-1000	M-W	R	s-M
2/9-4	86	1		3					1	7	1		-	TZHE				1	90	88-1000	P	R	I
2/8-6	86	1		9								1	1	TZHA				2	150	65-1700	M	R	s
2/8-1	85	2		7					-	1		1	-	TZ				4	160	88- 900	M	R	s
2/7-6	89	1		4						1	1	2	1	TZH				1	175	60- 800	M-W	R	s-M
2/7-3	90			4	-					1	1	1	-	TZGS				3	215	65- 800	P-M	R-W	s
1/7-4	93			4						-		1	1	TZH	P			1	110	62- 700	M	R	s
2/7-1	87			9					-	2		1	-	T				1	70	60- 125	VW	s-R	M-S
2/7-2	86			3			-		3	3		3	-	Z	MH?			2	250	52- 700	P-M	s-W	s
2/6-8	81	-		2					-	10	-		-	TZ				7	100	62- 200	W	s	I
1/6-2b	80			5				-	-	13			1	TZ				-	70	62- 125	W-VW	R	I
1/6-3	88			10			-			1	-		1	TZHR	M			-	150	50- 300	W-VW	s-R	S
1/6-1	92	1		5						-		1	1	TZH				-	95	60- 500	P-M	R	s-M
1/6-2A	85	-		7			1		-	-	2	2	3	TZH					125	60- 500	M-W	s-R	M-S
3-15	90	3		4			-			-	1		-	TZ				2	215	100-900	M-W	R	s-M
2/5-2	77			21	-						-		1	TZS				-	200	150-400	VW	R	S
2/5-5	91			1						7			-	TZH				1	100	62- 250	VW	s-R	I
1/5-2	90	1		4						-		1	3	H				1	215	70- 600	M-W	R	s-M
1/5-1	90			7						-		1	-	Z				2	190	65- 500	M-W	R	M-S
3-14	88	1		10							-		-					1	400	100-2800	M	R-W	s-M
A-1	87	1		1			-			-	4		1	TH				6	200	88- 800	W-VW	sA-s	M-S
2/4-3	88	-		7			-			2		1	1	TZ				1	150	70- 700	M-P	R	s
1/3-4	90	-		6						3				T				1	150	88- 800	W	R-W	S
A-2	85	1		6									1	TZ				7	250	90-1400	M-W	R	M
1/3-2	84			12						-				TZH				4	215	100-500	W-V	R	S
1/2-3	86			4						2	4	-	1					3	300	80- 710	M-W	R	M-S
1/2-1	74			14					1	2		1						8	200	80- 710	W-VW	V	S
3-13	47	3		1			1	-	-	5	40		2	T				1	150	50- 250	M-W	s	1-s
3-12	52	1		1						1	25	3	1	TZH				16	100	62- 500	M	sA	s-M
3-11	85	4		3			-				2		1	Z		-		5	150	80-2500	M	R-W	s-W
3-9	85	3		5				-		1	4		-	T				2	215	80-1500	P-M	W	s-M
3-10	86	3	-	2						2	2		-	Z		-		5	150	65-2800	M	R-W	s-M
C-4	81	2	-	6						6				T				5	215	100-3500	M-W	s-W	I
3-8	80	1		15	-		-			1	1			TH				2	250	150-2100	M	R	s-M
3-7	83	6	-	4			-				-	-	1	ZH	H			6	200	90-1700	M-P	R	s-M
3-6	82	5		8			-			-	1		-	TZH				4	260	90-2100	P	R	s
3-5	82	1		11						-	1		-					5	425	125-1000	W	s-R	M-S
3-4	78	-	?	1	-	-	-	-		13	7		-	TZHG				1	80	50- 700	P-M	sA-R	I
3-3	73	3		2	-	-				9	6		-	ZG		5	-	1		177-1500	P	R	I
C-3	65			-	-	-	1	-	-	5	23	1	1	Z				4	60	50- 170	P-M	s	I
3-2	79	1	?	10	-		1	1		1	1	2	-	H				4	125	62- 250	W	s-R	M-S
3-1	82	1	-	3	-	1	-	-	-	-	9		-	TZH				4	125	62- 250	W-VW	R	S
C-2	77	1		6						4	1		-	TZ				11	135	80- 800	W	R	M-S
C-1	67	-		4	1	-				9		6	-	TZH	H			10	50	20- 60	W	s-R	s

*mQ = monocrystalline quartz, pQ = polycrystalline quartz, cht = chert, over = quartz overgrowths, plag = plagioclase, micro = microcline, musc = muscovite, bio = biotite, chl = chlorite, clay = amorphous iron oxide/clay aggregates, i/s = illite/sericite, smec = smectite, kao = kaolinite, heav's = heavy minerals, opaq = opaque minerals, RF's = rock fragments, φ = porosity, roun = rounding.

[a] T = tourmaline, Z = zircon, H = hornblende, G = garnet, E = epidote, A = apatite, S = sphene, R = rutile.

[b] P = pyrite, H = hematite, M = magnetite.

[c] P = poorly sorted, M = moderately sorted, W = well-sorted, VW = very well-sorted.

[d] sA = subangular, s = subrounded, R = rounded, W = well-rounded, V = very well-rounded.

[e] I = immature, s = submature, M = mature, S = supermature.

APPENDIX B

DETRITAL PERCENTAGES RECONSTRUCTED FROM POINT-COUNTED DATA

Table B-1. Detrital Percentages Reconstructed from Point-Counted Data.

Sample	mQ*	pQ	cht	plag	micro	musc	bio	chl	'clay'	"unstable components" i/s+smec+kao
A-10	97	2				-	-		1	-
A-8	99	1							-	-
A-7	98	-							1	1
4-1	99	-								1
4-2	89	8							2	-
A-9	95	4				-			-	1
A-6	99	1							-	-
A-5	85	3				1	-			10
A-4	95	4	-						-	-
A-3	99	-				-				-
C-5	98							-	1	1
2/10-2	84					-	-		7	8
2/9-3	98							-	1	1
2/9-6	97	1							2	-
2/9-4	90	1				-		1	7	1
2/8-6	97	1								2
2/8-1	96	2						-	1	1
2/7-6	94	1							1	4
2/7-3	97			-					1	2
1/7-4	98							-	-	2
2/7-1	97								2	1
2/7-2	91					-		3	3	3
2/6-8	89	-						-	11	-
1/6-2b	85						-	-	14	1
1/6-3	98					-			1	1
1/6-1	97	1							-	2
1/6-2A	91	-				1		-	-	7
3-15	96	3				-			-	1
2/5-2	99			-						1
2/5-5	93								7	-
1/5-2	95	1							-	4
1/5-1	99								-	1
3-14	99	1								-
A-1	94	1				-			-	5
2/4-3	96	-							2	2
1/3-4	97	-							3	
A-2	98	1								1
1/3-2	100								-	
1/2-3	93								2	5
1/2-1	95							1	3	1
3-13	48	3				1	-	-	5	43
3-12	63	1							1	35
3-11	92	4				-				3
3-9	91	3					-		1	4
3-10	92	3	-						2	2
C-4	91	2							6	
3-8	96	1		-		-			1	1
3-7	92	7	-			-				1
3-6	93	2				-			-	1
3-5	98	1							-	1
3-4	80	-	?	-	-	-	-		13	7
3-3	80	3		-	-				10	6
C-3	68			-	-	1	-	-	5	25
3-2	92	1	?	-		1	1		1	3
3-1	88	1	-	-	1	-	-	-	-	10
C-2	93	1							5	1
C-1	79	-		4	-				10	7

*mQ = monocrystalline quartz, pQ = polycrystalline quartz, cht = chert, plag = plagioclase, micro = microcline, musc = muscovite, bio = biotite, chl = chlorite, 'clay' = amorphous iron oxide/clay aggregates, i/s = illite/sericite, smec = smectite, kao = kaolinite.

APPENDIX C

PALEOCURRENT MEASUREMENTS

Table C-1. Paleocurrent Measurements.

UNIPOLAR DIRECTIONAL INDICATORS

	Dip Azimuth	Dip Angle	Feature*
Hagan Shale (n=1)			
1.	39°	19°	T
Lower PVR (n=5)			
2.	162	25	PT
3.	157	20	PT
4.	155	20	PT
5.	330	30	PT
6.	157	20	T
Middle PVR (n=16)			
7.	306	17	PT
8.	300	29	PT
9.	328	16	CA
10.	276	21	PT
11.	231	3	PT
12.	309	10	PT
13.	42	11	T
14.	300	16	T
15.	302	17	T
16.	298	22	PT
17.	263	6	PT
18.	14	20	PT
19.	256	16	PT
20.	280	25	PT
21.	266	14	T
22.	273	7	T
Upper PVR (n=16)			
23.	298	30	PT
24.	302	28	PT
25.	138	24	PT
26.	322	27	PT
27.	20	28	PT
28.	350	48	PT
29.	0	39	PT
30.	341	37	PT
31.	336	10	PT
32.	88	10	T

Table C-1 (continued)

33.	269	14	PT
34.	78	16	T
35.	32	24	PT
36.	182	4	PT
37.	115	6	T
38.	70	42	PT
PVR (exact position unknown) (n=44)			
39.	298	30	PT
40.	311	37	T
41.	359	4	T
42.	8	23	T
43.	308	43	PT
44.	316	37	PT
45.	309	24	PT
46.	12	35	T
47.	309	23	T
48.	12	52	PT
49.	318	40	PT
50.	330	30	PT
51.	242	20	PT
52.	43	33	PT
53.	214	12	T
54.	357	41	PT
55.	348	52	PT
56.	346	48	PT
57.	5	38	PT
58.	303	42	PT
59.	326	46	PT
60.	332	51	PT
61.	317	28	PT
62.	322	38	T
63.	343	34	PT
64.	135	19	PT
65.	326	23	PT
66.	327	29	PT
67.	324	32	PT
68.	318	24	T
69.	322	25	T
70.	326	34	PT
71.	354	37	PT
72.	19	38	T
73.	332	40	PT
74	13	26	PT
75	352	37	PT
76.	8	30	PT
77.	332	36	PT

Table C-1 (continued)

78.	299	23	PT
79.	82	14	PT
80.	50	10	PT
81.	337	35	PT
82.	335	25	PT

BIDIRECTIONAL INDICATORS

	Dip Azimuth	Feature
1.	81	Rusophycus
2.	103	osc. ripples
3.	137	osc. ripples
4.	93	osc. ripples
5.	86	osc. ripples
6.	237	pebble streaks
7.	84	osc. ripples
8.	183	channel axis
9.	168	osc. ripples
10.	170	osc. ripples
11.	146	osc. ripples

*PT = planar-tabular cross-bed; T = trough cross-bed; CA = channel axis.

APPENDIX D

LITHOLOGIC DESCRIPTION

Table D-1. Lithologic Description.

Unit Thickness (m)	Cumulative Thickness (m)	
		HAGAN SHALE LITHOLOGIC DESCRIPTION (OUTCROP 3)
0	0	Contact with Juniata Formation
4.4	4.4	Clayey siltstone, brown, very thinly bedded, interbedded with clayshales, olive
1.7	6.1	Sandstone, pale olive, very fine to fine-grained, medium bedded, contains Planolites and Monocraterion, interbedded with claystone to siltstone (pink), burrow mottled, beds <15 cm thick
0.5	6.4	Sandstone, yellow-gray, fine- to medium-grained, planar tabular cross bedded (1 set) contains Skolithos in tops, Planolites on base, foresets are wavy and contain intraclasts
0.8	7.2	Sandstone, yellow-gray, fine- to medium grained, massively bioturbated, abundant Monocraterion
0.7	7.9	Sandstone, yellow-gray, fine-grained, interbedded with siltstone to very fine sandstone, gray-green, both commonly burrow-mottled
0.2	8.1	Sandstone, yellow-gray, very fine-grained, burrow-mottled, commonly exhibits trough cross-stratification
0.15	8.25	Sandstone, fine-grained, iron-stained, abundant Monocraterion
0.1	8.35	Siltstone, gray-green, burrow-mottled
0.1	8.45	Sandstone, fine-grained, iron-stained, common very thin Planolites on surface, may show oscillation-interference ripples
0.3	8.75	Siltstone, gray-green, burrow-mottled

Table D-1 (continued)

Unit Thickness (m)	Cumulative Thickness (m)	
0.1	8.85	Sandstone, iron-stained, fine-grained, thick-bedded, commonly shows planar-tabular cross stratification
0.3	9.15	Sandstone, iron-stained, fine-grained, planar-tabular cross-stratified
0.5	9.65	Siltstone (to claystone), gray-green, burrow-mottled, interbedded with sandstone, gray-green, commonly contains Planolites, and Monocraterion; siltstones rarely contain maroon-gray intraclasts
0.7	10.35	Sandstone, iron-stained, fine-grained, burrow-mottled, commonly exhibits very thin Planolites
0.5	10.85	Sandstone, gray-green, fine-grained, burrow-mottled, thinly bedded, interbedded with siltstone, gray-green, burrow-mottled, thinly bedded
0.15	11.0	Conglomeratic sandstone, green-gray, up to 3 mm in diameter pebbles in medium sandstone, abundant Skolithos
0.15	11.15	Siltstone, gray, thinly bedded, common very thin Planolites
0.6	11.75	Sandstone, green, medium- to thick-bedded, medium-grained, gray intraclasts at top, burrow-mottled, contains common Skolithos, possible Rusophycus, pebbles at top
0.15	11.90	Conglomerate, green, pebbles 4 mm to 15 mm diameter, clays and rock fragments common
0.4	12.30	Sandstone, iron-stained, medium-grained, possible Rusophycus
0.3	12.60	Siltstone, yellow-gray, not burrowed
2.3	14.90	Sandstone, light gray, medium to coarse sandstone, abundant Skolithos

Table D-1 (continued)

Unit Thickness (m)	Cumulative Thickness (m)	
POOR VALLEY RIDGE MEMBER LITHOLOGIC DESCRIPTION (OUTCROPS 3 AND 4)		
8.2	23.10	Sandstone, light gray, very fine- to fine-grained, abundant bioturbation and weathered-out intraclasts (10-15 cm diameter) towards top, contains rare planar-tabular cross-stratified interbeds of pink-purple, very fine sandstone, toward base is a bidirectional ripple surface topped by a rip-up lag (partially weathered out) topped by a coarse discontinuous sand quartz lag underlain by burrowed very fine sand containing abundant Skolithos, Arenicolites and an unidentifiable deposit-feeding trace; underlain by basal planar-tabular cross-beds
0.32	23.42	Sandstone, olive, medium- to coarse-grained planar-tabular cross-bedded, common ripple surfaces (ripples 1.7 cm wide, 15 cm long)
2.45	25.87	Sandstone, very pale brown, medium-grained, planar medium-bedded, iron-rich undulating horizon toward top; underlain by 50 cm thick slightly silty claystone; underlain by planar-tabular cross-beds and more planar bedding
1.4	27.27	Sandstone, white, medium-grained to very coarse sand, commonly oscillation rippled with reactivation surfaces, common reduction spots, gradational base
10.0	37.27	Sandstone, white, medium-grained, coarser toward top, flat based with sparse partially weathered-out clasts, fine pebble stringers abundant toward top, trace fossils become present (Skolithos and deposit feeders) toward middle, in irregular slabby beds; 50 cm thick planar-tabular cross-set; middle of unit is a thin fissile siltstone, gray, more bioturbated white sandstone with abundant iron staining, with small abundant reduction spots, common Cruziana (4.5 cm wide, 40 cm long) and Rusophycus, interbed of trough and planar-tabular cross-bedded,

Table D-1 (continued)

Unit Thickness (m)	Cumulative Thickness (m)	
		white, medium-grained sandstone at base, more planar-tabular cross-beds underlain by burrowed sandstone containing abundant Monocraterion and a granule layer
2.46	39.73	Sandy siltstone, light gray, very fine-grained, weathers to yellowish brown, evenly planar-bedded ranging from 3 mm to 10 cm, bedding fines up
3.05	42.78	Sandstone, white, fine- to medium-grained, medium bedded, siderite nodules are common along a horizon in the middle of the unit, a planar-tabular (intertongued with rare trough-) cross-bedded layer, medium-grained approximately 20 cm thick set, gray, with an erosive surface present near the base of the unit
0.06	42.84	Siltstone, dark gray, fissile, discontinuous
2.78	45.62	Sandstone, white, medium-grained, planar-bedded, with a planar-tabular cross-bedded horizon with a sharp base capped with a fine pebble lag occurring with some weathered out shale clasts
5.56	51.18	Covered
1.85	53.03	Sandstone, white, medium- to coarse-grained, planar-tabular cross-bedded (multidirectional current direction), sparse bidirectional ripples, sparse fine pebble stringers
0.92	53.95	Sandstone, white, medium-grained, bioturbated
2.32	56.27	Sandstone, white, medium-grained, with medium beds, with occasional fine pebble stringers
9.36	65.63	Sandstone, white, fine- to medium-grained, planar bedded with common fine pebble stringers overlain by planar-tabular cross-beds, in 7-25 cm thick sets, 1-3 cm thick bed overlain by a discontinuous very fine, dark gray, fissile, sandstone overlain by fine

Table D-1 (continued)

Unit Thickness (m)	Cumulative Thickness (m)	
		sandstone showing abundant Skolithos tubes capped by an Arthrophycus layer, in horizontal and rare planar-tabular cross-beds, overlain by greenish gray planar-tabular cross-beds, overlain by white planar-tabular cross-beds, planar beds sparse fine pebble layers, and rare fining-upward sequences
2.0	67.63	Sandstone, white, fine- to medium-grained, planar-bedded in top two-thirds, planar-tabular cross-bedded in lower third in sets approximately 10-25 cm thick with beds between 1 mm and 5 cm thick, common bioturbation in middle third of unit
2.3	69.63	Sandstone, white, fine- to medium-grained, very limited trough cross-beds, discontinuously cross-bedded in beds approximately 1 m thick, common bioturbation in upper half visible as punctures, Skolithos common towards base
0.7	70.63	Sandstone, white, fine- to medium-grained, planar-bedded in beds 20-70 cm thick
		Erosional upper surface
		LITHOLOGIC DESCRIPTION OF POOR VALLEY RIDGE OUTCROP 1
2.4		Sandstone, white to light gray, fine- to medium-grained, massively bioturbated (Diplocraterion and Skolithos), sparse unidirectional ripples and bidirectional ripples in fine sandstone
0.8		Sandstone, white to gray, very fine- to medium-grained, planar-bedded and trough cross-bedded (some truncated), very fine, fissile, sandstone drapes on medium sandstone cross-beds, all toe out into dark green-gray, very fine sandstone (pyrite nodules sparse) (base is Arthrophycus burrowed)

Table D-1 (continued)

Unit Thickness (m)	Cumulative Thickness (m)	
2.4		Sandstone, brown-gray, fine- to medium-grained, planar-bedded with common trough cross-beds with episodic and drapes toeing-out into a white siltstone, sparse homogeneous planar-tabular cross-beds, sparse burrowing, based with possible scour or irregular cross-beds
1.2		Sandstone, yellow-gray, fine grained, very low-angle planar-tabular cross-beds, bioturbated (Skolithos and Diplocraterion) towards bottom of unit, base is Arthrophycus burrowed
2.0		Sandstone, white, very fine- to fine-grained, trough cross-bedding present but rare, otherwise planar-bedded, draped bidirectional ripples present but rare (wavelength 2.25 m, 10 cm high, drapes 2.5-9 cm in thickness), large possible channel structure (10 m wide) with possible load structure (or smaller channel structure) within, top of unit has been truncated by the overlying unit, Arthrophycus burrowing in lower beds of unit
2.2		Sandstone, light gray, fine-grained, massively bioturbated (Arthrophycus visible at base)
		Erosional upper surface
	LITHOLOGIC DESCRIPTION OF POOR VALLEY RIDGE OUTCROP 2	
1.8		Sandstone, white, fine- to coarse-grained, uneven bedded with planar-tabular cross-beds and trough cross-beds, bioturbated showing Arthrophycus and Skolithos, otherwise horizontally laminated
3.3		Sandstone, gray (some iron stained areas), fine- to medium-grained, densely bioturbated (Skolithos and Arthrophycus), planar-tabular cross-bedded and planar laminated with extensive dish-and-pillar structures in some areas, bidirectional (oscillation) ripples (wavelength 6.5-30 cm, 0.5 to 2 cm high, bed thickness 8-15 cm), channel cuts may be visible

Table D-1 (continued)

Unit Thickness (m)	Cumulative Thickness (m)	
2.6		Sandstone, light gray to white, fine- to medium-grained, densely bioturbated showing Skolithos and Diplocraterion, areas of soft-sediment deformation exhibiting dish-and-pillar structures
1.5		Sandstone, light gray, medium-grained, planar-laminated, with some planar-tabular cross-bedding, limited areas of bidirectional (oscillation) ripple marks
0.2		Siltstone, gray, very thinly bedded, friable, commonly weathered out
3.1		Sandstone, light gray, medium-grained, planar-laminated with some trough cross-stratification, possible scour surfaces; some areas well-bioturbated showing Arthrophycus
1.6		Sandstone, light gray, medium-grained, planar-laminated, burrowed (shows Arthrophycus on bases of beds)
1.7		Sandstone, light gray, medium-grained, planar-tabular cross-bedded but most commonly planar-bedded
		Erosional upper surface

VITA

Amy Elizabeth Schoner was born and raised in the Washington, D.C. area, living in both Maryland and Virginia. She attended public schools in Oxon Hill, Maryland, and Fairfax County, Virginia, graduating from Herndon High School in June of 1978. The following August she entered the College of William and Mary and received a Bachelor of Science degree in Geology with a minor in Anthropology in May of 1982.

After accepting a teaching assistantship from The University of Tennessee, Knoxville, she joined the Department of Geological Sciences in September of 1982. She received the Master of Science degree majoring in Geology in June of 1985.

Ms. Schoner is a member of the Geological Society of America, the American Association of Petroleum Geologists, and Sigma Gamma Epsilon.